Development of Catalytic Asymmetric Payne–Type Oxidations under the Catalysis of Chiral Triaminoiminophosphoranes

キラルトリアミノイミノホスホランを触媒とする不斉ペイン型酸化反応の開発

TSUTSUMI Ryosuke

Department of Applied Chemistry, Graduate School of Engineering

Nagoya University

Contents

Chapter 1

General Introduction and Summary

1.1   Organic Base Catalyst

A Brønsted base is defined as a chemical species capable of abstracting a proton from other molecules. In the context of organic transformations, this deprotonation event is regarded as one of the most fundamental and important elementary reactions because the resulting anion can be involved in various C–C bond or C–heteroatom bond formations. Aside from conventional metal bases such as n-BuLi, LDA, ^{t}BuOK, organic base has advantages over them from the aspect of mildness and ease of construction of catalytic (stereoselective) reaction system. Common basic core functions such as amine, more basic guanidine[1] and amidine[2] have been explored to facilitate target reactions.[3,4] As a consequent, in addition to the prevalent tertiary amine catalysts, several guanidine-based optically active catalysts have been designed, and a variety of catalytic asymmetric transformations have been achieved by using them, while successful asymmetric reactions catalyzed by chiral amidines are rare (Scheme 1.1).

Scheme 1.1 Selected examples of chiral amine-, guanidine- and amidine-catalyzed asymmetric transformations (top[4a], middle[4b] and bottom[2a] respectively)
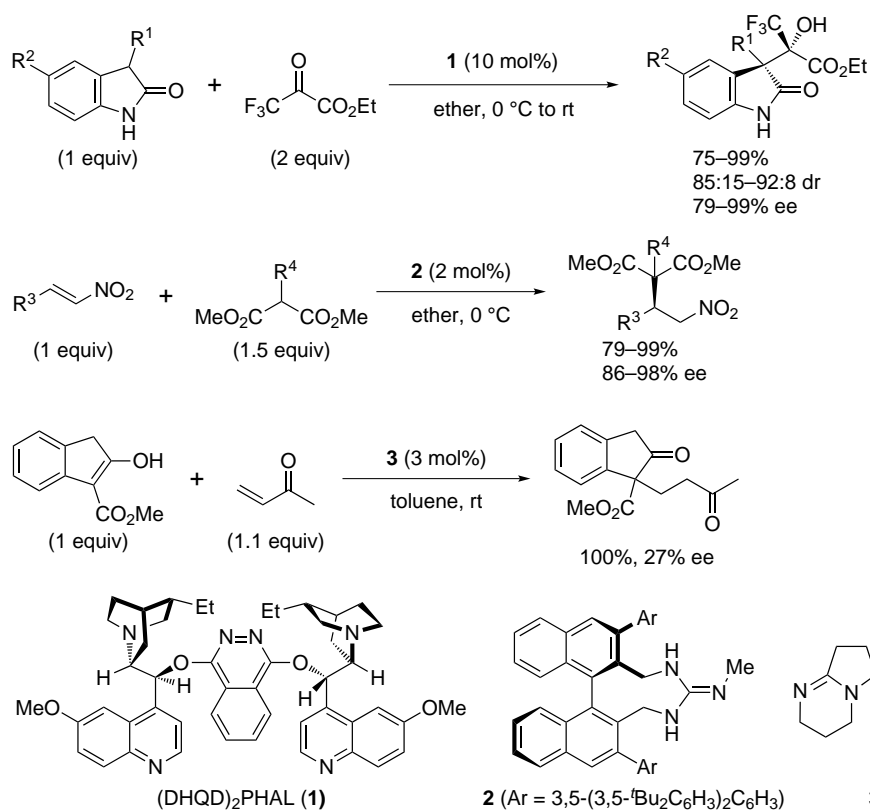
Lambert and coworkers have recently developed a highly basic cyclopropenimine catalyst (**4**)[5] whose conjugated acid is doubly stabilized by nitrogen lone pairs and aromaticity and exhibited their effectiveness for the Michael addition (Scheme 1.2)[5a] and Mannich reaction[5b] of glycine imine.

Scheme 1.2 Chiral cyclopropeneimine-catalyzed Michael addition [5a]
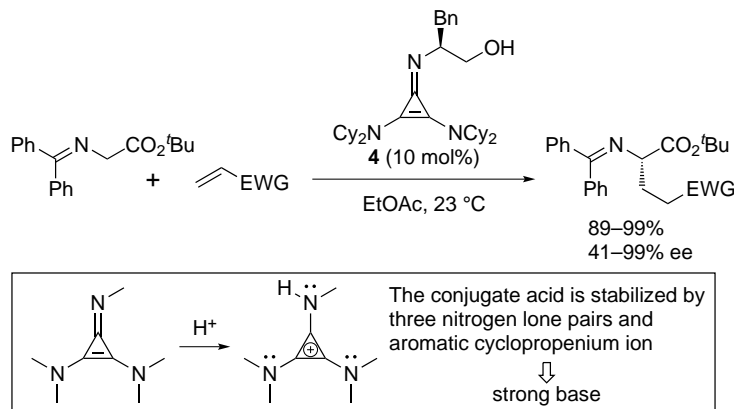
1.2 Phosphazene Base [3b]

In 1985, Schwesinger reported a series of phosphazene (triaminoiminophosphorane) bases which contain pentavalent phosphorous atom(s) bonded to four nitrogen atoms one of which is linked by a P=N double bond.6 Their basicities are greater than those of amidines and guanidines (Figure 1.1), and thus they are one of the strongest uncharged organic bases whose pK_{BH^+} values generally range from 26 to 47 (in acetonitrile).
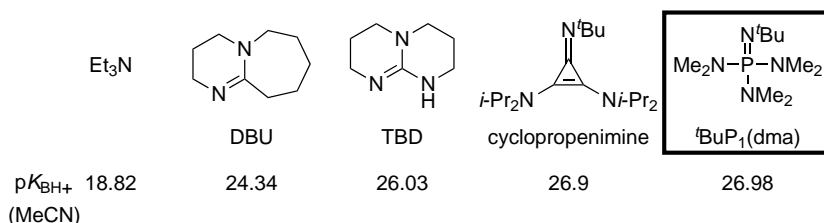

Figure 1.1 pK_{BH^+} of Et_3N, DBU, TBD, cyclopropenimine (see Scheme 1.2) and a phosphazene base (^tBuP1(dma)) in acetonitrile [5a,7]

The strong basicity of phosphazene bases was ascribed to the efficient delocalization of the positive charge through the conjugation system in the protonated molecule, [6d] though the center phosphorus atom is in a tetrahedral-like structure in a solid state according to X-ray crystallographic analysis. [6d,e] Phosphazene bases possessing additional triaminoiminophosphorane moieties in the molecule have also been synthesized, and they are referred to as Pn phosphazene where n is the number of triaminoiminophosphorane units. [6c−e] It is known that the basicity of Pn phosphazene is increased with increasing the number n, though the basicity reaches saturation when $n = 5$. [6c] When n are equal, a "branched" base is more basic than a "linear" one (for example, the pK_{BH^+} of a "linear" P3 base ^tBuP$_3$(dma) is lower than that of a "branched" ^tBuP$_3$(dma)Me (see Figure 1.2)). [6e]

P1   R$_2$N–P(**N**R')–NR$_2$ | NR$_2$ R = R' = Me (MeP$_1$(dma)): 27.52[7]
R = Me, R' = ^{t}Bu (^{t}BuP$_1$(dma) or ^{t}Bu-P$_1$): 26.98[7]
R = Me, R' = Ph (PhP$_1$(dma)): 21.25[7]
R = –(CH$_2$)$_4$–, R' = ^{t}Bu (^{t}BuP$_1$(pyrr) or BTPP): 28.42[7]

Me, N / **N**^{t}Bu
P–NEt$_2$
N
Me
BEMP: 27.5[8]

P2   R$_2$N–P(**N**R')–N=P(NR$_2$)–NR$_2$ R = R' = Me (MeP$_2$(dma)): 32.72[6e]
R = Me, R' = ^{t}Bu (^{t}BuP$_2$(dma) or ^{t}Bu-P$_2$): 33.49[6e]
R = Me, R' = Ph (PhP$_2$(dma)): 26.46[7]
R = –(CH$_2$)$_4$–, R' = Ph (PhP$_2$(pyrr)): 27.55[7]

P3   R$_2$N–P(**N**R')–N=P(NR$_2$)–N=P(NR$_2$)–NR$_2$ R = Me, R' = ^{t}Bu (^{t}BuP$_3$(dma)): 36.6[6e]
R = Me, R' = Ph (PhP$_3$(dma)): 31.48[7]

NMe$_2$ **N**^{t}Bu NMe$_2$
Me$_2$N–P=N–P–N=P–NMe$_2$
NMe$_2$ NMe$_2$ NMe$_2$
^{t}BuP$_3$(dma)Me or ^{t}Bu-P$_3$
38.6[6e]

P4   R$_2$N–P=N–P(**N**R')–N=P–NR$_2$ (with R$_2$N–P–NR$_2$ / NR$_2$ branch)   R = Me, R' = ^{t}Bu (^{t}Bu-P$_4$): 42.7[6e]
R = –(CH$_2$)$_4$–, R' = ^{t}Bu: 44.0[6e]

P5   R$_2$N–P=N–P(**N**R')–N=P–N=P–NR$_2$ (with R$_2$N–P–NR$_2$ / NR$_2$ branch)   R = Me, R' = ^{t}Bu (^{t}Bu-P$_5$): 45.3[6e]
R = –(CH$_2$)$_4$–, R' = ^{t}Bu: 46.9[6e]

NMe$_2$ NMe$_2$ **N**^{t}Bu NMe$_2$ NMe$_2$
Me$_2$N–P=N–P=N–P–N=P–N=P–NMe$_2$
NMe$_2$ NMe$_2$ N^{i}Pr$_2$ NMe$_2$ NMe$_2$
44.0[6e]

P7   NMe$_2$ NMe$_2$ **N**^{t}Bu NMe$_2$ NMe$_2$
Me$_2$N–P=N–P=N–P–N=P–N=P–NMe$_2$
NMe$_2$ NMe$_2$ N   NMe$_2$ NMe$_2$
Me$_2$N–P–NMe$_2$
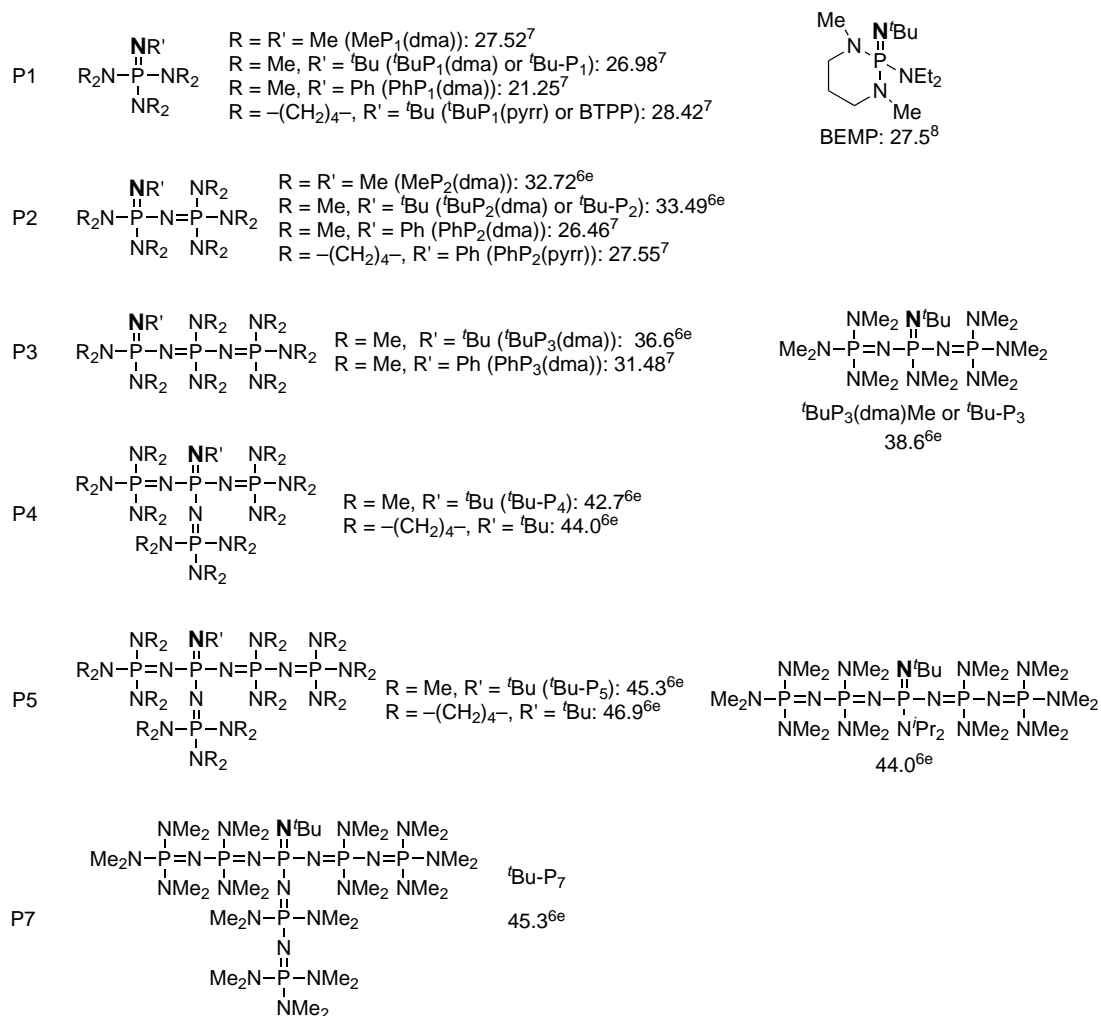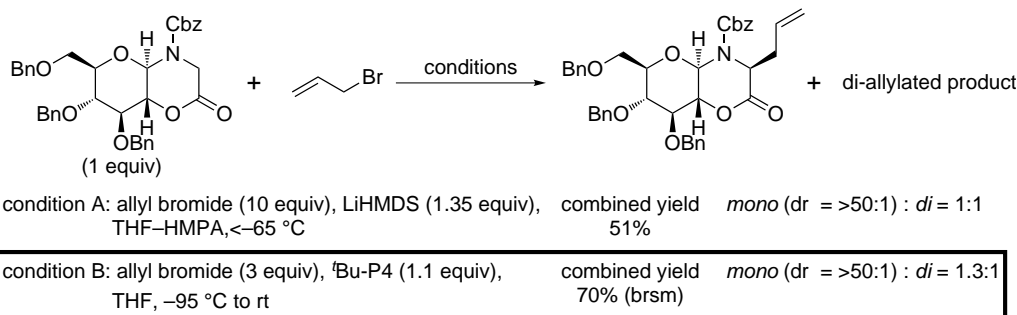N
Me$_2$N–P–NMe$_2$
NMe$_2$
^{t}Bu-P$_7$
45.3[6e]

Figure 1.2 Examples of phosphazene bases; nitrogen atoms that are protonated are indicated in boldface; pK_{BH^+} values in acetonitrile are shown. [6e,7,8]

^{t}Bu-P4, which is the most basic among commercially available phosphazene bases, exhibits basicity comparable to organolithium bases. For example, a weakly acidic α-proton of an oxazi-none derivative can be abstracted by ^{t}Bu-P4 to afford the allylated product after treatment with allyl bromie (Scheme 1.3). [9] In this case the yield is better than that of the reaction via the corresponding lithium enolate.

Scheme 1.3 Allylation of ester enolate using ^{t}Bu-P4 as a base [9]

| condition A: allyl bromide (10 equiv), LiHMDS (1.35 equiv), THF–HMPA,<–65 °C | combined yield 51% | *mono* (dr = >50:1) : *di* = 1:1 |
| condition B: allyl bromide (3 equiv), ^{t}Bu-P4 (1.1 equiv), THF, –95 °C to rt | combined yield 70% (brsm) | *mono* (dr = >50:1) : *di* = 1.3:1 |

The deprotonation of a hydrogen atom on an aromatic ring, which is known to be difficult by using conventional organic base, was achieved by ^{t}Bu-P4 phosphazene[10]. In the reaction shown in Scheme 1.4, the existence of ZnI_2 as an additive was beneficial for the efficiency of the reactions. [11]

Scheme 1.4 Deprotonative functionalization of aromatics using ^{t}Bu-P4 [11]
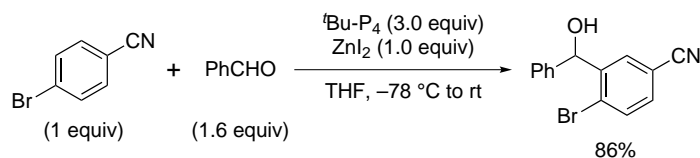
1.3   Chiral [5.5]-*P*-Spiro Triaminoiminophosphorane

1.3.1   General Description

Our research group designed [5.5]-*P*-spiro chiral tetraaminophosphonium salts **5**·HX and **6**·HX focusing on its function as an ion-paired catalyst, and has reported various highly stereoselective C–C and C–heteroatom bond formations by using them. [12] The structure and the design concept of the catalyst are depicted in Figure 1.3. The molecule has phosphorus-centered [5.5]-spirocycles composed of two chiral 1,2-diamine units derived from amino acid. Alkyl substituents on diazaphosphacycles can be altered by changing the starting amino acid. And aryl substituents are sterically and electronically tunable by introducing appropriate aromatics during the preparation process of 1,2-diamine. The key function of the tetraaminophosphonium ion is the recognition of the anion via hydrogen bonding and electrostatic interaction. Oriented double hydrogen bonds donated from two N–H protons define the position of reactive counterion and regulate the stereoselectivity of the reaction in which it is involved. Anion recognition via hydrogen bonding interaction by tetraaminophosphonium ion **5**·H and **6**·H is supported by X-ray crystallographic analysis of L-valine-derived phosphonium salts (*M,S*)-**5a**·HCl and (*P,S*)-**6a**·HCl (Figure 1.4).
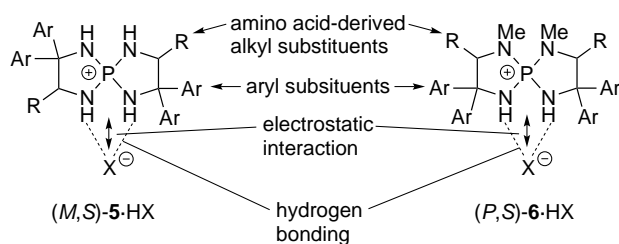
Figure 1.3 The structure and the design concept of the tetraaminophosphonium salt
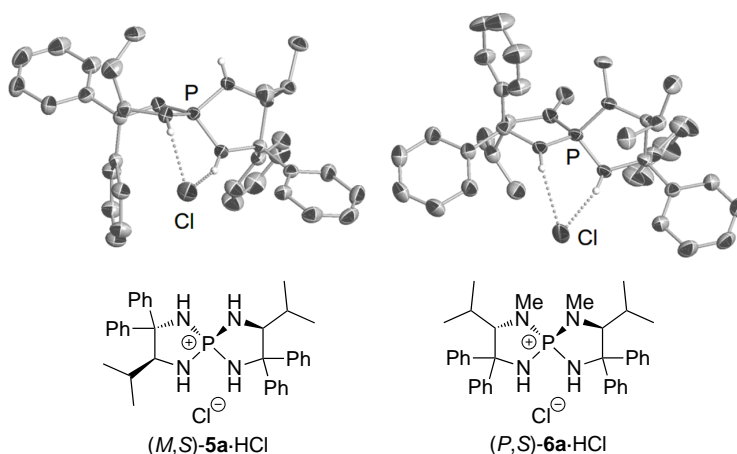

Figure 1.4 Three-dimensinal structures of (*M,S*)-**5a**·HCl and (*P,S*)-**6a**·HCl [12]

As a part of research program exploiting the unique feature of these tetraaminophosphonium salts, our group have demonstrated the potential of triaminoiminophosphoranes of type **5** and **6**, conjugate bases of tetraaminophosphonium ion **5**·H and **6**·H, through the development of highly stereoselective catalysis. [13]

1.3.2   Stereoselective Direct Henry Reaction

Triaminoiminophosphorane **5** was first applied to the highly stereoselective Henry reaction (Scheme 1.5).   In this reaction, the pronucleophile, nitroalkane was deprotonated by the triaminophosphorane 5b which was *in situ* generated from the corresponding tetraaminophosphonium chloride **5b**·HCl and ^{t}BuOK to form tetraaminophosphonium nitronate. The tetraaminophosphonium ion **5b**·H recognizes the nitronate, which is known as a bidentate hydrogen bonding acceptor. This "structured ion pair" undergoes the stereoselective addition to aldehyde to form the product and regenerate **5b** (Figure 1.5).

Scheme 1.5 Stereoselective Henry reaction [13a]
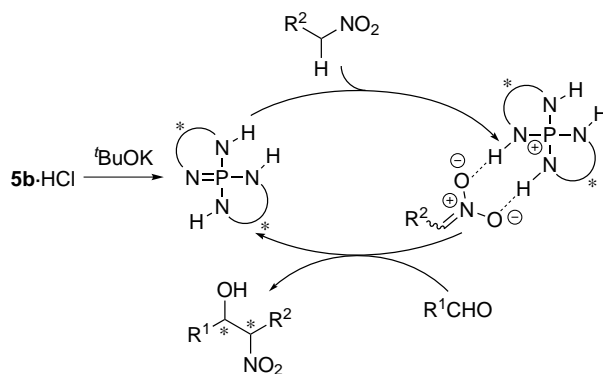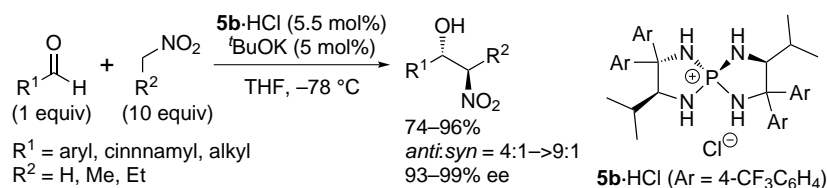

Figure 1.5 Catalytic cycle of Henry reaction [13a]

The Henry reaction also proceeds with good stereoselectivity when pyruvate derivative was employed as the electrophile. [13b]

Henry reaction between nitroalkanes and ynals was also reported. [13c] In the initial attempt, the reaction of 3-phenylpropynal (**7a**) with nitroethane using *in situ* generated **5a** as the catalyst was examined. Although the desired *anti*-Henry adduct was obtained almost exclusively (*anti*:*syn* = ¿20:1) with 86% ee, the yield was quite low (22%) (Scheme 1.6). Analysis of the crude mixture revealed the decomposition of **5a**·H. The origin of this phenomenon was attributed to the relatively low pK_a of the product, β-nitro secondary propargylic alcohol, because the tetraaminophosphonium cation **5a**·H was stable in the reactions with aromatic or aliphatic aldehydes under similar conditions. It means that the high acidity of the product might prevent the facile proton abstraction from **5a**·H. Instead, the propargylic alkoxide might attack the cationic phosphorus center to give rise to the decomposition of **5a**·H (Figure 1.6). To confirm this assumption, 4-methyl-4-nitro-1-phenylpent-1-yn-3-ol, the Henry adduct of **7a** and 2-nitropropane, was treated with the iminophosphorane **5a** preformed from **5a**·HCl and ᵗBuOK in THF at −98 °C. Upfield shift of the original ³¹P NMR signal of the iminophosphorane **5a** (δ = 47.2 to 37.7 ppm) confirmed the presumed formation of phosphonium alkoxide **A**.

Scheme 1.6 Initial attempt of Henry reaction with ynal [13c]
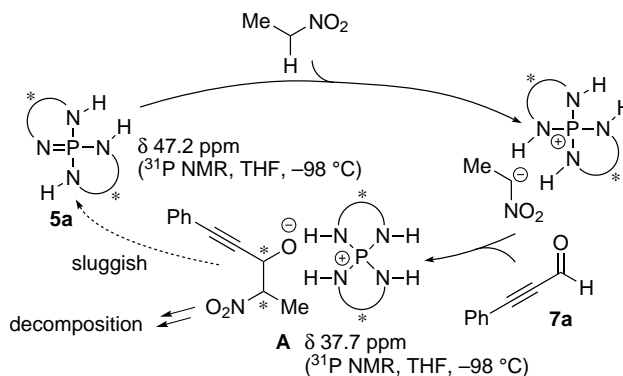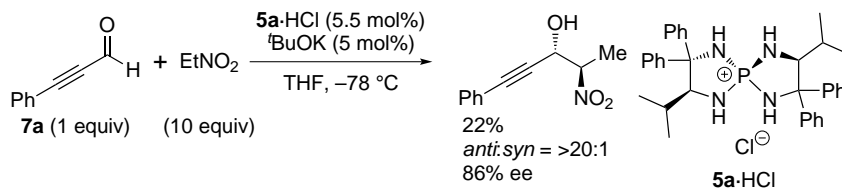
Figure 1.6 Postulated decomposition pathway of **5a**·H [13c]

The above problem was solved by using *N,N*-dimethylformamide (10 v/v%) as a co-solvent, and the conversion of the starting ynal **7a** improved at the slight expense of stereoselectivity (¿99%, 12:1, 83% ee), probably because the polarity of the solvent system has a beneficial effect on the stabilization of the phosphonium alkoxide intermediate **A**. Under this optimized condition, the reaction with various ynal **7** and nitroalkane proceeds in high yield, high *anti*-selectivity and high enantioselectivity by using **5c**·HCl as a precatalyst. The synthetic utility of this method was demonstrated by the concise syntheses of (*2S,3R*)-(+)-xestoaminol C and (−)-codonopsinines (Scheme 1.7).

Scheme 1.7 The highly stereoselective Henry reaction of ynals and concise syntheses of (*2S,3R*)-(+)-xestoaminol C and (−)-codonopsinines [13c]
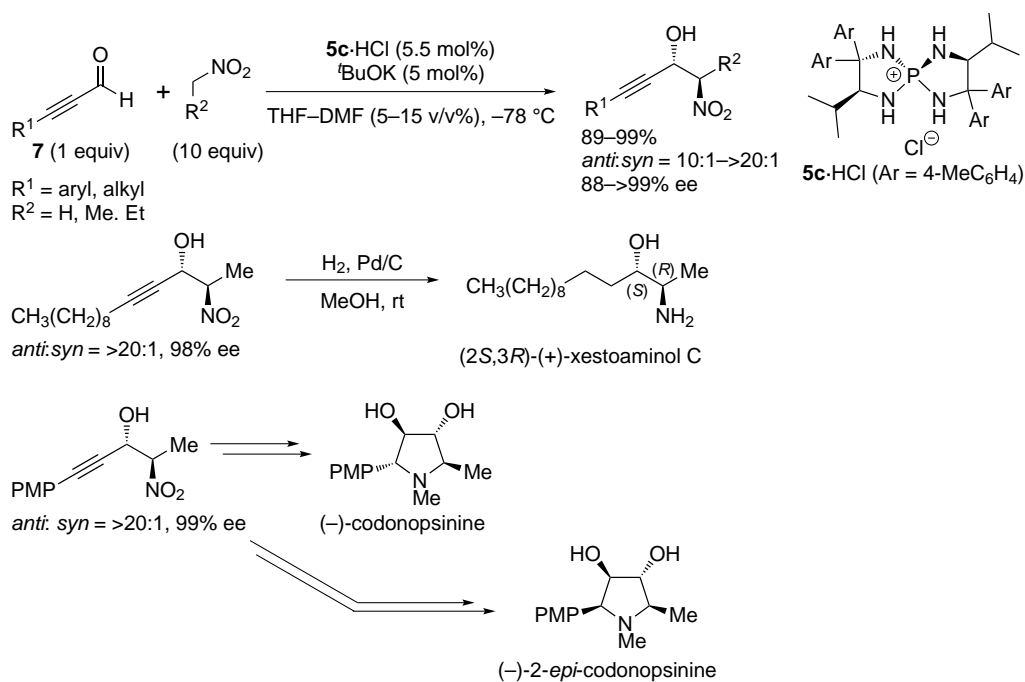
1.3.3   Stereoselective Aldolization of α-Hydroxy Phosphonate

Highly stereoselective aldol reaction between an α-hydroxy phosphonate and aldehydes was developed (Scheme 1.8) [13d]. In this reaction, iminophosphorane **6a** initially deprotonates α-hydroxy moiety of the phosphonate to afford phosphonium alkoxide. Then it undergoes facile phospha-Brook rearrangement to form chiral phosphonium enolate which stereoselectively adds to aldehyde. Subsequent phosphinate migration leads to the final product (Figure 1.7).

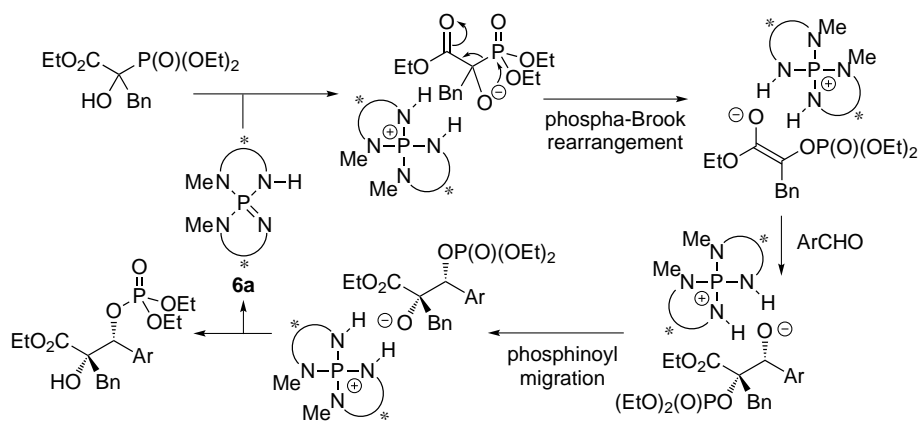**Scheme 1.8** Stereoselective aldolization of α-hydroxy phosphonate [13d]
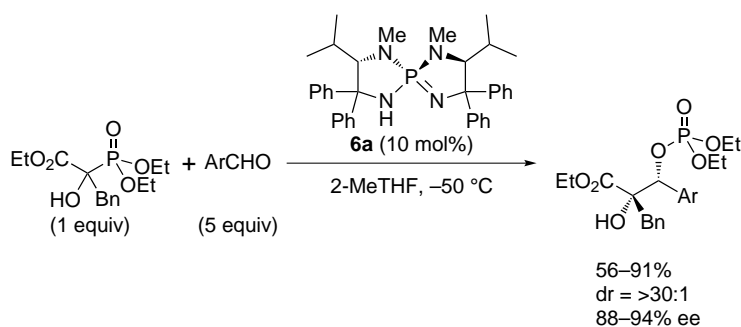
Figure 1.7 Proposed reaction mechanism of the aldolization of α-hydroxy phosphonate via phospha-Brook rearrangement [13d]

1.3.4 Other Catalytic Asymmetric Reactions Using Triaminoiminophosphoranes 5 and 6

1.3.4.1 Enantioselective Hydrophosphonylation

The strong basicity of iminophoshorane **5** and its ability of donating double hydrogen bond was utilized for the development of highly stereoselective hydrophosphonylation—the addition of dialkyl phosphonates to aldehydes or ketones. [13e] To realize hydrophophonylation with dialkyl phosphonates, the predominant contribution of phosphonate form to the equilibrium in the phosphonate–phosphite tautomerism should be considered because the latter is believed to be the actual nucleophilic species in the bond-forming event (Figure 1.8). As this equilibrium shifts to the phosphite form under basic condition, the choice of appropriate base catalyst may play an important role in promoting hydrophosphonylation.
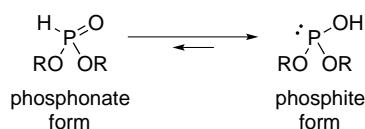

Figure 1.8 Phosphonate–phosphite tautomerism

Preliminary ^{31}P NMR analysis of the mixture of dimethyl phosphonate and several organic bases implicated the importance of the stabilization of the phosphite anion especially by double hydrogen bonding donated by counterion to increasing the contribution of phosphite form in the aforementioned equilibrium.

Iminophosphorane **5a** prepared *in situ* from phosphonium chloride **5a·**HCl and ^{t}BuOK, which showed a good result in the above NMR experiment, indeed exhibited high catalytic activity in the reaction between benzaldehyde and dimethyl phosphonate. With the optimized catalyst **5c**, the hydrophosphonylation of various aldehydes proceeded with good efficiency and excellent enan-

tioselectivities (Scheme 1.9). [13e]

Scheme 1.9 Enantioselective hydrophosphonylation of aldehydes [13e]
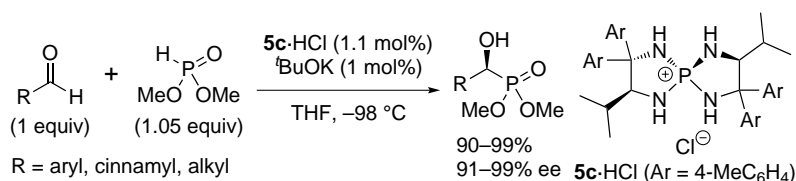
The hydrophosphonylation of alkylnyl methyl ketones also proceeds with good enantioselectivity to afford the corresponding α-hydroxyphosphonates. [13f]

1.3.4.2   Stereoselective Michael Addition of Azlactones to Electron-Deficient Triple Bonds

A catalyst-controlled, stereodivergent asymmetric Michael addition of azlactones to methyl propiolate was achieved. Interestingly, the *E/Z* stereochemistry of the olefin moiety in the product **8** and **9** depends on the catalyst employed (Table 1.1). [13g]

Table 1.1 *E*- and *Z*-selective asymmetric Michael addition of azlactones to methyl propiolate [13g]

entry	catalyst	R	yield (%)	*E/Z*	ee (%)	product
1	**5d**	Bn	92	1:>20	90	**8**
2	**5d**	4-ClC$_6$H$_4$CH$_2$	93	1:>20	85	**8**
3	**5d**	4-MeOC$_6$H$_4$CH$_2$	95	1:>20	85	**8**
4	**5d**	Me$_2$CHCH$_2$	89	1:16	58	**8**
5	**6b**	Bn	97	>20:1	93	**9**
6	**6b**	4-ClC$_6$H$_4$CH$_2$	98	18:1	90	**9**
7	**6b**	4-MeOC$_6$H$_4$CH$_2$	92	>20:1	93	**9**
8	**6b**	Me$_2$CHCH$_2$	92	7:1	87	**9**

This complete switch of *E/Z* configuration was accounted for by the difference of protonation pathway of the intermediary allenic enolate. When **5d** was used as the catalyst, the allenic enolate

is protonated by **5d·**H in the α,β-π plane from the same side as a hydrogen atom, which is kinetically favorable (Figure 1.9, path *a*). On the other hand, **6b·**H, which has more spatially congested environment around the acidic N–H protons than that of **5d·**H (see Figure 1.4), may protonate the allenic enolate on the oxygen atom (path *c*) rather than on the sterically demanding carbon atom in the α,β-π plane (paths *a* and *b*).
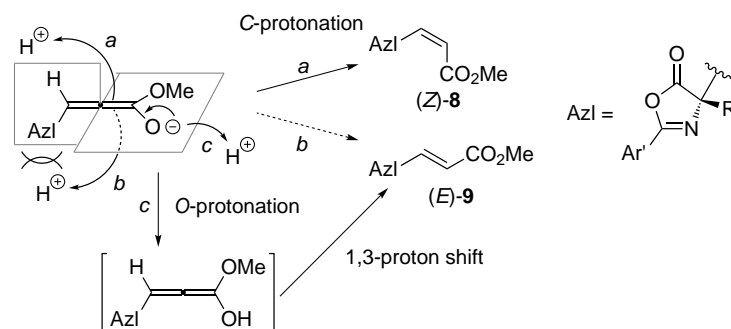

Figure 1.9 Possible protonation pathways of the allenic enolate

This interpretation was supported by conducting the Michael addition of azlactones to cyanoacetylene with **6b** as a catalyst, where *N*-protonation of the α-cyano vinylic anion intermediate is negligible. The reaction gave the product exclusively in (*Z*) form, even though **6b** was the *E*-selective catalyst in the addition of azlactone to methyl propiolate, which suggests the contribution of *O*-protonation pathway in the **6b**-catalyzed stereoselective Michael addition of azlactone to methyl propiolate.

This *Z*-selective Michal addition to cyanoacetylene was applicable to azlactones of broad substrate scope, and gave the products in good yields and excellent enantioselectivities (Scheme 1.10).
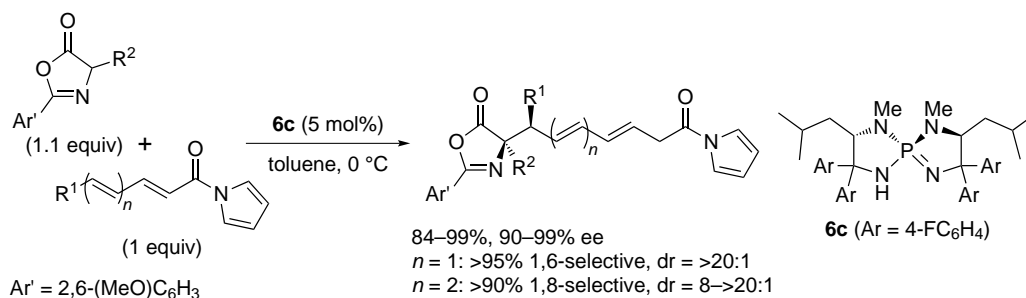
Scheme 1.10 *Z*- and enantioselective Michael addition of azlactones to cyanoacetylene [13g]
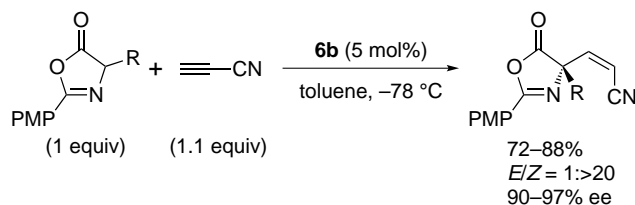
1.3.4.3   Regio-, Diastereo-, and Enantioselective 1,6- and 1,8-Additions of Azlactones to Di- and Trienyl *N*- Acylpyrroles

Regio-, diastereo-, and enantiocontrolled conjugate additions have been achieved using L-leucine-derived iminophosphorane **6c** as the catalyst. It catalyzes unprecedented 1,6- and 1,8-addition of azlactones to di- and trienyl *N*-acylpyrroles (Scheme 1.11). [13h]

Scheme 1.11 Regio-, diastereo-, and enantioselective 1,6- and 1,8-additions of azlactones to di- and trienyl *N*-acylpyrroles [13h]

84–99%, 90–99% ee
n = 1: >95% 1,6-selective, dr = >20:1
n = 2: >90% 1,8-selective, dr = 8–>20:1
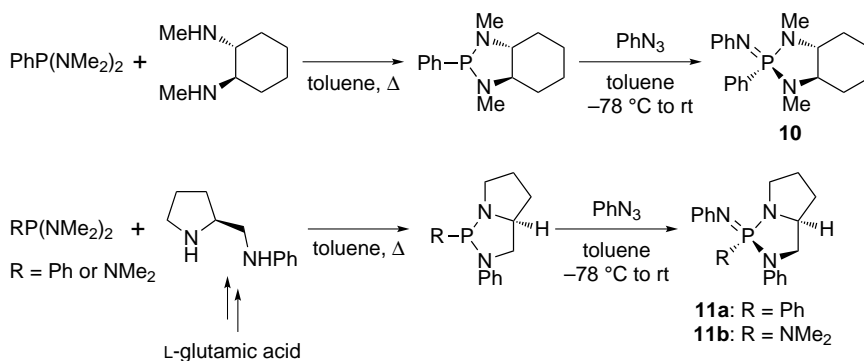
6c (Ar = 4-FC₆H₄)

Ar' = 2,6-(MeO)C₆H₃

1.4 Miscellaneous Examples of Chiral Phosphazene Bases and Their Application to Catalytic Asymmetric Transformations
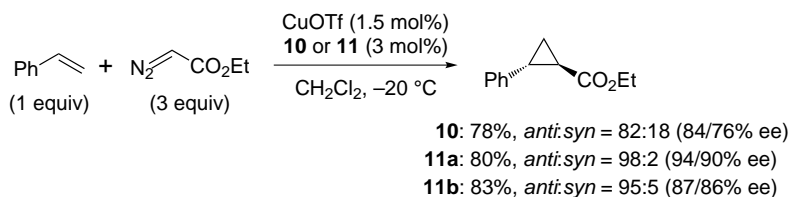
Examples of syntheses of chiral phosphazenes other than ours are described in this section, some of which were applied to catalytic asymmetric reactions.

Buono and coworkers reported the preparation of chiral iminophosphoranes from (*R*,*R*)-*N*,*N'*-dimethyl-cyclohexane-1,2-diamine or L-glutamic acid (Scheme 1.12). Iminophosphoranes **10** and **11** were utilized as chiral ligands of copper(I) to mediate asymmetric cyclopropanation of olefins (Scheme 1.13). [14]

**Scheme 1.12** Preparation of chiral iminophosphoranes **10** and **11** [14]

Scheme 1.13 Asymmetric cyclopropanation of olefins by ethyl diazoacetate [14]

10: 78%, *anti*:*syn* = 82:18 (84/76% ee)
11a: 80%, *anti*:*syn* = 98:2 (94/90% ee)
11b: 83%, *anti*:*syn* = 95:5 (87/86% ee)

Anders and coworkers prepared chiral P1 phosphazenes **12** from commercially available 5-oxo-L-proline and characterized them as their hydrogen tetrafluoroborate salts (Scheme 1.14). [15]

They argued that the newly synthesized **12a** may be approximately nine pK_a units more basic than $^tBuP1(pyrr)$, that is it should have $^{MeCN}pK_{BH+}$ value of 35–37 based on the DFT calculation of the free energy change of the acid–base reaction between liberated **12a** and $^tBuP1(pyrr)\cdot H$ in gas phase.

Scheme 1.14 Preparation of chiral triaminoiminophosphoranes **12** [15]

**Scheme 1.15** Preparation of chiral bisphosphazide **13** [16]
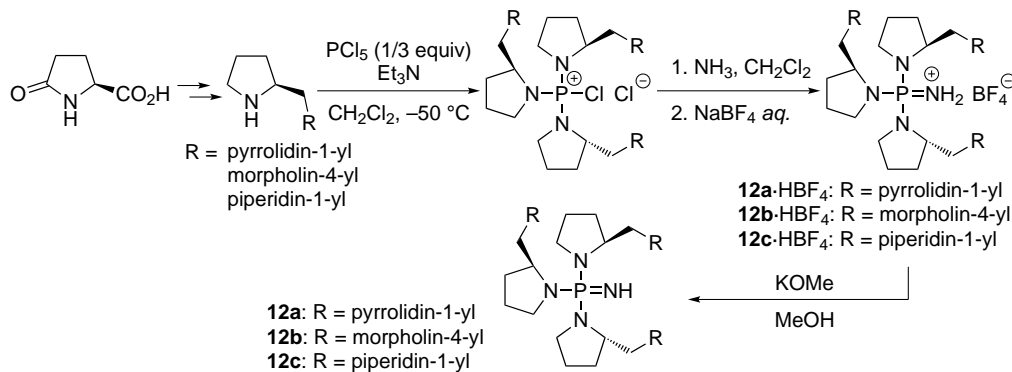
Kondo, Naka and coworkers synthesized chiral bisphosphazide **13** in three steps from commercially available (*R,R*)-hydrobenzoin (Scheme 1.15) and demonstrated the catalytic activity of its lithium complex in enantioselective Michael addition of dialkyl malonates to chalcone derivatives (Scheme 1.16). [16] The dual functionality of **13** as Brœnsted (for malonate) and Lewis base (for lithium) and cooperation of **13** with lithium ion in the catalytic cycle were proposed.

**Scheme 1.15** Preparation of chiral bisphosphazide **13** [16]
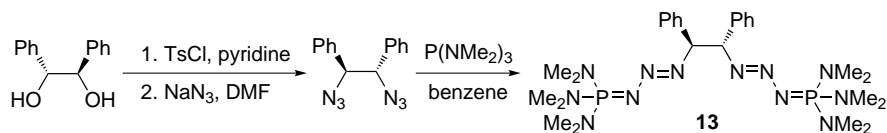
Scheme 1.16 Enantioselective Michael addition of dialkyl malonates to chalcone derivatives [15]
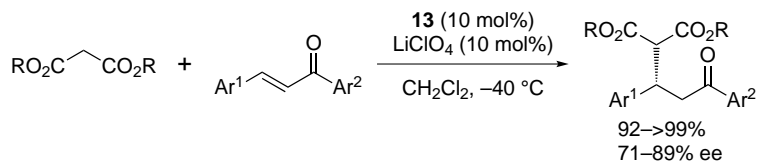
Terada and Takeda have recently developed a chiral bis(guanidino)iminophosphorane **14** and exploited its strong basicity and potential stereocontrolling ability via hydrogen bonding for the asymmetric amination of ketones (Scheme 1.17). [17]

Scheme 1.17 Asymmetric amination of ketones [15]

(5 equiv)   (1 equiv)

X = –(CH$_2$)$_n$– (n = 1–3)
–OCH$_2$–, –SCH$_2$–

7–>99%
10–98% ee

(M)-**14**
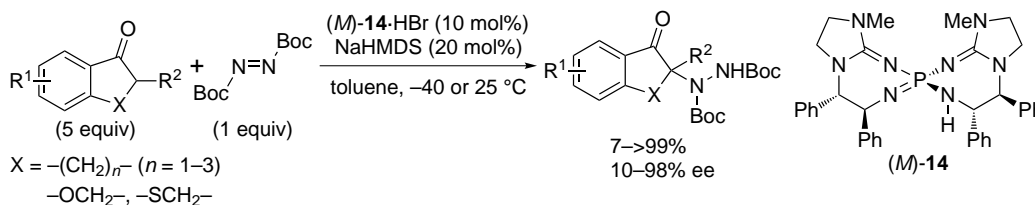
The same group has also reported the preparation of chiral spirocyclic P3 phosphazenes **15** as their hydrogen halide salts utilizing the optical resolution of their racemic forms by preparative chiral HPLC, though their liberation to free base and application to organic transformation was not mentioned (Figure 1.10). [18]
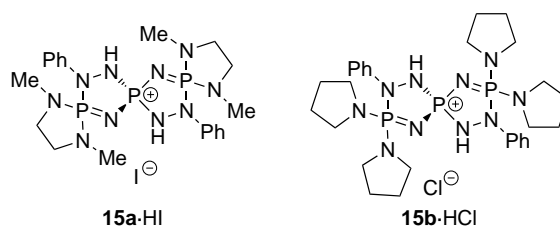

15a·HI   **15b**·HCl

Figure 1.10 Chiral spirocyclic P3 phosphazenes **15** in their hydrogen halide salt forms

1.5 Hydrogen Peroxide in Catalytic Asymmetric Reactions

As described in sections 1.3.2 and 1.3.3, during the course of the development of catalytic asymmetric transformations using iminophosphoranes of type **5** and **6**, the formation of tetraaminophosphonium alkoxide was observed especially when the acidity of the corresponding alcohol is relatively high. Based on this observation, the author hypothesized that these iminophosphoranes could also activate hydrogen peroxide as phosphonium hydroperoxide, even thoug it is a fairly weak acid (pK_a = 11.64 (water) [19]). Exploitation of this reactive species would lead to the development of catalytic asymmetric oxidation with hydrogen peroxide, further broadening the scope of our research (Figure 1.11).

5 or **6**   hydrogen peroxide   tetraaminophosphonium hydroperoxide   catalytic asymmetric oxidation
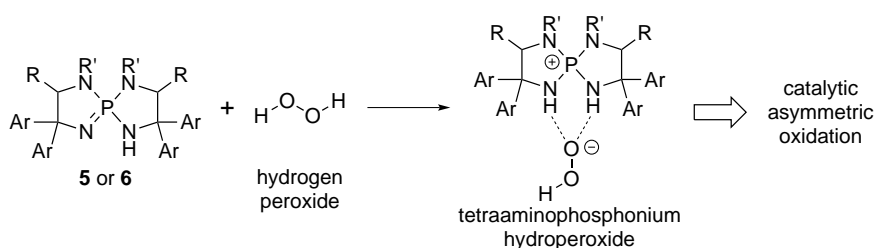
Figure 1.11 Postulated formation of phosphonium hydroperoxide species

In the context of activating hydrogen peroxide whose sole oxidizing ability is usually insuffi-

cient for general use in organic synthesis, organocatalytic asymmetric oxidations using hydrogen peroxide [20,21] are overviewed in the following sections, especially focusing on the activation mode.

1.5.1 Activation of Hydrogen Peroxide as Hydroperoxide Ion under Basic Condition

One of the most common method for epoxidizing electron-deficient olefins is treating the substrate with alkaline hydrogen peroxide, namely Weitz–Scheffer reaction. [22] Under this condition, hydrogen peroxide is deprotonated by an inorganic base and "activated" as hydroperoxide ion with enhanced nucleophilicity (Figure 1.12). Conjugated addition of the hydroperoxide anion at the β-position of an electron-deficient olefin affords β-peroxyenolate intermediate. Subsequent intramolecular S_{N2} substitution at the oxygen atom gives rise to cleavage of the O–O bond and affords an epoxide. Asymmetric Weitz–Scheffer reactions have been most commonly achieved by using chiral catalysts under biphasic (or triphasic) conditions (1.5.1.1 and 1.5.1.2). [23]
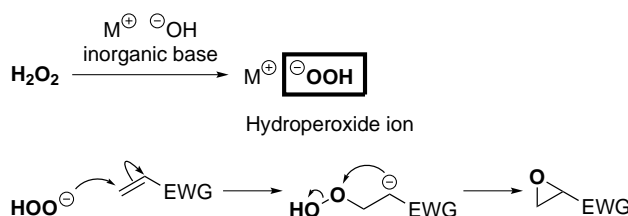

Figure 1.12 Activation of hydrogen perxode as hydroperoxide and Weitz–Scheffer reaction

1.5.1.1 Asymmetric Epoxidation with Phase-Transfer Catalysts (PTCs)

Phase-transfer catalysis is considered to be one of the most powerful tools in organic synthesis for preparing chiral compounds. [24] The application of phase-transfer catalysis to Weitz–Scheffer epoxidation was pioneered by Wynberg *et al.* [25] Under the catalysis of quaternary ammonium salt **16** derived from quinine, chalcone derivatives were converted to the corresponding epoxy ketones with moderate enantiomeric excesses (Scheme 1.18). [25b] After their achievement, Shioiri and Arai, Gao and Jew and Park reported improved protocols for asymmetric Weitz–Scheffer epoxidation using cinchona alkaloid-derived quaternary ammonium salts as PTCs. [26]

Scheme 1.18   Asymmetric Weitz–Scheffer epoxidation using cinchona alkaloid-derived catalysts [25b]
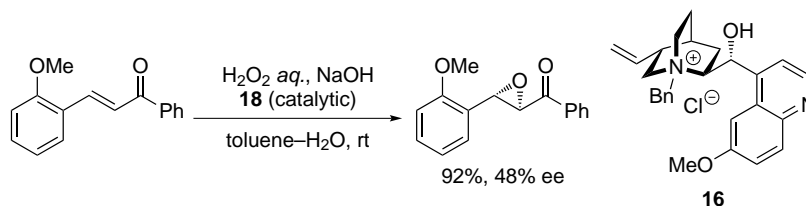
1.5.1.2 Juliá–Colonna Epoxidation

Juliá–Colonna-type epoxidation is defined as a poly-amino acid-catalyzed epoxidation of electron-deficient olefins with hydrogen peroxide.[27] Since the first report by Juliá in 1980 describing the asymmetric epoxidation using insoluble poly-L-alanine as a catalyst under triphasic condition (Scheme 1.19, top),[28] many variants including homogeneous version using polymer catalysts that are soluble in organic solvent have been developed (Scheme 1.19, bottom).[29] It is suggested that the catalytic activity is originated from the binding of β-hydroperoxy enolate to the three amidic N–H protons of the poly-amino acid catalyst in an α-helix form, which provides the appropriate chiral environment around the β-carbon atom of the substrate.[30]

Scheme 1.19 Examples of Juliá–Colonna-type epoxidation: the originally reported triphasic condition (top)[27] and homogeneous condition (bottom)[29]
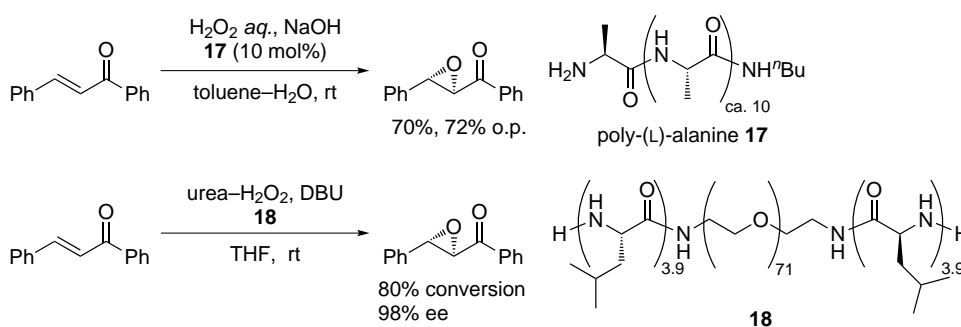
1.5.1.3 Organic Base-Catalyzed Epoxidation of Electron-Deficient Olefins

Strong organic base such as guanidine can catalyze the epoxidation of electron-deficient olefins by hydrogen peroxide. This type of reactions in a homogeneous media could be included in the broad sense of Weitz–Scheffer reaction. Terada and coworkers reported the asymmetric oxidation of chalcone derivatives catalyzed by BINOL-derived chiral guanidine **19** yielding the corresponding epoxides with moderate enantiomeric excesses (Scheme 1.20).[31]

Scheme 1.20 Chiral guanidine-catalyzed epoxidation of enones[31]
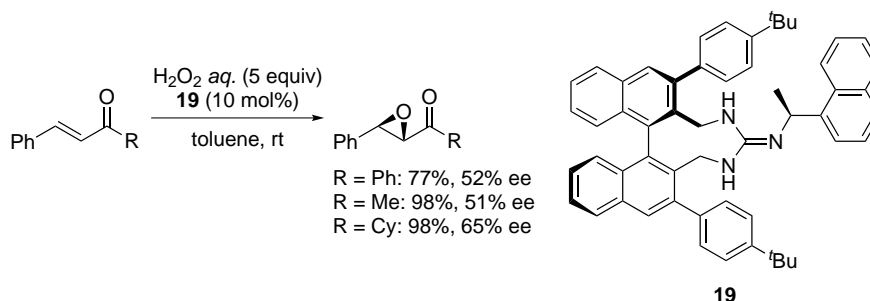
Nagasawa and coworkers demonstrated the effectiveness of their guanidine-urea bifunctional catalyst **19** for asymmetric Weitz–Scheffer-type epoxidation (Scheme 1.21).[32] The interaction of

urea groups with the substrate was proposed as the key feature in addition to the activation of hydrogen peroxide by the guanidine moiety (Figure 1.13).

Scheme 1.21 Chiral guanidine-urea **20** catalyzed epoxidation of chalcones [32]
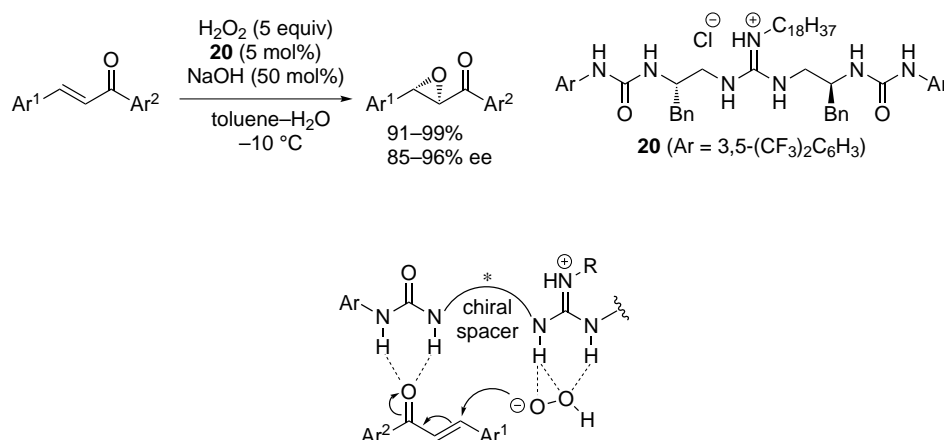

Figure 1.13 Cooperative interactions of guanidine-urea catalyst **20** with enone and hydrogen peroxide [32]

1.5.2 Direct Electrophilic Activation of Hydrogen Peroxide through Non-covalent Interaction

List and coworkers have recently disclosed the applicability of the electrophilic activation of hydrogen peroxide for catalytic asymmetric oxidation. They hypothesized that chiral Brønsted acid could electrophilically activate hydrogen peroxide by noncovalent interaction to promote the attack by the nucleophilic substrates, resulting in enantioselective oxygen-transfer (Figure 1.14).
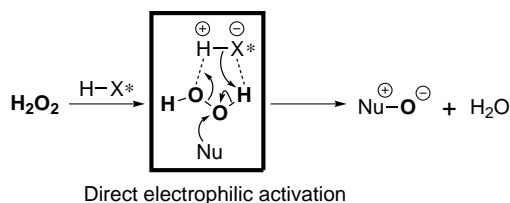

Direct electrophilic activation

Figure 1.14 Direct electrophilic activation of hydrogen peroxide by chiral Brønsted acid

This scenario was realized in the enantioselective oxidation of sulfides using bisphosphoryl imide (**21**) as the catalyst. Brœnsted acid **21** efficiently catalyzes the reaction to afford sulfoxides in good yields and good enanitoselectivities (Scheme 1.22). [33]

Scheme 1.22 Chiral bisphosphoryl imide **21** catalyzed enantioselective sulfoxidation [33]
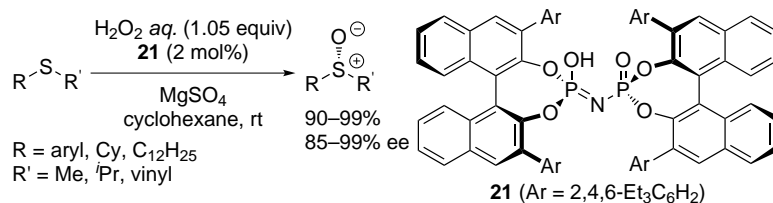
1.5.3   *In Situ* Conversion of Hydrogen Peroxide to More Reactive Species

Another potent method for activating hydrogen peroxide is to catalytically generate reactive oxidative species from hydrogen peroxide in reaction systems. Chiral ketones, carboxylic acids, iminium salts, and flavins have been employed as the activators; they react with hydrogen peroxide (making new covalent bonds) to form active oxidants in the reaction systems.

1.5.3.1   *In Situ* Generation of Chiral Dioxirane

During the course of the development of chiral ketone-catalyzed epoxidations, [34,35] Shi and coworkers discovered that hydrogen peroxide can work as the terminal oxidant in this reaction system. [36] By using (D)-fructose-derived ketone **22** as the catalyst, various olefins including unfuctionalized ones undergo oxidation to yield the corresponding epoxides with good to excellent enantioselectivities (Scheme 1.23). [36b] In this reaction, hydrogen peroxide is finally activated as the form of dioxirane, the same active species in the conventional procedure wherein Oxone is used as the terminal oxidant. They proposed the involvement of peroxyimidic acid intermediate (see section 1.6) in the conversion of hydrogen peroxide to the dioxirane (Figure 1.15).

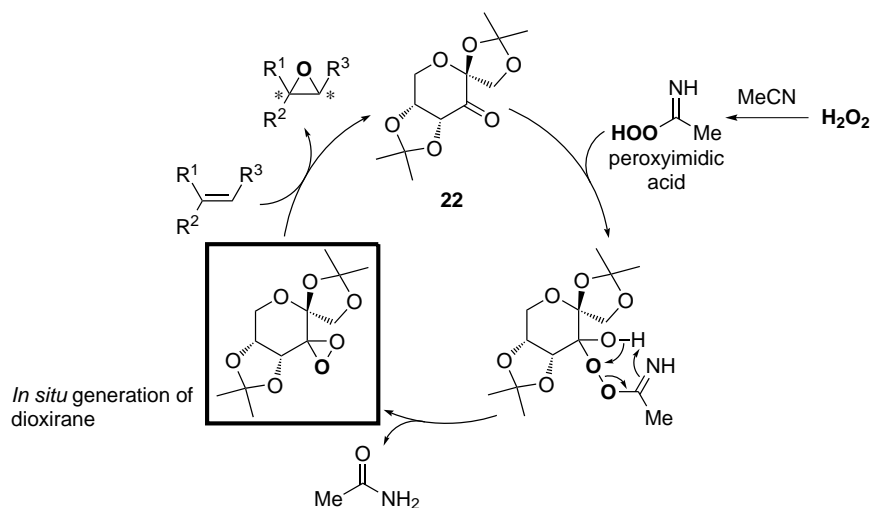**Scheme 1.23** Chiral ketone **22** catalyzed epoxidation of olefins [36b]
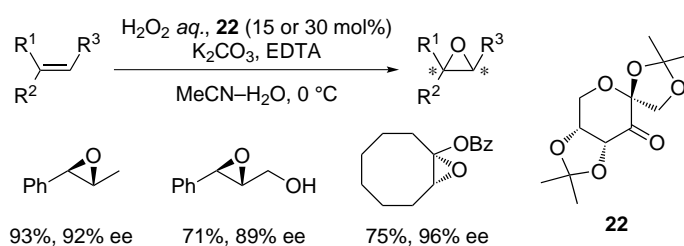
Figure 1.15 Proposed catalytic cycle of **22** catalyzed epoxidation of olefins: *in situ* generation of dioxirane [36b]

1.5.3.2 *In Situ* Generation of Chiral Peroxy Acid

Miller and coworkers achieved enantioselective epoxidation of non-electron-deficient olefins with hydrogen peroxide using peptide catalyst **23** (Scheme 1.24) [37]. The key feature of this reaction system is the generation of chiral peroxy acid from **23** and hydrogen peroxide. The carboxylic acid moiety in the aspartatic acid residue of **23** is first activated by diisopropylcarbodiimide (DIC) followed by the condensation with hydrogen peroxide with the aid of DMAP co-catalyst to form chiral the peroxy acid which is considered to be the active species (Figure 1.16). The system was found to be uniquely effective for the carbamate-protected allylic alcohols and the carbamate function in the substrate may interact with **23** via hydrogen bonding, which is assumed to be important for attaining high enantioselsectivity.

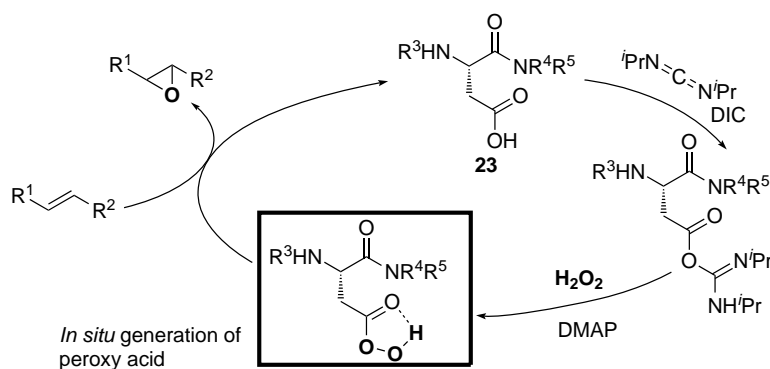**Scheme 1.24** Peptide **23** catalyzed asymmetric epoxidation of olefins [37]
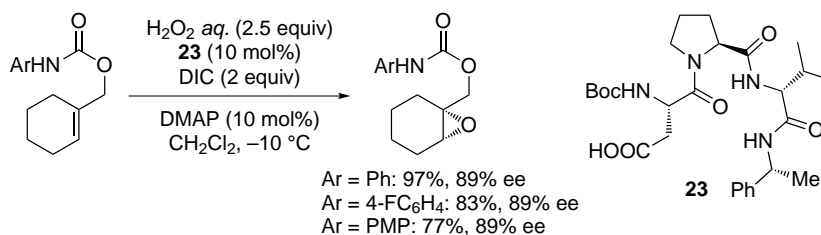
Figure 1.16 Catalytic cycle of **23** catalyzed epoxidation: *in situ* generation of peroxy acid [37]

The concept of *in situ* generation of the chiral peroxy acid was also applied to the oxidation of indole derivatives [38] and Baeyer–Villiger oxidation. [39]

1.5.3.3 *In Situ* Generation of Chiral Oxaziridinium Salt

Since the work by Lusinchi *et al.*, [40] asymmetric epoxidation of non-electron-deficient alkenes have been conducted by using various chiral iminium salt catalysts combined with appropriate stoichiometric oxidants. [35,41] In these oxidation systems, Oxone have been usually chosen as the oxidant for iminium salts to generate active species, oxaziridinium salts. Page and coworkers have reported that hydrogen peroxide can be used as the terminal oxidant for this purpose. They disclosed the epoxidation of 1-phenylcyclohexene using chiral iminium salt **24** as the catalyst yielding the corresponding epoxide with moderate enantiomeric excess (Scheme 1.25). [42] They suggested two possible pathways in which percarbonate participates or not (Figure 1.17).

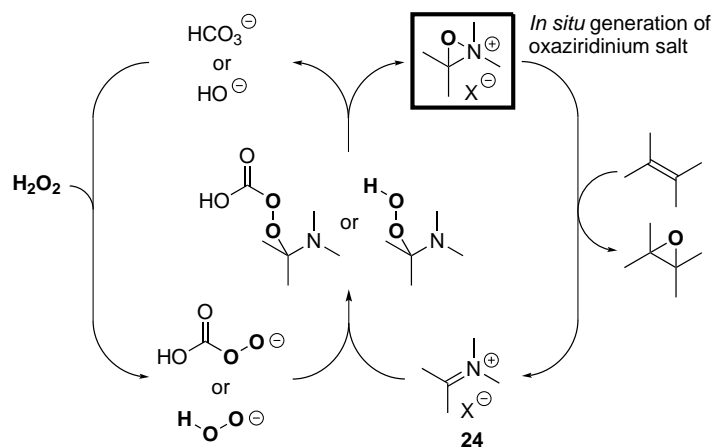**Scheme 1.25** Iminium salt **24** catalyzed asymmetric epoxidation [42]
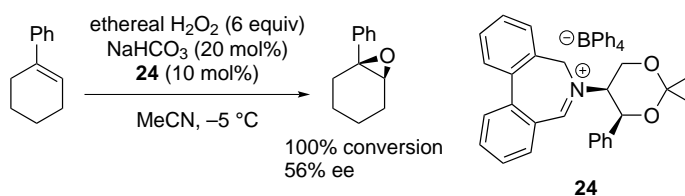
Figure 1.17 Proposed catalytic cycles of **24** catalyzed epoxidation: *in situ* generation of oxaziridinium salt [42]

1.5.3.4   Flavin-Catalyzed Oxidation

Flavin-containing monooxygenases (FMOs) together with cytochrome P450 oxidatively metabolize xenobiotic substances in mammalian hepatic tissue. [43] The enzymatic oxygenation involves the activation of molecular oxygen by enzyme-bound reduced flavin to afford 4a-hydroperoxyflavin, which transfers the oxygen atom to heteroatoms such as nitrogen and sulfur. [44] The model study of mimicking the function of FMOs was carried out by Bruice *et al.* They synthesized 4a-hydroperoxyflavin by treating 5-ethyl-3,7,8,10-tetramethylisoalloxazinium perchlorate (**25**) with hydrogen peroxide, and disclosed their high oxidizing ability toward amines and sulfides. [45] Murahashi and coworkers demonstrated that this oxidation can be performed catalytically in flavin. [46] The catalytic cycle is shown in Figure 1.18. In this cycle, hydrogen peroxide reacts with **25** to give active oxidative species, 4a-hydroperoxyflavin. After the oxidation of the substrate, the resultant 4-hydroxyflavin undergoes dehydration to regenerate **25**. Inspired by these reports, efforts have been made for the design of chiral organic molecules based on flavin or related structures and the development of catalytic asymmetric oxidation with them. [47]
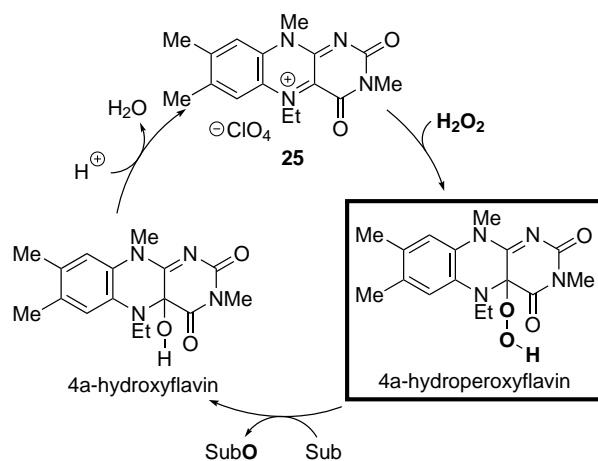
Figure 1.18 Catalytic cycle of the oxidation using flavin catalyst and hydrogen peroxide

Shinkai and coworkers reported enantioselective oxidation of sulfides with planar-chiral flavinophane **26** giving aryl methyl sulfoxides with modest enantioselectivities (Scheme 1.26). [48]

Scheme 1.26 Chiral flavinophane **26** catalyzed enantioselective sulfoxidation [48]
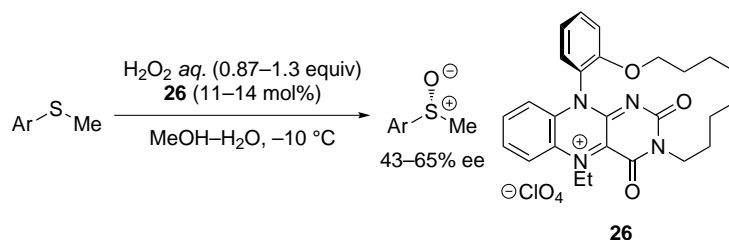
Murahashi and coworkers reported the first organocatalytic Baeyer–Villiger oxidation using bisflavinium perchlorate **27** as the catalyst. 3-Arylcyclobutanones were converted to the corresponding γ-lactams with moderate enantioselectivities (Scheme 1.27). [49] They proposed that hydrogen peroxide first reacts with **27** to form hydroperoxyflavin intermediate, which subsequently undergoes nucleophilic addition to the carbonyl group to form a Criegee intermediate. The asymmetric induction was ascribed to the π-π interaction between the aromatic ring of the catalyst **27** and the 3-aryl group of the substrate, which directs the approach of the ketone to the hydroperoxyflavin intermediate.

Scheme 1.27 Bisflavin perchlorate **27** catalyzed asymmetric Baeyer–Villiger oxidation [49]
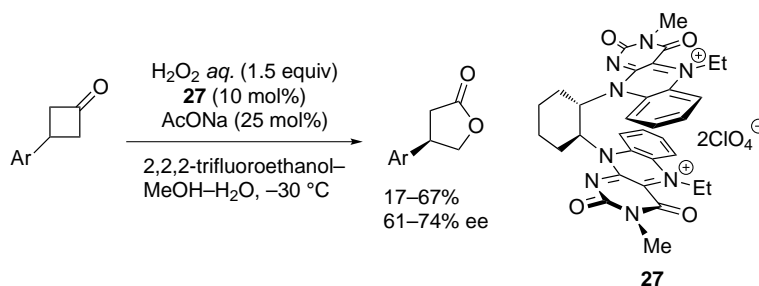
1.5.4   Substrate Activation in Oxidations Using Hydrogen Peroxide

Besides the activation of hydrogen peroxide described above, activation of substrate is another
effective strategy for the organocatalytic oxidation using hydrogen peroxide.

1.5.4.1   Epoxidation of α,β-Unsaturated Carbonyls by Iminium Activation

Asymmetric epoxidation of α,β-unsaturated aldehydes has been a challenging transformation. This
long-standing issue was solved by exploiting iminium activation of the formyl moiety by amine
catalysts. In these cases, the activation of substrate (aldehyde to iminium) is the important factor
for promoting the reaction rather than the activation of hydrogen peroxide (Figure 1.19).
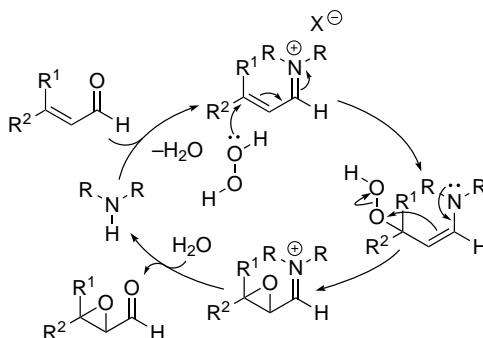
Figure 1.19 Epoxidation of α,β-unsaturated aldehydes by the iminium activation of the substrate

Jœrgensen and coworkers reported the first organocatalytic asymmetric epoxidation of α,β-
unsaturated aldehydes using hydrogen peroxide as oxidant. *O*-TMS diarylprolinol **28** was selected
as the catalyst, and epoxyaldehydes were obtained in moderate to good yields with good stereose-
lectivities (Scheme 1.28).[50]

Scheme 1.28 *O*-TMS diarylprolinol **28** catalyzed asymmetric epoxidation of α,β-unsaturated
aldehydes[50]
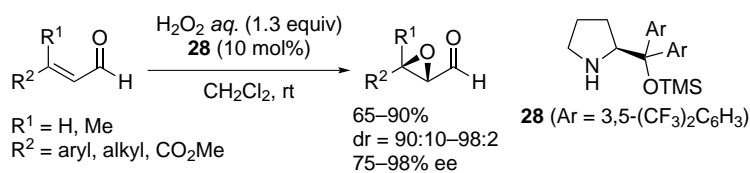
In 2008, List and coworkers developed a catalytic asymmetric epoxidation of cyclic enones
using chiral primary diamine–acid salts **29** or **30** as catalysts (Scheme 1.29).[51] They suggested
the formation of iminium ion **A**, in which the second basic amine moiety may direct the attack of
hydrogen peroxide toward one enantioface of the double bond.

Scheme 1.29 Chiral diamine–acid salts **28** and **29** catalyzed asymmetric epoxidation of cyclic enones [51]
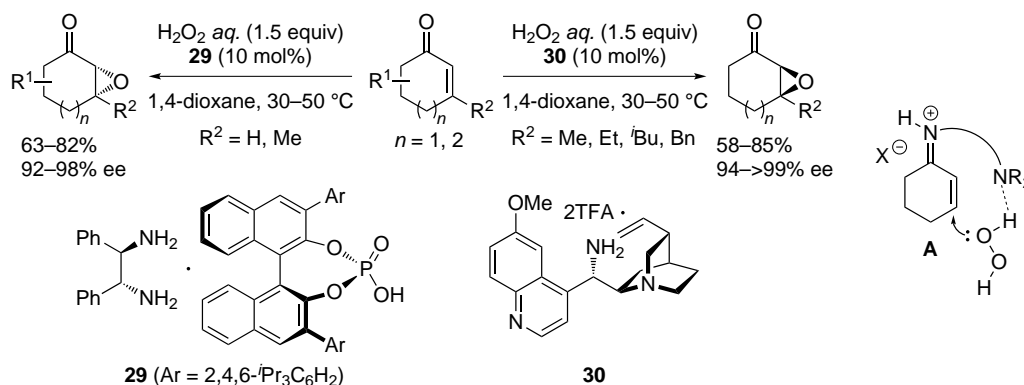
1.5.4.2 Chiral Brœnsted Acid Catalyzed Asymmetric Baeyer–Villiger Oxidation

Ding and coworkers reported asymmetric Baeyer–Villiger oxidation using chiral phosphoric acid **31** as the catalyst. 3-Arylcyclobutanones were oxidized to the corresponding γ-lactams in excellent yields with moderate to good enantioselectivities (Scheme 1.30). [52] The kinetic and theoretical study revealed that the reaction proceeds via a two-step concerted mechanism in which the catalyst **31** functions as a bifunctional catalyst to activate the reactants or the Criegee intermediate in a synergistic manner (Figure 1.20).

Scheme 1.30 Chiral phosphoric acid **31** catalyzed asymmetric Baeyer–Villiger oxidation [52]
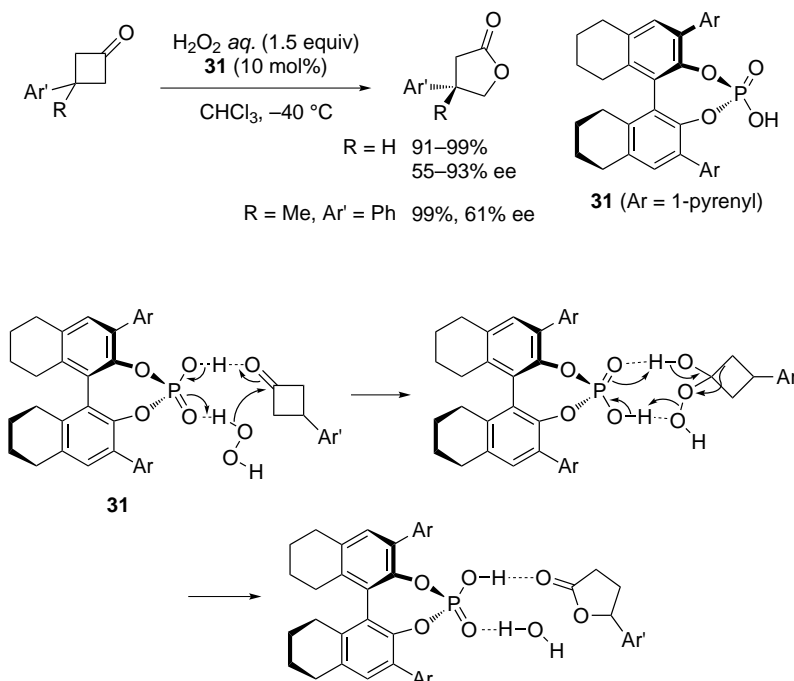
Figure 1.20 The mechanism of **31** catalyzed Baeyer–Villiger oxidation [52]

1.6 Payne Oxidation

As argued in section 1.5.3, *in situ* conversion of hydrogen peroxide to more reactive species with the aid of catalytic amount of chiral molecule is a powerful strategy from the viewpoint of the activation of hydrogen peroxide and the stereocontrol of the oxidations. Based on this concept, the author focused attention on Payne oxidation where formation of a peroxy acid-like species from hydrogen peroxide is considered to be critical. In 1961, Payne and coworkers discovered that the epoxidation of electronically neutral olefins proceeds in the presence of hydrogen peroxide and organic nitriles such as acetonitrile, benzonitrile, and trichloroacetonitrile (Scheme 1.31).[53] Slow addition of hydrogen peroxide along with simultaneous slow addition of excess alkali to maintain the optimum pH (7.5–8) was needed for efficient conversion of the starting olefin.

Scheme 1.31 Payne oxidation: epoxidation of electron-non-deficient olefins [53]
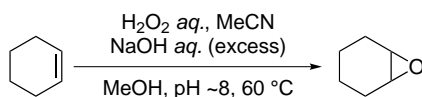
The active species of the Payne oxidation is believed to be peroxyimidic acid which is *in situ* generated from hydrogen peroxide and a nitrile by the action of base; it has an isoelectronic structure of peroxy acid and seems to have the similar reactivity (Figure 1.21).
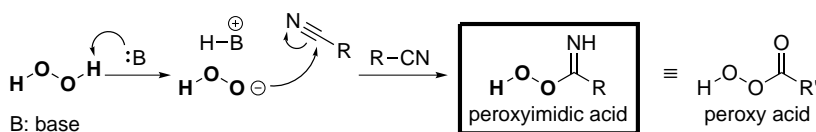
Figure 1.21 Formation of peroxyimidic acid from hydrogen peroxide and nitrile

The applications of the Payne condition to the oxidation of heteroatoms are also known (Scheme 1.32).[54]

Scheme 1.32 Applications of the Payne conditions: oxidation of sulfides (top)[54b] and oxidation of 4-*N*-dialkylaminopyridines (bottom)[54c]

The applications of Payne oxidation to asymmetric synthesis were reported by Ben Hassine *et*

al. They employed stoichiometric amount of a chiral helicene-derived nitrile **32** in the enantiose-lective epoxidation of olefins. (Scheme 1.33, top). [55] They also achieved stereoselective oxidation of imines by using amino acid-derived nitrile **33** (Scheme 1.33, middle and bottom).
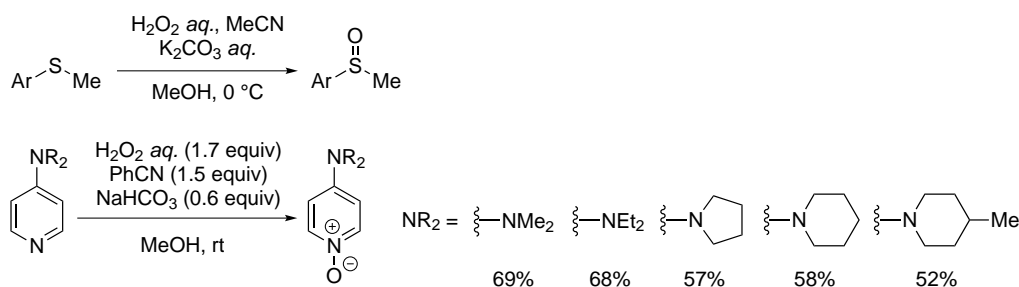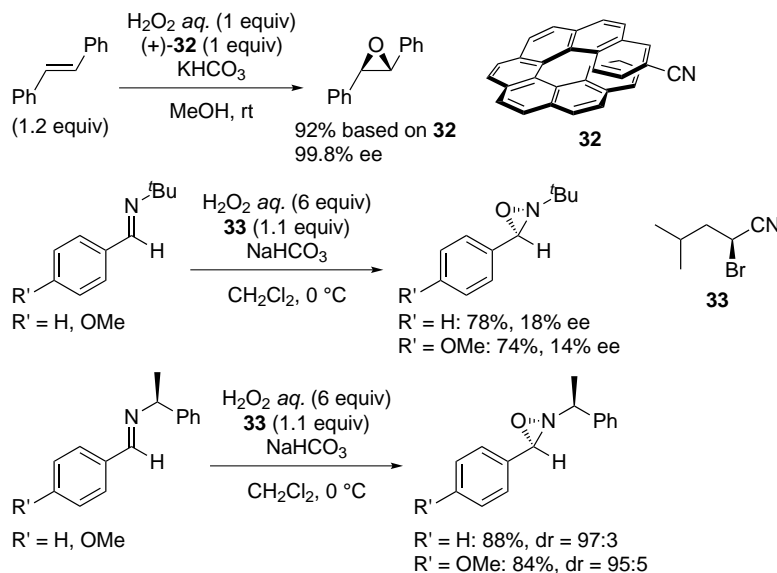
Scheme 1.33 Enantioselective Payne oxidations: asymmetric epoxidation of olefins using chiral helicenecarbonitrile **32** (top) [55a,b] and asymmetric oxidation of imines by using amino acid-derived chiral nitrile **33** (middle and bottom) [55c]

Despite the potential utility of Payne oxidation which realizes synthetically meaningful trans-formations by the combination of relatively inexpensive reagents, the examples of practical use in organic synthesis has been extremely limited compared with the standard protocols using peroxy acids such as *m*CPBA. Moreover, the attempt for the development of catalytic enantioselective ones has never been reported.

1.7   Development of Catalytic Payne-Type Oxidations under the Catalysis of Triaminoiminophosophorane

The author hypothesized that a catalytic Payne oxidation can be achieved by utilizing the high basicity of triaminoiminophosphorane of type **5** or **6** and prominent anion recognition ability of their conjugate acid **5**·H or **6**·H. In analogy with the conventional Payne oxidation mechanism using a stoichiometric amount of inorganic base (Figure 1.21), phosphonium hydroperoxide generated by the deprotonation of hydrogen peroxide by **5** or **6** would react with a nitrile to afford chiral phosphonium peroxyimidate, which could give rise to asymmetric oxidation that cannot be realized just by hydrogen peroxide and base catalyst (Figure 1.22). In contrast to Miller's system (see 1.5.3.2) wherein the repetitive generation of chiral peroxy acid is the core feature, this is the first attempt for controlling achiral peroxy acid or its equivalent by a chiral catalyst and its application to catalytic asymmetric oxidation.
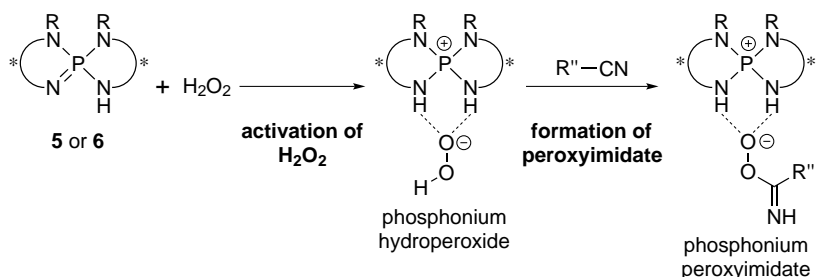
Figure 1.22 Postulated generation of chiral phosphonium peroxyimidate

The author's research according to this concept is briefly summarized in the following sections.

1.7.1 Catalytic Asymmetric Oxidation of *N*-Sulfonyl Imines with Hydrogen Peroxide–Trichloroacetonitrile System (Chapter 2)

N-Sulfonyl imine was chosen as the model substrate for the above described catalytic asymmetric Payne–type oxidation. The author assumed that the chiral phosphoium peroxyimidate would enantioselectively add to the imine to give the key intermediate **B** (Figure 1.23). The intermediate **B** would subsequently undergo rapid ring-closure driven by the high leaving ability of the amidate ion to afford chiral *N*-sulfonyl oxaziridine. The amidate ion coproduced in this cyclization would be basic enough to abstract the the N–H proton of the counter ion **5·H** or **6·H** to regenerate the catalyst **5** or **6**.
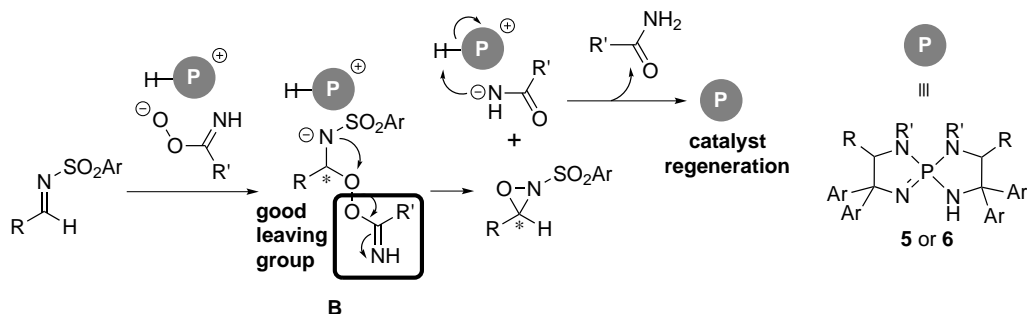
Figure 1.23 Postulated reaction course of the asymmetric oxidation of *N*-sulfonyl imines under the catalytic Payne-type oxidation condition

The proof of the above hypothesis was initiated by the oxidation of *N*-Ts 4-nitrobenzaldimine (**34a**) with hydrogen peroxide by using **6a** as the catalyst. Under the condition shown in Scheme 1.34, the corresponding *N*-Ts oxaziridine **35a** smoothly formed with moderate enantioselectivity by using trichloroacetonitrile as an additive. The shutdown of the reaction without trichloroacetonitrile suggested the operation of the proposed Payne-type mechanism.

Scheme 1.34 Initial attempt for the catalytic enantioselective oxidation of *N*-sulfonyl imines
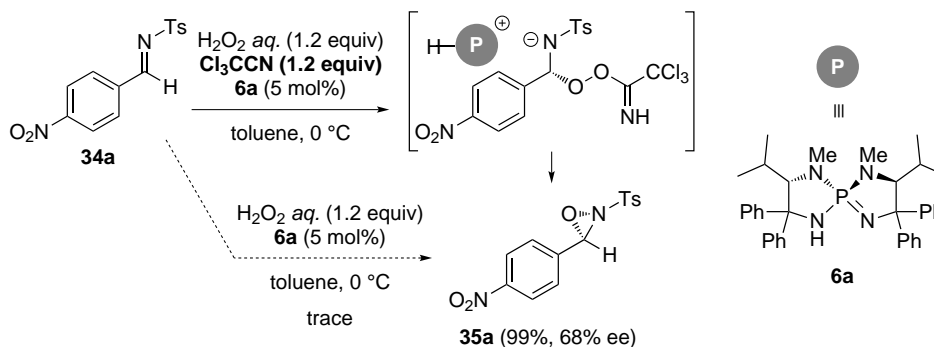
By optimization of the reaction condition and the catalyst structure, the reaction proceeds with a variety of aromatic and aliphatic imines as the substrates and gives the corresponding oxaziridines in good yields with excellent enantioselectivities (Scheme 1.35). The synthetic value of the present procedure was demonstrated in the derivatization utilizing the oxygen and nitrogen atom-transferring ability of the products (Scheme 1.36).

Scheme 1.35 Iminophosphorane **6d** catalyzed enantioselective oxidation of *N*-sulfonyl imines
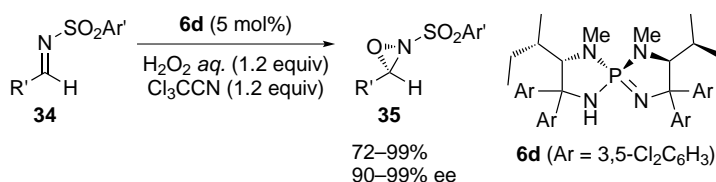
Scheme 1.36 Derivatization of the chiral *N*-sulfonyl oxaziridines
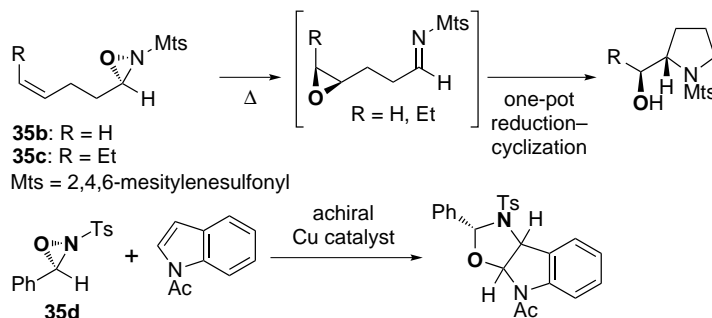
1.7.2   Mechanistic Study on the Oxidation of *N*-Sulfonyl Imines with Hydrogen Peroxide–Trichloroacetonitrile System (Chapter 3)

The mechanism of the *N*-sulfonyl imine oxidation using hydrogen peroxide and trichloroacetonitrile was revealed through a series of competetive reactions.

Aside from the initially postulated Payne-type oxidation mechanism (Figure 1.24, path *a*), another possibility of the reaction pathway could be considered wherein hydrogen peroxide initially

added to imine **34** to give a peroxyhemiaminal intermediate **C**, followed by the reaction of **C** with trichloroacetonitrile to generate the key intermediate **B** (path *b*).

The predominant pathway was determined by comparing the reactivity of imine **33** and the peroxyhemiaminal **C·H** under the influence of **6** and trichloroacetonitrile.

First, a solution of peroxyhemiaminal derived from *N*-Mts isovaleraldimine (**34b**) was prepared by the treatment of **34b** (1 equiv) with ethereal hydrogen peroxide [56] (2 equiv) in the presence of chiral iminophosphorane **6d** (5 molin CDCl$_3$. To the solution was added a solution of **N**-Mts hydrocinnamaldimine (**34c**, Mts = 2,4,6-mesitylenesulfonyl) (1 equiv) and trichloroacetonitrile (10 equiv) in CDCl$_3$. The ^{1}H NMR analysis of the reaction mixture showed almost exclusive formation of 3-phenethyl-2-Mts-1,2-oxaziridine (**35f**) (Figure 1.25, top), which indicated the predominant contribution of path *a*. A similar product distribution was also observed in the experiment conducted by exchanging the roles of **34b** and **34c** (Figure 1.25, bottom). These observations strongly suggested that hydroperoxide ion rather than the peroxyhemiaminal ion preferentially attacked to trichloroacetonitrile with the aid of **6d** to form the oxaziridines derived from the imines added afterward under the conditions. As a consequence, the author concluded that the present oxaziridination proceeds via path *a*, the initially proposed catalytic Payne-type oxidation mechanism.
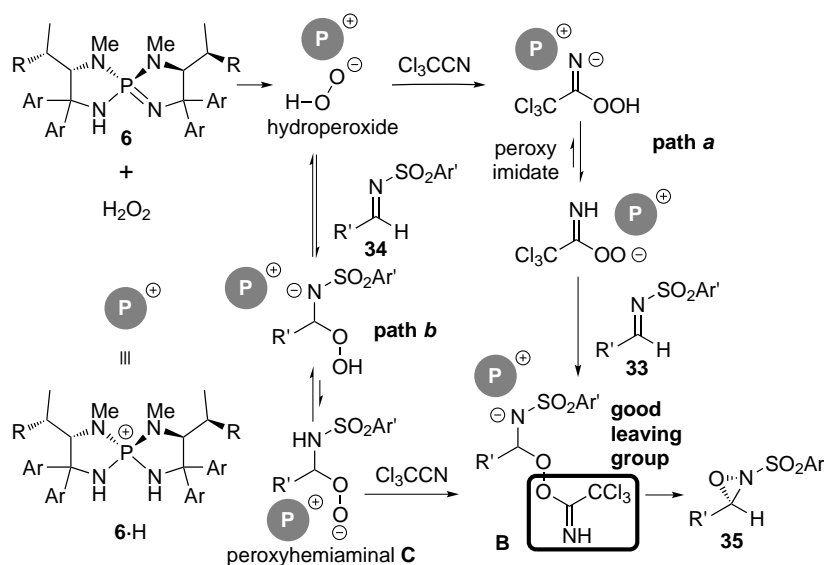
Figure 1.24 Two possible reaction courses of the oxaziridination
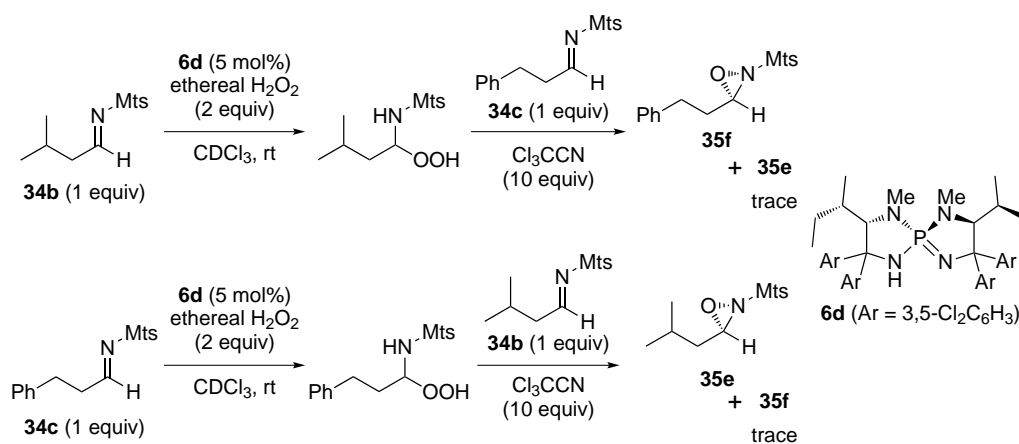
Figure 1.25 Cross-over experiment for determination of the reaction pathway

1.8 Conclusion

In this doctoral course study, the first catalytic enantioselective Payne-type oxidation has been
achieved by using chiral triaminoiminophosphorane catalyst, which demonstrates the fact that it
is possible to generate chiral peroxyimidate from hydrogen peroxide and nitrile and control the
stereochemical outcome of the reaction with the aid of a chiral base catalyst. This novel catalytic
oxidation system was applied to the enantioselective oxidation of *N*-sulfonyl imines, which led
to the development of the practical preparative method of synthetically relevant optically-active
N-sulfonyl oxaziridines of broad substrate scope. The mechanistic aspect of this reaction was also
investigated, and the operation of Payne-type oxidation mechanism was confirmed. The author
hopes that this study would stimulate the development of catalytic (asymmetric) reactions based
on the concept of the catalytic generation of reactive oxidative species from hydrogen peroxide
and its control by the power of chiral catalysts.

References and notes

(1) For reviews on enantioselective catalysis by using chiral guanidine, see: (a) Ishikawa, T.; Isobe, T. *Chem.—Eur. J.* **2002**, *8*, 552–557. (b) Ishikawa, T.; Kumamoto, T. *Synthesis* **2006**, 737–752. (c) Leow, D.; Tan, C.-H. *Chem.—Asian J.* **2009**, *4*, 488–507. (d) Sohtome, Y.; Nagasawa, K. *Synlett* **2010**, 1–22. (e) Terada, M. *J. Synth. Org. Chem., Jpn.* **2010**, *68*, 1185–1194.

(2) (a) Ostendorf, M.; Dijkink, J.; Rutjes, F. P. J. T.; Hiemstra, H. *Eur. J. Org. Chem.* **2000**, 115–124. (b) Kotsuki, H.; Sugino, A.; Sakai, H.; Yasuoka, H. *Heterocycles* **2000**, *53*, 2561–2567.

(3) For reviews on organic base catalysis, see: (a) Palomo, C,; Oiarbide, M.; Ló pez, R. *Chem. Soc. Rev.* **2009**, *38*, 632–653. (b) *Superbases for Organic Synthesis: Guanidines, Amidines, Phosphazenes and Related Organocatalysts*; Ishikawa, T., Ed.; John Wiley & Sons: West Sussex, U. K., 2009.

(4) Selected examples of organic base catalyzed asymmetric transformations: (a) Ogawa, S.; Shibata, N.; Inagaki, J.; Nakamura, S.; Toru, T.; Shiro, M. *Angew. Chem. Int. Ed.* **2007**, *46*, 8666–8669. (b) Terada, M.; Ube, H.; Yaguchi, Y. *J. Am. Chem. Soc.* **2006**, *128*, 1454–1455.

(5) (a) Bandar, J. S.; Lambert, T. H. *J. Am. Chem. Soc.* **2012**, *134*, 5552–5555. (b) Bandar, J. S.; Lambert, T. H. *J. Am. Chem. Soc.* **2013**, *135*, 11799–11802.

(6) (a) Schwesinger, R. *Chimia* **1985**, *39*, 269–272. (b) Schwesinger, R.; Schlemper, H. *Angew. Chem. Int. Ed.* **1987**, *26*, 1167–1169. (c) Schwesinger, R.; Schlemper, H. *Angew. Chem. Int. Ed.* **1993**, *32*, 1361–1363. (d) Schwesinger, R.; Willaredt, J.; Schlemper, H.; Keller, M.; Schmitt, D.; Fritz, H. *Chem. Ber.* **1994**, *127*, 2435–2454. (e) Schwesinger, R.; Schlemper, H.; Hasenfratz, C.; Willaredt, J.; Dambacher, T.; Breuer, T.; Ottaway, C.; Fletschinger, M.; Boele, J.; Fritz, H.; Putzas, D.; Rotter, H. W.; Bordwell, F. G.; Satish, A. V.; Ji, G.-Z.; Peters, K.; von Schnering, H. G. *Liebigs Ann.* **1996**, 1055–1081.

(7) $^{MeCN}pK_{BH^+}$ values of various organic bases were measured by Leito *et al.*: Kaljurand, I.; Kütt, A.; Sooväli, L.; Rodima, T.; Mäemets, V.; Leito, I.; Koppel, I. A. *J. Org. Chem.* **2005**, *70*, 1019–1028.

(8) Xu, W.; Mohan, R.; Morrissey, M. M. *Bioorg. Med. Chem. Lett.* **1998**, *8*, 1089–1092.

(9) Keynes, M. N.; Earle, M. A.; Sudharshan, M.; Hultin, P. G. *Tetrahedron* **1996**, *52*, 8685–8702.

(10) For a review, see: Imahori, T. *J. Pharm. Soc. Jpn.* **2004**, *124*, 509–517.

(11) Imahori, T.; Kondo, Y. *J. Am. Chem. Soc.* **2003**, *125*, 8082–8083.

(12) Uraguchi, D.; Ooi, T. *J. Synth. Org. Chem., Jpn.* **2010**, *68*, 1185–1194.

(13) (a) Uraguchi, D.; Sakaki, S; Ooi, T. *J. Am. Chem. Soc.* **2007**, *129*, 12392–12393. (b) Uraguchi, D.; Ito, T.; Nakamura, S.; Sakaki, S.; Ooi, T. *Chem. Lett.* **2009**, *38*, 1052–1053. (c) Uraguchi, D.; Nakamura, S.; Ooi, T. *Angew. Chem. Int. Ed.* **2010**, *49*, 7562–7565. (d) Corbett, M. T.; Uraguchi, D.; Ooi, T.; Johnson, J. S. *Angew. Chem. Int. Ed.*

2012, *51*, 4685–4689. (e) Uraguchi, D.; Ito, T.; Ooi, T. *J. Am. Chem. Soc.* **2009**, *131*, 3836–3867. (f) Uraguchi, D.; Ito, T.; Nakamura, S.; Ooi, T. *Chem. Sci.* **2010**, *1*, 488–490. (g) Uraguchi, D.; Ueki, Y.; Sugiyama, A.; Ooi, T. *Chem. Sci.* **2013**, *4*, 1308–1311. (h) Uraguchi, D.; Yoshioka, K.; Ueki, Y.; Ooi, T. *J. Am. Chem. Soc.* **2012**, *134*, 19370–19373.

(14) Brunel, J. M.; Legrand, O.; Reymond, S.; Buono, G. *J. Am. Chem. Soc.* **1999**, *121*, 5807–5808.

(15) Köhn, U.; Schulz, M.; Schramm, A.; Günther, W.; Görls, H.; Schenk, S.; Anders, E. *Eur. J. Org. Chem.* **2006**, 4128–4134.

(16) Naka, H.; Kanase, N.; Ueno, M.; Kondo, Y. *Chem. Eur. J.* **2008**, *14*, 5267–5274.

(17) Takeda, T.; Terada, M. *J. Am. Chem. Soc.* **2013**, *135*, 15306–15309.

(18) Terada, M.; Goto, K.; Oishi, M.; Takeda, T.; Kwon, E.; Kondoh, A. *Synlett* **2013**, *24*, 2531–2534.

(19) In *Lange's Handbook of Chemistry 15th Ed.*; Dean, J. A., Ed.; McGraw-Hill: New York, 1998; p 8.20.

(20) For a review, see: Russo, A.; De Fusco, C.; Lattanzi, A. *ChemCatChem* **2012**, *4*, 901–916.

(21) For reviews on metal-catalyzed asymmetric oxidations with hydrogen peroxide, see: (a) Srour, H.; Le Maux, P.; Chevance, S.; Simonneaux, G. *Coord. Chem. Rev.* **2013**, *257*, 3030–3050. (b) De Faveri, G.; Ilyashenko, G.; Watkinson, M. *Chem. Soc. Rev.* **2011**, *40*, 1722–1760. (c) Lane, B. S.; Burgess, K. *Chem. Rev.* **2003**, *103*, 2457–2473.

(22) (a) Weitz, E.; Scheffer, A. *Ber. Dtch Chem. Ges.* **1921**, *54*, 2327; for a review see: (b) In *Comprehensive Organic Name Reactions and Reagents*; Wang, Z., Ed.; John Wiley & Sons: West Sussex, U. K., 2009; pp 2975–2979.

(23) For a review on organocatalytic asymmetric epoxidation of electron-deficient olefins see: Weiß, K. M.; Tsogoeva, S. B. *Chem. Rec.* **2011**, *11*, 18–39.

(24) For reviews, see: (a) Asymmetric Phase Transfer Catalysis; Maruoka, K., Ed.; Wiley-VCH: Weinheim, Germany, 2008. (b) Ooi, T.; Maruoka, K. *Angew. Chem. Int. Ed.* **2007**, *46*, 4222. (c) Hashimoto, T.; Maruoka, K. *Chem. Rev.* **2007**, *107*, 5656–5682.

(25) (a) Helder, R.; Hummelen, J. C.; Laane, R. W. P. M.; Wiering, J. S.; Wynberg, H. *Tetrahedron Lett.* **1976**, 1831. (b) Wynberg, H.; Greijdanus, B. *J. Chem. Soc., Chem. Commun.* **1978**, 427–438. (c) Wynberg, H.; Hummelen, J. C. *Tetrahedron Lett.* **1978**, 1089. (d) Wynberg, H.; Marsman, B. *J. Org. Chem.* **1979**, *44*, 2312–2314. (e) Wynberg, H.; Marsman, B. *J. Org. Chem.* **1980**, *45*, 158. (f) Pluim, H.; Wynberg, H. *J. Org. Chem.* **1980**, *45*, 2498.

(26) (a) Arai, S.; Tsuge, H.; Shioiri, T. *Tetrahedron Lett.* **1998**, *39*, 7563. (b) Arai, S.; Oku, M.; Miura, M.; Shioiri, T. *Synlett* **1998**, 1201. (c) Arai, S.; Tsuge, H.; Oku, M.; Miura, M.; Shioiri, T. *Tetrhedron* **2002**, *58*, 1623. (d) Liu, X. D.; Bai, X. L.; Qiu, X. P.; Gao, L. X. *Chin. Chem. Lett.* **2005**, *16*, 975. (e) Jew, S.-S.; Lee, J.-H.; Jeong, B.-S.; Yoo, M.-S.; Kim, M.-J.; Lee, Y.-J.; Lee, J.; Choi, S.-H.; Lee, K.; Lah, M. S.; Park, H.-G. *Angew. Chem. Int. Ed.* **2005**, *44*, 1383.

(27) For reviews, see Ref. 23 and: Kelly, D. R.; Roberts, S. M. *Biopolymers (Peptide Science)* **2006**, *84*, 74–89.

(28) Julia, S.; Masana, J.; Vega, J. C. *Angew. Chem. Int. Ed.* **1980**, *19*, 929.

(29) Flood, R. W.; Geller, T. P.; Petty, S. A.; Roberts, S. M.; Skidmore, J.; Volk, M. *Org. Lett.* **2001**, *3*, 683.

(30) Kelly, D. R.; Roberts, S. M. *Chem. Commun.* **2004**, 2018.

(31) Terada, M.; Nakano, M. *Heterocycles* **2008**, *76*, 1049–1055.

(32) Tanaka, S.; Nagasawa, K. *Synlett* **2009** 667–670.

(33) Liao, S.; Čorič, I.; Wang, Q.; List, B. *J. Am. Chem. Soc.* **2012**, *134*, 10765–10768.

(34) Shi, Y. *Acc. Chem. Res.* **2004**, *37*, 488–496.

(35) For reviews on chiral ketone and iminium catalyzed asymmetric epoxidations, see: (a) Wong, O. A.; Shi, Y. In *Asymmetric Organocatalysis*; List, B., Ed.; Topics in Current Chemistry 291; Springer: Berlin, Germany, 2009; pp 201–232. (b) Wong, O. A.; Shi, Y. *Chem. Rev.* **2008**, *108*, 3958–3987.

(36) (a) Shu, L.; Shi, Y. *Tetrahedron Lett.* **1999**, *40*, 8721–8724. (b) Shu, L.; Shi, Y. *Tetrahderon* **2001**, *57*, 5213–5218. (c) Burke, C. P.; Shu, L.; Shi, Y. *J. Org. Chem.* **2007**, *72*, 6320–6323.

(37) Peris, G.; Jakobsche, C. E.; Miller, S. J. *J. Am. Chem. Soc.* **2007**, *129*, 8710–8711.

(38) Kolundzic, F.; Noshi, M. N.; Tjandra, M.; Movassaghi, M.; Miller, S. J. *J. Am. Chem. Soc.* **2011**, *133*, 9104–9111.

(39) Peris, G.; Miller, S. J. *Org. Lett.* **2008**, *10*, 30498–3052.

(40) (a) Milliet, P.; Picot, A.; Lusinchi, X. *Tetrahedron Lett.* **1976**, *17*, 1573. (b) Milliet, P.; Picot, A.; Lusinchi, X. *Tetrahedron Lett.* **1976**, *17*, 1577. (c) Lusinchi, X.; Hanquet, G. *Tetrahedron* **1997**, *53*, 13727. (d) Bohé, L.; Lusinchi, M.; Lusinchi, X. *Tetrahedron* **1999**, *55*, 141.

(41) Selected examples: (a) Aggarwal, V. K.; Wang, M. F. *Chem. Commun.* **1996**, 191–192. (b) Wong, M.-K.; Ho, L.-M.; Zheng, Y.-S.; Ho, C.-Y.; Yang, D. *Org. Lett.* **2001**, *3*, 2587–2590. (c) Lacour, J.; Monchaud, D.; Marsol, C.; *Tetrahedron Lett.* **2002**, *43*, 8257–8260. (d) Głuszyńska, A.; Maćkowska, I.; Rozwadowska, M. D.; Sienniak, W. *Tetrahedron: Asymmetry* **2004**, *15*, 2499–2505 (e) Vachon, J.; Pérollier, C.; Monchaud, D.; Marsol, C., Ditrich, K.; Lacour, J. *J. Org. Chem.* **2005**, *70*, 5903–5911. (f) Gonçalves, M.-H.; Martinez, A.; Grass, S.; Page, P. C. B.; Lacour, J. *Tetrahedron Lett.* **2006**, *47*, 5297–5301. (g) Vachon, J.; Rentsch, S.; Martinez, A.; Marsol, C.; Lacour, J. *Org. Biomol. Chem.* **2007**, *5*, 501–506.

(42) Page, P. C. B.; Parker, P.; Rassias, G. A.; Buckley, B. R.; Bethell, D. *Adv. Synth. Catal.* **2008**, *350*, 1867–1874.

(43) Ballou, D. P. Flavoprotein Monooxygenases. In *Flavins and Flavoproteins*, Massey, V., Williams, C. H., Eds.; Elsevier: New York, 1982, pp 301–310.

(44) (a) Poulsen, L. L.; Ziegler, D. M. *J. Biol. Chem.* **1979**, *254*, 6449–6455. (b) Beaty, N. B.: Ballou, D. P. *J. Biol. Chem.* **1980**, *255*, 3817–3819.

(45) Ball, S.; Bruice, T. C. *J. Am. Chem. Soc.* **1979**, *101*, 4017–4019.

(46) Murahashi, S.; Oda, T.; Masui, Y. *J. Am. Chem. Soc.* **1989**, *111*, 5002–5003.

(47) Selected examples: (a) Jurok, R.; Cibulka, R.; Dvořáková, H.; Hampl, F.; Hodaćová, J. *Eur. J. Org. Chem.* **2010**, 5217–5224. (b) Mojr, V.; Herzig, V.; Buděšínský, M.; Cibulka, R.; Kraus, T. *Chem. Commun.* **2010**, *46*, 7599–7601. (c) Mojr, V.; Buděšínský, M.; Cibulka, R.; Kraus, T. *Org. Biomol. Chem.* **2011**, *9*, 7318–7326. (d) Hartman, T.; Herzig, V.; Buděšínský, M.; Jindřich, J.; Cibulkaa, R.; Kraus, T. *Tetrahedron: Asymmetry* **2012**, *23*, 1571–1583. (e) Iida, H.; Iwahana, S.; Mizoguchi, T.; Yashima, E. *J. Am. Chem. Soc.* **2012**, *134*, 15103–15113.

(48) Shinkai, S.; Yamaguchi, T.; Manabe, O.; Toda, F. *J. Chem. Soc., Chem. Commun.* **1988**, 1399–1401.

(49) Murahashi, S.; Ono, S.; Imada, Y. *Angew. Chem. Int. Ed.* **2004**, *43*, 1566–1568.

(50) Marigo, M.; Franzén, J.; Poulsen, T. B.; Zhuang, W.; Jœrgensen, K. A. *J. Am. Chem. Soc.* **2005**, *127*, 6964–6965.

(51) Wang, X.; Reisinger, C. M.; List, B. *J. Am. Chem. Soc.* **2008**, *130*, 6070–6071.

(52) (a) Xu, S.; Wang, Z.; Zhang, X.; Zhang, X.; Ding, K. *Angew. Chem. Int. Ed.* **2008**, *47*, 2840–2843. (b) Xu, S.; Wang, Z.; Li, Y.; Zhang, X.; Wang, H.; Ding, K. *Chem. Eur. J.* **2010**, *16*, 3021–3035.

(53) Payne, G. B.; Deming, P. H.; Williams, P. H. *J. Org. Chem.* **1961**, *26*, 659–663.

(54) (a) Page, P. C. B.; Graham, A. E.; Bethell, D.; Park, B. K. *Synth. Commun.* **1993**, 1507. (b) Berhell, D.; Graham, A. E.; Heer, J. P.; Markopoulou, O.; Page, P. C. B.; Park, B. K. *J. Chem. Soc. Perkin Trans. 2* **1993**, 2161–2162. (c) Katritzky, A. R.; Rasala, D.; Brito-Palma, F. *J. Chem. Res., Synop.* **1988**, 42–43.

(55) (a) Ben Hassine, B.; Gorsane, M.; Geerts-Evrard, F.; Pecher, J.; Martin, R. H.; Castelet, D. *Bull. Soc. Chim. Belg.* **1986**, *95*, 547–556. (b) Ben Hassine, B.; Gorsane, M.; Pecher, J.; Martin, R. H. *Bull. Soc. Chim. Belg.* **1986**, *95*, 557–566. (c) Tka, N.; Kraïem, J.; Ben Hassine, B. *Synth. Commun.* **2012**, *42*, 2994–3003.

(56) (a) Saito, I.; Nagata, R.; Yuba, K.; Matsuura, T. *Tetrahedron Lett.* **1983**, *24*, 1737. (b) Sasakura, N.; Nakano, K.; Ichikawa, Y.; Kotsuki, H. *RSC Adv.* **2012**, *2*, 6135.

Chapter 2

Catalytic Asymmetric Oxidation of *N*-Sulfonyl Imines with Hydrogen Peroxide–Trichloroacetonitrile System

2.1 Introduction

Organic peroxy acids, such as peracetic acid, *m*-chloroperbenzoic acid (*m*CPBA), and magnesium monoperoxyphthalate, are convenient yet reactive oxidizing agents in synthetic chemistry and are frequently used for the oxidation of organic functional groups and low-valent metal species. [1] The primary factors responsible for their competent reactivity are vulnerability of the oxygen–oxygen bond and good leaving ability of the acyloxy moiety. At the same time, however, these characteristics are tightly linked with their thermal instability and potentially explosive nature, thus impeding the application to large-scale operations. Therefore, the development of a reliable method for the in situ catalytic generation of a peroxy acid or its equivalent is desirable to reduce hazardousness of this synthetically useful oxidation process.

Besides the practical issues associated with the reactivity, stereoselectivity control is another important subject of interest in peroxy acid-mediated oxidations. Although substrate-directed stereospecific oxidations have been well established, asymmetric catalysis using peroxy acids as a source of active oxygen atom has scarcely been developed. [2,3] The landmark thesis was released from Miller group in 2007, wherein a small peptide architecture was elaborated as a catalytic promoter with remarkable performance. [3a] A free carboxylic acid moiety of an aspartic acid residue in the catalyst was condensed with hydrogen peroxide (H$_2$O$_2$) with the aid of a stoichiometric amount of carbodiimide to repetitively generate the requisite chiral peroxy acid for the enantioselective epoxidation of unactivated olefins with a secondary carbamate as the directing group. The effectiveness of this approach was also demonstrated in the Baeyer–Villiger oxidation of cyclic ketones and the hydroxylation of substituted indoles. [3c,d] On the other hand, a method for controlling the stereochemical outcome of the oxidation with an *in situ*-generated achiral peroxy acid by a catalytic quantity of a chiral molecule remains virtually unknown and is considered to be rather problematic. This is partially because the corresponding carboxylic acid is inevitably formed as the side product in this type of oxidation, preventing the selective activation of the peroxy acid by the chiral catalyst.

In this context, the Payne oxidation, where the active oxidant is an *in situ*-generated peroxyimidic acid, appears to be a uniquely attractive system. [4] This reaction was originally discovered in the study directed toward the epoxidation of acrylonitrile with H$_2$O$_2$ and was subsequently applied to the epoxidation of simple olefins. [4a] The oxidation process is initiated by the addition of H$_2$O$_2$ to a nitrile in the presence of excess base to afford the peroxyimidic acid intermediate thatinstantly transfers active oxygen to the substrate (Scheme 2.1), forming the corresponding amide as the side product unlike the carboxylic acid produced in the standard peroxy acid-mediated oxidations. Because the pKa of the resulting amide ion is expected to be higher than H$_2$O$_2$, it could regenerate a hydroperoxide ion ($^-$OOH). This notion clearly indicates the inherent feasibility of rendering the Payne oxidation catalytic in base. However, such a system has never been developed, much less the catalytic asymmetric variant, probably because of the lack of an appropriate chiral base

catalyst.

Scheme 2.1 Mechanism of the Payne Oxidation
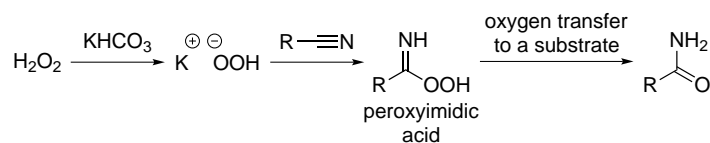
As a part of our research program aiming at the molecular design and synthetic applications of *P*-spiro chiral tetraaminophosphonium salts as organic ion-pair catalysts,[5] we have demonstrated the potential of their conjugate bases, triaminoiminophosphoranes of type **1** (Figure 2.1),[6,7] as chiral organic superbases through the development of a series of highly stereoselective transformations.[8]

1a: R = Me, Ar = Ph   **1f**: R = Me, Ar = 3,5-Me$_2$C$_6$H$_3$
1b: R = Me, Ar = 4-MeC$_6$H$_4$ **1g**: R = Me, Ar = 3,5-Cl$_2$C$_6$H$_3$
1c: R = Me, Ar = 4-ClC$_6$H$_4$ **1h**: R = Me, Ar = 3,5-F$_2$C$_6$H$_3$
1d: R = Me, Ar = 3-MeC$_6$H$_4$ **1i**: R = Et, Ar = 3,5-Cl$_2$C$_6$H$_3$
1e: R = Me, Ar = 3-ClC$_6$H$_4$
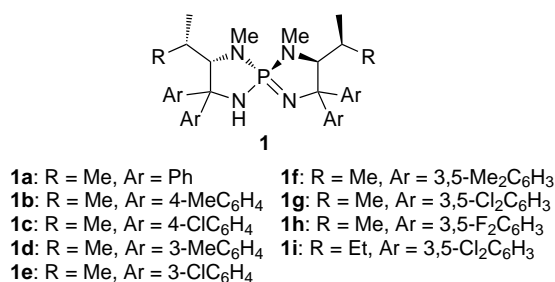
Figure 2.1 *P*-Spiro chiral triaminoiminophosphoranes **1**

In particular, iminophosphorane **1a** catalyzes the stereoselective glycolate aldol reaction that involves the *P*-Brook rearrangement of α-hydroxy phosphonates triggered by their deprotonation with **1a** (Scheme 2.2).[8e]

Scheme 2.2 Chiral iminophosphorane **1a**-catalyzed glycolate aldol reaction
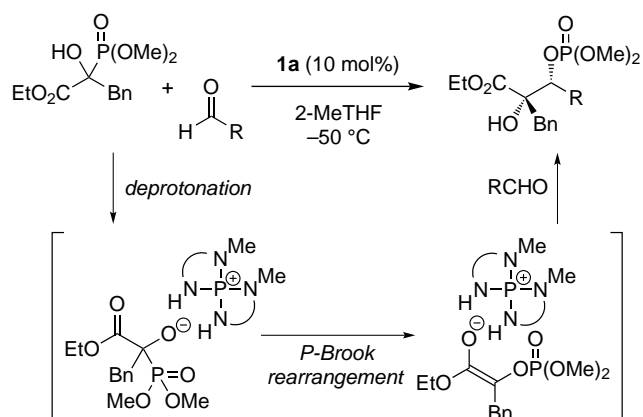
The ability of iminophosphorane **1** to generate the aminophosphonium alkoxide in this direct aldolization hinted at the possibility that **1**, upon treatment with H$_2$O$_2$, could catalytically generate the corresponding hydroperoxide **1**·HOOH, which would be sufficiently reactive for the facile addi-

tion to nitrile to form the aminophosphonium peroxyimidate as the key intermediate for achieving the catalytic asymmetric Payne-type oxidation. In the following sections, the author describes the details of the endeavor to substantiate this hypothesis in the establishment of the catalytic, highly enantioselective oxidation of *N*-sulfonyl imines as a broadly applicable method for the synthesis of optically active *N*-sulfonyl oxaziridines. [9]

2.2 Results and Discussion

2.2.1 Optimization of the Reaction Conditions

The feasibility of the asymmetric Payne-type oxidation under the catalysis of the iminophosphorane was investigated in the oxidation of *N*-sulfonyl imines to chiral *N*-sulfonyl oxaziridines. [10–18] Chiral *N*-sulfonyl oxaziridine is one of the unique organic oxidants in synthetic chemistry and used for the oxygen-transfer reactions to electron-rich functional groups such as enolates and heteroatoms. [15,16] While diastereoselective oxidation of *N*-sulfonyl imines with a chiral backbone has been utilized for the preparation of stereochemically defined *N*-sulfonyl oxaziridines, a reliable method for their enantioselective synthesis is rather underdeveloped. [14,16] In 2011, Jørgensen pioneered the catalytic asymmetric oxidation of *N*-sulfonyl imines with *m*CPBA using a cinchona alkaloid derivative as the chiral base catalyst. [12] Although this protocol requires over-stoichiometric amount of peroxy acid, a variety of aromatic and aliphatic imines can be converted into the corresponding *N*-sulfonyl oxaziridines with moderate-to-excellent enantioselectivity. Yamamoto also succeeded in the catalytic oxidation of *N*-sulfonyl imines by the combined use of a chiral hafnium(IV)-complex, which was originally introduced as an effective catalyst for the epoxidation of *N*-sulfonyl allylic amines, and cumenhydroperoxide. [13] Excellent enantioselectivity was observed not only for aldimines but also for a ketimine, although the scope of this system was not fully studied. The author's approach was based on the catalytic formation of chiral aminophosphonium peroxyimidate **1**·HOOC(=NH)R as the key intermediate by the reaction of aminophosphonium hydroperoxide **1**·HOOH, generated from iminophosphorane **1** and H_2O_2, with an appropriate nitrile (RCN) as illustrated in Figure 2.2. The nucleophilic peroxyimidate ion of this chiral ion pair subsequently attacks electrophilic imine **2** enantioselectively followed by an expected smooth ring closure owing to the high leaving ability of the amidate ion $RCONH^-$ to afford the three-membered product and aminophosphonium amidate **1**·H_2NC(=O)R. The amidate ion is basic enough to abstract a proton from aminophosphonium ion **1**·H to regenerate parent iminophosphorane **1**, thus completing the catalytic cycle.
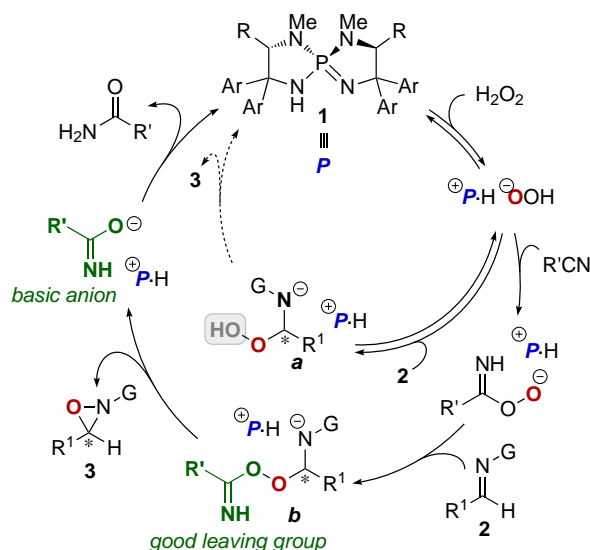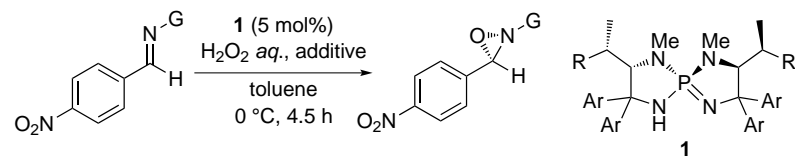
Figure 2.2 Working hypothesis

Initially, trichloroacetonitrile (Cl$_3$CCN) was chosen as a requisite stoichiometric promoter, and carried out the oxidation of *N*-Ts-4-nitrobenzaldimine **2a** (Ts = tosyl) with an aqueous solution of H$_2$O$_2$ in the presence of Cl$_3$CCN and iminophosphorane **1a** (5 mol%) in toluene at 0 °C, which resulted in the quantitative isolation of the desired *N*-sulfonyl oxaziridine**3a** as anticipated, butwith moderate enantioselectivity (Table 2.1, entry 1). An attempt without Cl$_3$CCN led to complete suppression of the reaction probably because leaving ability of the hydroxide ion was insufficient for *N*-sulfonyl amidate ion, a soft nucleophile, to attack the nearby oxygen atom in intermediate **a** (Figure 2.2) for the rapid ring closure (entry 2).[9] The formation of only a trace amount of **3a** was detected in the reactions with other electron-deficient nitriles (entry 3). These results demonstrate not only the crucial role of Cl$_3$CCN as a uniquely effective promoter but also the operation of the Payne-type oxidation mechanism. The author then pursued the structural modification of the iminophosphorane for the improvement in the enantioselectivity (entries 4–10). With the L-valine-derived iminophosphoranes, the steric and electronic properties of the aromatic substituents (Ar) had a significant influence on the selectivity profile. In particular, the introduction of halogen atoms to the appropriate position of the aromatic nuclei was found to be beneficial; **1g** with a 3,5-dichlorophenyl substituent allowed for the production of **3a** in 86% yield with 94% ee (entry 9). The identity of the parent amino acid of the diamine backbone was also responsible for the stereo-controlling ability of iminophosphorane **1**, and L-isoleucine-derived **1i** was singled out as the best catalyst (entry 11).

Table 2.1 Optimization of the catalyst structure[a]

entry	catalyst	imine	G	additive	yield (%)[b]	ee (%)[c]	product
1	**1a**	**2a**	Ts	Cl$_3$CCN	99	68	**3a**
2	**1a**	**2a**	Ts	none	trace	–	–
3	**1a**	**2a**	Ts	R'CN[d]	trace	–	–
4	**1b**	**2a**	Ts	Cl$_3$CCN	88	44	**3a**
5	**1c**	**2a**	Ts	Cl$_3$CCN	83	74	**3a**
6	**1d**	**2a**	Ts	Cl$_3$CCN	84	65	**3a**
7	**1e**	**2a**	Ts	Cl$_3$CCN	94	85	**3a**
8	**1f**	**2a**	Ts	Cl$_3$CCN	89	70	**3a**
9	**1g**	**2a**	Ts	Cl$_3$CCN	86	94	**3a**
10	**1h**	**2a**	Ts	Cl$_3$CCN	88	91	**3a**
11	**1i**	**2a**	Ts	Cl$_3$CCN	89	98	**3a**
12	**1i**	**4a**	Mts[e]	Cl$_3$CCN	75	99	**5a**
13	**1i**	**6**	Mtr[e]	Cl$_3$CCN	87	97	**7**
14	**1i**	**8**	Bs	Cl$_3$CCN	89	97	**9**
15	**1i**	**10**	Ms	Cl$_3$CCN	86	93	**11**

[a]Unless otherwise noted, reactions were performed on 0.1 mmol scale with 1.2 equiv of a 35% aqueous solution of H$_2$O$_2$, 1.2 equiv of Cl$_3$CCN, and 5 mol% of **1** in toluene (2.0 mL) at 0 °C. [b]Isolated yields were reported. [c]Enantiomeric excess was analyzed by chiral stationary phase HPLC. Absolute configuration of **3a** was assigned according to the literature data.[12s] [d]R' = Me, Ph, C$_6$F$_5$, 3,5-(CF$_3$)$_2$C$_6$H$_3$. [e]Mts = mesitylenesulfonyl, Mtr = 4-methoxy-2,3,6-trimethylbenzenesulfonyl. For this type of abbreviation for multi-substituted benzenesulfonyl groups, see ref 21.

It is noteworthy that over 1 g of **2a** was quantitatively converted into **3a** with virtually complete enantiocontrol in the presence of only 1 mol% of **1i** under otherwise similar conditions, demonstrating the scalability of this asymmetric oxidation (Scheme 2.3).[20]

Scheme 2.3 Catalytic asymmetric Payne oxidation on practical scale
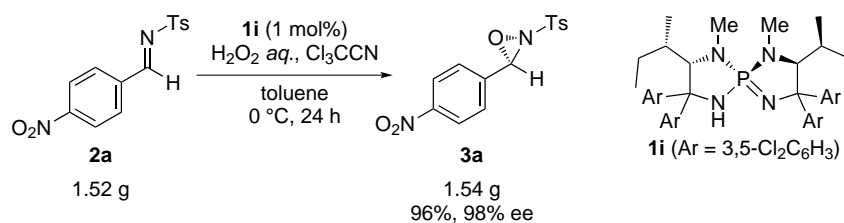
Furthermore, we confirmed that the variation in the *N*-sulfonyl group of the imines was feasible (entries 12–15); the asymmetric catalysis of **1i** accommodated imines **4a** and **6** bearing sterically demanding mesitylenesulfonyl (Mts) and 4-methoxy-2,3,6-trimethylbenzenesulfonyl (Mtr)

groups, respectively (entries 12 and 13)[21] and imine **10** with the smallest methanesulfonyl (Ms) group (entry 15).

2.2.2   Generality

With the optimal catalyst structure, we thoroughly evaluated the generality of this **1i**-catalyzed asymmetric Payne oxidation of *N*-sulfonyl imines, and the results are summarized in Table 2.2. This system is applicable to a wide range of aromatic *N*-Ts imines with substituents of different steric and electronic attributes and the corresponding *N*-sulfonyl oxaziridines were obtained with uniformly excellent enantioselectivity (entries 1–11). Notably, potentially oxidizable furyl and thienyl functionalities were tolerated (entries 12 and 13), indicating the nucleophilic nature of the intermediary formed aminophosphonium peroxyimidate **1i**·HOO(C=NH)CCl$_3$ (Figures 2.2 and **??**). With α,β-unsaturated aldimines, the 1,2-addition of the peroxyimidate ion occurred exclusively with rigorous stereocontrol, leaving the olefin moiety intact (entry 14). In the oxidation of aliphatic imines, slight modifications of the reaction conditions were necessary for attaining high chemical yield except for α-quaternary imines (entries 15 and 16). When *N*-Ts-cyclohexylaldimine **2r** was exposed to the standard conditions using **1i** as the catalyst, the starting material was smoothly consumed, while only a trace amount of the desired oxaziridine **3r** was detected in the ^{1}H NMR spectrum of the crude aliquot. The major product was assigned as a diastereomeric mixture of dimeric peroxide **12** with dr = 1.7:1 (Figure 2.3). This outcome could be attributed to the considerable effect of the inherent steric and electronic differences between the aromatic and aliphatic imines on the equilibrium in the addition of $^-$OOH to the imine (Figure 2.2). Although this problem was overcome by simply performing the reaction in dichloromethane at ambient temperature in the case of α-branched imines, installation of the bulky Mts group on the imine nitrogen was critical for promoting the enantioselective oxidation of α-unsubstituted imines with high efficiency (entries 17–23).[22] In addition, *N*-Mts imines **4e** and **4f** with non-conjugated, electron-rich olefins were oxidized to the enantioenriched oxaziridines **5e** and **5f** without any difficulties (entries 22 and 23).

Table 2.2 Substrate scope of the Payne oxidation[a]

$$R^1 \overset{\displaystyle N \diagup G}{\underset{\displaystyle H}{\big\|}} \quad \xrightarrow[\text{toluene, 0 °C}]{\substack{\textbf{1i} \text{ (5 mol\%)} \\ H_2O_2 \ aq., Cl_3CCN}} \quad R^1 \overset{O\cdots N \diagup G}{\underset{H}{\diagdown}}$$

| entry	R^1	G	imine	time (h)	yield (%)[b]	ee (%)[c]	product
1	Ph	Ts	**2b**	2.5	90	95	**3b**
2	2-FC$_6$H$_4$	Ts	**2c**	4	83	95	**3c**
3	2-ClC$_6$H$_4$	Ts	**2d**	3.5	72	95	**3d**
4	2-BrC$_6$H$_4$	Ts	**2e**	3.5	78	95	**3e**
5	2-MeC$_6$H$_4$	Ts	**2f**	2.5	86	96	**3f**
6	3-BrC$_6$H$_4$	Ts	**2g**	2	84	97	**3g**
7	3-MeOC$_6$H$_4$	Ts	**2h**	3.5	99	95	**3h**
8	4-ClC$_6$H$_4$	Ts	**2i**	1.5	89	96	**3i**
9	4-BrC$_6$H$_4$	Ts	**2j**	4	86	96	**3j**
10	4-MeC$_6$H$_4$	Ts	**2k**	4.5	91	95	**3k**
11	2-naphthyl	Ts	**2l**	4.5	99	90	**3l**
12	3-furyl	Ts	**2m**	4	96	93	**3m**
13	3-thienyl	Ts	**2n**	2.5	91	94	**3n**
14	(*E*)-PhCH=CH	Ts	**2o**	3.5	85	96	**3o**
15	Me$_3$C	Ts	**2p**	2	85	98	**3p**
16	CH$_2$=CHCH$_2$C(Me)$_2$	Ts	**2q**	3	79	98	**3q**
17[d]	*cyclo*-hexyl	Ts	**2r**	1	91	98	**3r**
18[d]	Me$_2$CH	Ts	**2s**	1	78	95	**3s**
19[d]	Me$_2$CHCH$_2$	Mts	**4b**	1	92	95	**5b**
20[d]	Ph(CH$_2$)$_2$	Mts	**4c**	0.5	87	96	**5c**
21[d]	Me(CH$_2$)$_4$	Mts	**4d**	1	87	94	**5d**
22[d]	CH$_2$=CH(CH$_2$)$_2$	Mts	**4e**	1	83	96	**5e**
23[d]	(*Z*)-EtCH=CH(CH$_2$)$_2$	Mts	**4f**	1	76	95	**5f**

[a]Unless otherwise noted, reactions were performed on 0.1 mmol scale with 1.2 equiv of a 35% aqueous solution of H$_2$O$_2$, 1.2 equiv of Cl$_3$CCN, and 5 mol% of **1i** in toluene (2.0 mL) at 0 °C. [b]Isolated yields were reported. [c]Enantiomeric excesses were analyzed by chiral stationary phase HPLC. Absolute configurations of oxaziridines were assigned to be *R* by analogy to the known compounds. [12] [d]Reaction was conducted at 25 °C in dichloromethane (2.0 mL).
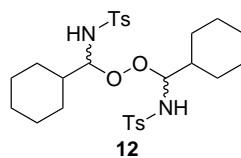
Figure 2.3 Unexpectedly obtained dimeric peroxide **12**

2.2.3   Kinetic Resolution of α-Chiral Aldimines

Because this protocol for the catalytic asymmetric Payne oxidation was remarkably effective for a broad structural range of *N*-sulfonyl imines, the author was interested in the application to the oxidative kinetic resolution of racemic α-chiral imines (Scheme 2.4). If aminophosphonium peroxyimidate intermediate **1i**·HOO(C=NH)CCl$_3$ could discriminate the chirality of a stereogenic carbon at the α-position of the aliphatic imine, one of the enantiomers would be preferentially oxidized to afford a single diastereomer of four possible diastereomeric products. This possibility was explored in the reaction of the racemic mixture of α-tert-butyldimethylsiloxy propanaldimine (**4g**) under the reaction conditions similar to those optimized for the *N*-Mts-aliphatic aldimines except for the use of *rac*-**4g** in double the amount. Indeed, one of the diastereomers of the corresponding oxaziridine **5g** formed predominantly with high enantioselectivity, proving the prominent ability of the chiral peroxyimidate to recognize the stereocenter in the starting imine.

Scheme 2.4 Catalytic asymmetric Payne oxidation on practical scale
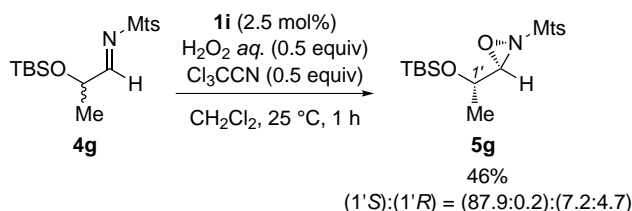
2.2.4   Derivatization

The synthetic utility of this catalytic imine oxidation protocol was highlighted through the fruitful derivatization of the chiral oxaziridines (Scheme 2.5). With the expectation of intramolecular oxygen-transfer reaction on the basis of the intrinsic character of the oxaziridine as an organic oxidant, [24−26] **5e** (96% ee) was simply heated at 60 °C in chloroform and indeed transformed into the corresponding epoxy imine **13a**. The subsequent Lewis acid-promoted reduction of the C–N double bond triggered the 5-*exo-tet* cyclization to furnish the pyrrolidine methanol derivative **14a** in good yield with 95% ee (Scheme 2.5a). The conservation of enantiomeric purity throughout this process reflects the cyclic transition state (TS) at the oxygen-transfer stage. The result of the cross-over experiment (see **??**) also suggests the participation of the intramolecular oxygen-transfer process. In a similar manner, chiral secondary alcohol **14b** was prepared from **5f** (95% ee) via *N*-sulfonyl imine **13b** with an internal *cis*-epoxide moiety (Scheme 2.5b). Finally, enantioenriched aromatic oxaziridine **3b** (95% ee) was subjected to the Yoon's conditions for the copper salt-catalyzed oxyamination of *N*-acetyl indole, taking the advantage of the recent progress in methodology development for utilizing oxaziridines as versatile intermediates; tricyclic indoline derivative **15** was obtained without loss of enantiomeric excess (Scheme 2.5c). [25j]

Scheme 2.5 Catalytic asymmetric Payne oxidation on practical scale
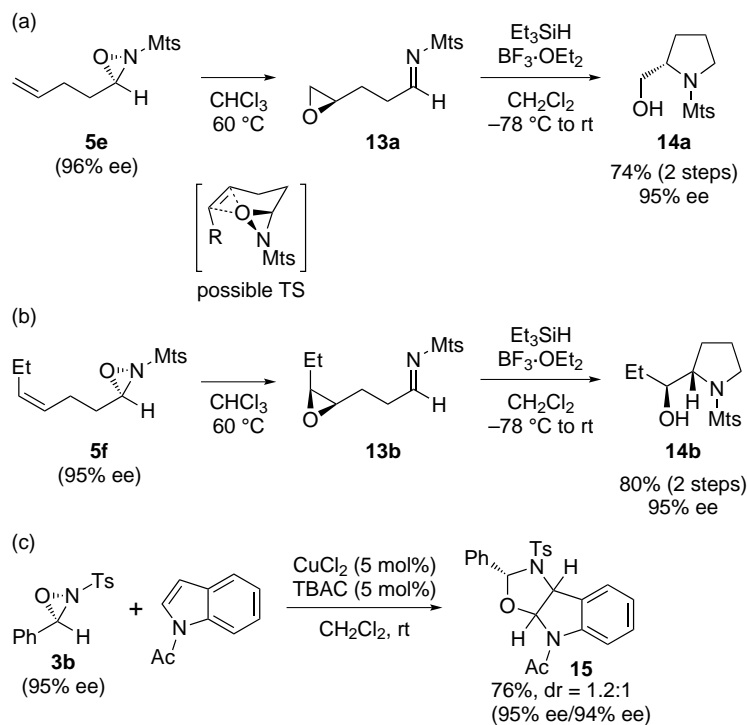
2.3   Conclusion

The first catalytic asymmetric Payne oxidation of *N*-sulfonyl imines was developed under the catalysis of *P*-spiro chiral triaminoiminophosphoranes. This protocol is applicable to structurally diverse aromatic and aliphatic imines, which makes the chiral oxaziridines easily accessible yet synthetically valuable reagents and building blocks. Furthermore, the success in the catalytic use of a chiral base for the Payne oxidation would stimulate further research on the asymmetric oxidations based on the H$_2$O$_2$–nitrile system.

2.4 Experimental Section

2.4.1 General Information

Infrared spectra were recorded on a Shimadzu IRAffinity-1 spectrometer. ^{1}H NMR spectra were recorded on a JEOL JNM-ECS400 (400 MHz) or a Bruker AVANCE III-OneBasy500 (500 MHz) spectrometer. Chemical shifts are reported in ppm from tetramethylsilane (0.0 ppm) resonance as the internal standard (CDCl$_3$). Data are reported as follows: chemical shift, integration, multiplicity (s = singlet, d = doublet, t = triplet, q = quartet, m = multiplet, br = broad), and coupling constants (Hz). ^{13}C NMR spectra were recorded on a JEOL JNM-ECS400 (101 MHz) or a Bruker AVANCE III-OneBasy500 (126 MHz) spectrometer with complete proton decoupling. Chemical shifts are reported in ppm from the solvent resonance as the internal standard (CDCl$_3$; 77.36 ppm, C$_6$D$_6$; 128.06 ppm). ^{31}P NMR spectra were recorded on a JEOL JNM-ECS400 (162 MHz) spectrometer with complete proton decoupling. Chemical shifts are reported in ppm from H$_3$PO$_4$ (0.0 ppm) resonance as the external standard. ^{19}F NMR spectra were recorded on a JEOL JNM-ECS400 (376 MHz) spectrometer with complete proton decoupling. Chemical shifts are reported in ppm from benzotrifluoride (−64.0 ppm) resonance as the external standard. Optical rotations were measured on a HORIBA SEPA-500 polarimeter. The high resolution mass spectra were conducted on Thermo Fisher Scientific Exactive. Analytical thin layer chromatography (TLC) was performed on Merck precoated TLC plates (silica gel 60 GF254, 0.25 mm). Flash column chromatography was performed on PSQ60AB (spherical, av. 55 μm; Fuji Silysia Chemical ltd.). Enantiomeric excesses were determined by HPLC analysis using chiral columns [ϕ 4.6 mm × 250 mm, DAICEL CHIRALCEL OD-3 (OD3), CHIRALCEL OJ-3 (OJ3), CHIRALPAK AD-3 (AD3), CHIRALPAK IB (IB), and CHIRALPAK IC-3 (IC3)] with n-hexane (H), 2-propanol (IPA), and ethanol (EtOH) as eluent. Toluene and dichloromethane (CH$_2$Cl$_2$) were supplied from Kanto Chemical Co., Inc. as "Dehydrated" and further purified by passing through neutral alumina under nitrogen atmosphere. Aminophosphonium chlorides **1**·HCl, [8f] iminophosphoranes **8f**, and N-sulfonyl imines **2**, **4**, **6**, **8**, **10** [27] were prepared by following the literature procedures. Trifluoroacetic acid (TFA) and trifluoromethanesulfonic acid (TfOH) were kindly supplied from Asahi Glass Co., Ltd. and Central Glass Co., Ltd., respectively. Other simple chemicals were purchased and used as such.

2.4.2   Experimental Procedures and Characterization

### 2.4.2.1   Characterization of Chiral Iminophosphorane 1i
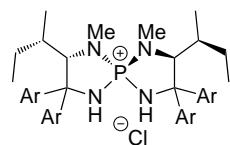
1i·HCl (Ar = 3,5-Cl$_2$C$_6$H$_3$): White solid; mp 204–206 °C (decomp); ^{1}H NMR (400 MHz, CD$_3$OD) δ 7.72 (4H, brd, *J* = 1.6 Hz), 7.61 (2H, t, *J* = 1.6 Hz), 7.55 (2H, t, *J* = 1.6 Hz), 7.40 (4H, br), 4.23 (2H, dd, *J*$_{P-H}$ = 20.4 Hz, *J*$_{H-H}$ = 4.3 Hz), 2.07 (6H, d, *J*$_{P-H}$ = 10.0 Hz), 1.85–1.72 (2H, m), 1.53–1.40 (2H, m), 1.16–1.01 (2H, m), 0.90 (6H, t, *J* = 7.3 Hz), 0.79 (6H, d, *J* = 6.9 Hz), N–H protons were missing due to deuterium exchange; ^{13}C NMR (101 MHz, CD$_3$OD) δ 151.4, 143.6 (d, *J*$_{P-C}$ = 12.6 Hz), 137.5, 136.6, 129.9, 129.6, 127.4, 126.7, 72.8 (d, *J*$_{P-C}$ = 10.6 Hz), 71.0 (d, *J*$_{P-C}$ = 11.6 Hz), 37.8, 33.0 (d, *J*$_{P-C}$ = 5.8 Hz), 26.3, 18.8, 12.2; ^{31}P NMR (162 MHz, CD$_3$OD) δ 35.5; IR (film) 2970, 2930, 2874, 1568, 1558, 1420, 1356, 1179, 1005, 862, 856, 802 cm^{-1}; HRMS (ESI) Calcd for C$_{38}$H$_{40}$N$_4$^{35}Cl$_8$P$^+$ ([M−Cl]$^+$) 863.0493. Found 863.0495. [α]$_D^{22}$ −158.1 (*c* = 1.00, CH$_2$Cl$_2$).
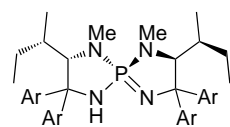
1i: White solid; mp 133–135 °C (decomp); ^{1}H NMR (400 MHz, CD$_3$OD) δ 7.72 (4H, d, *J* = 1.7 Hz), 7.47 (4H, br), 7.44 (2H, t, *J* = 1.7 Hz), 7.39 (2H, t, *J* = 1.7 Hz), 3.93 (2H, dd, *J*$_{P-H}$ = 19.5 Hz, *J*$_{H-H}$ = 3.9 Hz), 2.02–1.87 (2H, m), 1.96 (6H, d, *J*$_{P-H}$ = 9.1 Hz), 1.43–1.29 (2H, m), 1.13–0.98 (2H, m), 0.83 (6H, t, *J* = 7.3 Hz), 0.77 (6H, d, *J* = 7.3 Hz), N–H proton was missing due to deuterium exchange; ^{13}C NMR (101 MHz, CD$_3$OD) δ 154.9, 147.6, 136.5, 135.9, 128.4, 128.3, 127.8, 127.1, 74.0 (d, *J*$_{P-C}$ = 15.5 Hz), 72.0 (d, *J*$_{P-C}$ = 7.7 Hz), 38.5, 32.9 (d, *J*$_{P-C}$ = 4.8 Hz), 26.2, 19.3, 12.4; ^{31}P NMR (162 MHz, CD$_3$OD) δ 42.2; IR (film) 2968, 2930, 2872, 1558, 1418, 1204, 1136, 1121, 854 cm^{-1}; HRMS (ESI) Calcd for C$_{38}$H$_{40}$N$_4$^{35}Cl$_8$P$^+$ ([M+H]$^+$) 863.0493. Found 863.0499. [α]$_D^{22}$ −218.9 (*c* = 1.00, CH$_2$Cl$_2$).

### 2.4.2.2   Characterization of *N*-Sulfonyl Imines
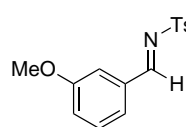
2h: White solid; mp 71–72 °C; ^{1}H NMR (400 MHz, CDCl$_3$) δ 8.99 (1H, s), 7.89 (2H, d, *J* = 8.5 Hz), 7.50–7.46 (1H, m), 7.45 (1H, d, *J* = 7.7, 1.1 Hz), 7.40 (1H, t, *J* = 7.7 Hz), 7.35 (2H, d, *J* = 8.5 Hz), 7.16 (1H, ddd, *J* = 7.7, 2.7, 1.1 Hz), 3.84 (3H, s), 2.44 (3H, s); ^{13}C NMR (101 MHz, CDCl$_3$) δ 170.5, 160.4, 145.0, 135.3, 134.0, 130.4, 130.1, 128.5, 125.7, 122.6, 113.5, 55.9, 22.0; IR (film) 3003, 2938, 2833, 1576, 1321, 1302, 1273, 1155, 1086, 1040, 806 cm^{-1}; HRMS (ESI) Calcd for C$_{15}$H$_{15}$NNaO$_3$S$^+$ ([M+Na]$^+$) 312.0665. Found 312.0663.
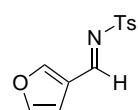
2m: Off-white solid; mp 126–127 °C; ^{1}H NMR (400 MHz, CDCl$_3$) δ 9.00 (1H, s), 8.09 (1H, t, *J* = 1.4 Hz), 7.86 (2H, d, *J* = 8.2 Hz), 7.50 (1H, t, *J* = 1.4 Hz), 7.34 (2H, d, *J* = 8.2 Hz), 6.84 (1H, d, *J* = 1.4 Hz), 2.44 (3H, s); ^{13}C NMR (101 MHz, CDCl$_3$) δ 162.1, 152.4, 145.7, 144.9, 35.4, 130.1, 128.3, 123.6, 108.3, 22.0; IR (film) 3130, 3026, 2970, 1601, 1315, 1283, 1150, 1086, 870, 827, 808 cm^{-1}; HRMS (ESI) Calcd for C$_{12}$H$_{11}$NNaO$_3$S$^+$

([M+Na]$^+$) 272.0352. Found 272.0350.
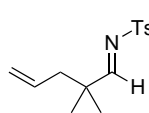
2q: White solid; mp 57–58 °C; ^{1}H NMR (500 MHz, CDCl$_3$) δ 8.44 (1H, s), 7.79 (2H, d, J = 8.4 Hz), 7.33 (2H, d, J = 8.4 Hz), 5.64 (1H, ddt, J = 17.1, 10.4, 7.3 Hz), 5.03 (1H, dq, J = 10.4, 1.0 Hz), 5.01 (1H, dq, J = 17.1, 1.0 Hz), 2.45 (3H, s), 2.24 (2H, dt, J = 7.3, 1.0 Hz), 1.12 (6H, s); ^{13}C NMR (126 MHz, CDCl$_3$) δ 184.0, 144.9, 135.2, 133.1, 130.1, 128.4, 119.3, 44.2, 41.2, 23.9, 22.0; IR (film) 2974, 2928, 1628, 1468, 1323, 1159, 1092, 922, 804 cm^{-1}; HRMS (ESI) Calcd for C$_{14}$H$_{19}$NNaO$_2$S$^+$ ([M+Na]$^+$) 288.1029. Found 288.1028.
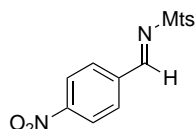
4a: Pale yellow solid; mp 178–179 °C; ^{1}H NMR (400 MHz, CDCl$_3$) δ 9.13 (1H, s), 8.34 (2H, d, J = 8.7 Hz), 8.11 (2H, d, J = 8.7 Hz), 7.01 (1H, s), 2.71 (6H, s), 2.33 (3H, s); ^{13}C NMR (101 MHz, CDCl$_3$) δ 166.6, 151.4, 144.3, 140.9, 138.0, 132.4, 132.1, 131.4, 124.5, 23.4, 21.4; IR (film) 1593, 1522, 1342, 1317, 1215, 1155, 1036, 854, 839 cm^{-1}; HRMS (ESI) Calcd for C$_{16}$H$_{16}$N$_2$NaO$_4$S$^+$ ([M+Na]$^+$) 355.0723. Found 355.0723.
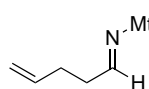
4e: Colorless oil; ^{1}H NMR (400 MHz, CDCl$_3$) δ 8.60 (1H, t, J = 4.2 Hz), 6.97 (2H, s), 5.79 (1H, ddt, J = 17.1, 10.2, 6.9 Hz), 5.04 (1H, dq, J = 17.1, 1.3 Hz), 5.01 (1H, dq, J = 10.2, 1.3 Hz), 2.66–2.58 (2H, m), 2.63 (6H, s), 2.39 (2H, q, J = 6.9 Hz), 2.31 (3H, s); ^{13}C NMR (101 MHz, CDCl$_3$) δ 176.6, 143.8, 140.7, 136.2, 132.2, 131.7, 116.6, 35.2, 29.0, 23.3, 21.4; IR (film) 2978, 2939, 1628, 1443, 1317, 1155, 1055, 916, 853 cm^{-1}; HRMS (ESI) Calcd for C$_{14}$H$_{20}$NO$_2$S$^+$ ([M+H]$^+$) 266.1209. Found 266.1203.
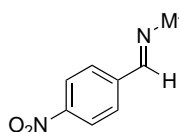
6: Yellow solid; mp 191–192 °C; ^{1}H NMR (400 MHz, CDCl$_3$) δ 9.11 (1H, s), 8.33 (2H, d, J = 8.7 Hz), 8.11 (2H, d, J = 8.7 Hz), 6.64 (1H, s), 3.87 (3H, s), 2.72 (3H, s), 2.66 (3H, s), 2.17 (3H, s); ^{13}C NMR (101 MHz, CDCl$_3$) δ 165.9, 160.9, 151.3, 141.1, 140.4, 138.2, 132.0, 126.5, 126.0, 124.5, 112.6, 56.0, 24.5, 19.0, 12.3; IR (film) 1593, 1520, 1342, 1315, 1275, 1150, 1121, 839 cm^{-1}; HRMS (ESI) Calcd for C$_{17}$H$_{19}$N$_2$O$_5$S$^+$ ([M+H]$^+$) 363.1009. Found 363.1009.
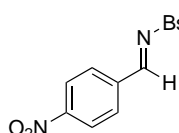
8: Pale yellow solid; mp 190–191 °C; ^{1}H NMR (400 MHz, CDCl$_3$) δ 9.14 (1H, s), 8.34 (2H, d, J = 8.8 Hz), 8.13 (2H, d, J = 8.8 Hz), 8.04 (2H, d, J = 7.8 Hz), 7.69 (1H, t, J = 7.8 Hz), 7.60 (2H, t, J = 7.8 Hz); ^{13}C NMR (101 MHz, CDCl$_3$) δ 168.1, 151.6, 137.7, 137.5, 134.5, 132.3, 129.7, 128.7, 124.6; IR (film) 1597, 1522, 1348, 1321, 1217, 1161, 1088, 843 cm^{-1}; HRMS (ESI) Calcd for C$_{13}$H$_{10}$N$_2$NaO$_4$S$^+$ ([M+Na]$^+$) 313.0253. Found 313.0252.
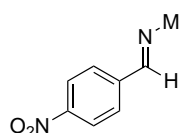
10: White solid; mp 186–187 °C; ^{1}H NMR (500 MHz, CDCl$_3$) δ 9.14 (1H, s), 8.39 (2H, d, J = 8.6 Hz), 8.16 (2H, d, J = 8.6 Hz), 3.20 (3H, s); ^{13}C NMR (126 MHz, CDCl$_3$) δ 169.5, 151.7, 137.4, 132.2, 124.7, 40.6; IR (film) 1618, 1593, 1522, 1346, 1310, 1217, 1146, 864, 841 cm^{-1}; HRMS (ESI) Calcd for C$_8$H$_8$N$_2$NaO$_4$S$^+$ ([M+Na]$^+$) 251.0097. Found 251.0096.

2.4.2.3   General Procedure 1 for Catalytic Asymmetric Payne Oxidation of Aromatic *N*-Sulfonyl Imines (R = aryl, *tert*-alkyl)
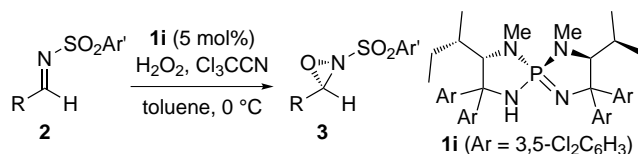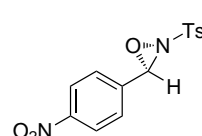

To a solution of chiral iminophosphorane **1i** (4.33 mg, 0.0050 mmol, 0.05 equiv), *N*-sulfonyl imine **2** (0.100 mmol, 1 equiv), and Cl_3CCN (12.0 μL, 0.120 mmol, 1.2 equiv) in toluene (2.0 mL) was added an aqueous 35% solution of H_2O_2 (10.5 μL, 1.2 equiv, titrated by using $KMnO_4$) at 0 °C under Ar atmosphere. After being stirred for indicated time, the reaction was quenched by the addition of a saturated aqueous solution of Na_2SO_3 (5 mL). The aqueous phase was extracted with ethyl acetate (EA, 2 × 10 mL). The combined organic extracts were dried over Na_2SO_4. After filtration, the organic phase was concentrated under reduced pressure. The residue thus obtained was purified by column chromatography on silica gel (H/EA as eluent) to afford oxaziridine **3**. The enantiomeric excess of **3** was determined by HPLC analysis.
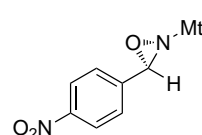
2.4.2.4   General Procedure 2 for Catalytic Asymmetric Payne Oxidation of Aliphatic *N*-Sulfonyl Imines (R = *sec*-, *prim*-alkyl)
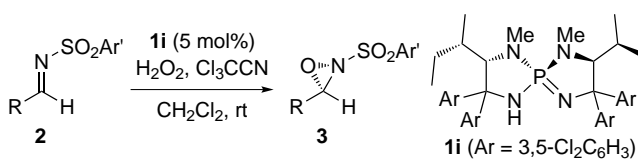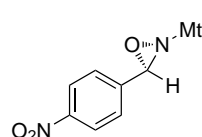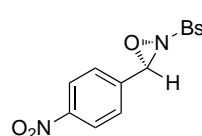

A solution of chiral iminophosphorane **1i** (4.33 mg, 0.0050 mmol, 0.05 equiv), *N*-sulfonyl imine **2** (0.100 mmol, 1.0 equiv), and Cl_3CCN (12.0 μL, 0.120 mmol, 1.2 equiv) in CH_2Cl_2 (2.0 mL) was treated with an aqueous 35% solution of H_2O_2 (10.5 μL, 1.2 equiv, titrated by using $KMnO_4$) at 25 °C under Ar atmosphere. The resulting reaction mixture was stirred for indicated time and then, remaining peroxides were quenched by the addition of a saturated aqueous solution of Na_2SO_3 (5 mL). After extraction of the aqueous phase with EA (2 × 10 mL), the combined organic extracts were dried over Na_2SO_4 and filtered. The organic phase was concentrated and the residual crude mixture was purified by column chromatography on silica gel (H/EA as eluent) to afford oxaziridine **3**. The enantiomeric excess of **3** was determined by HPLC analysis.

2.4.2.5 Characterization of *N*-Sulfonyl Oxaziridines

3a [12]: Prepared from *N*-Ts-4-nitrobenzaldimine **2a** (1.52 g, 5.00 mmol, 1 equiv) by general procedure 1 as a white solid (1.54 g, 4.82 mmol, 96%) with 98% ee as determined by HPLC analysis; HPLC OJ3, H/IPA = 60:40, flow rate = 1.0 mL/min, λ = 232 nm, 32.8 min (major isomer), 42.1 min (minor isomer); mp 121–123 °C; ^{1}H NMR (400 MHz, CDCl$_3$) δ 8.27 (2H, d, *J* = 8.3 Hz), 7.93 (2H, d, *J* = 8.2 Hz), 7.63 (2H, d, *J* = 8.7 Hz), 7.46 (2H, d, *J* = 8.7 Hz), 5.56 (1H, s), 2.52 (3H, s); ^{13}C NMR (101 MHz, CDCl$_3$) δ 150.1, 147.2, 137.6, 131.4, 130.5, 129.8, 129.7, 124.2, 74.7, 22.2; IR (film) 1595, 1529, 1346, 1298, 1188, 1175, 1161, 1109, 1068, 827 cm^{-1}; HRMS (ESI) Calcd for C$_{14}$H$_{12}$N$_2$NaO$_5$S$^+$ ([M+Na]$^+$) 343.0359. Found 343.0360; $[\alpha]_D^{22}$ +74.3 (*c* = 1.00, CHCl$_3$).

5a: Prepared from *N*-Mts-4-nitrobenzaldimine **4a** (32.2 mg, 0.0968 mmol, 1 equiv) by general procedure 1 as a white solid (25.4 mg, 0.0729 mmol, 75%) with 99% ee as determined by HPLC analysis; HPLC AD3, H/IPA = 10:1, flow rate = 1.0 mL/min, λ = 210 nm, 22.6 min (major isomer), 28.3 min (minor isomer); mp 137–139 °C; ^{1}H NMR (500 MHz, CDCl$_3$) δ 8.27 (2H, d, *J* = 8.6 Hz), 7.65 (2H, d, *J* = 8.6 Hz), 7.06 (2H, s), 5.60 (1H, s), 2.73 (6H, s), 2.36 (3H, s); ^{13}C NMR (126 MHz, CDCl$_3$) δ 150.0, 145.6, 142.4, 138.0, 132.6, 129.7, 129.5, 124.2, 74.1, 23.5, 21.5; IR (film) 2922, 1715, 1603, 1524, 1458, 1344, 1238, 1163, 1107, 1040, 826 cm^{-1}; HRMS (ESI) Calcd for C$_{16}$H$_{16}$N$_2$NaO$_5$S$^+$ ([M+Na]$^+$) 371.0672. Found 371.0671; $[\alpha]_D^{21}$ +81.6 (*c* = 1.00, CHCl$_3$).

7: Prepared from *N*-Mtr-4-nitrobenzaldimine **6** (36.3 mg, 0.100 mmol, 1 equiv) by general procedure 1 as a white solid (32.8 mg, 0.0867 mmol, 87%) with 97% ee as determined by HPLC analysis; HPLC AD3, H/IPA = 80:20, flow rate = 1.0 mL/min, λ = 210 nm, 19.0 min (minor isomer), 24.2 min (major isomer); mp 128–129 °C; ^{1}H NMR (500 MHz, CDCl$_3$) δ 8.27 (2H, d, *J* = 8.7 Hz), 7.66 (2H, d, *J* = 8.7 Hz), 6.67 (1H, s), 5.61 (1H, s), 3.90 (3H, s), 2.73 (3H, s), 2.70 (3H, s), 2.19 (3H, s); ^{13}C NMR (126 MHz, CDCl$_3$) δ 161.7, 150.0, 142.4, 142.2, 138.2, 129.7, 126.3, 124.5, 124.2, 112.7, 74.2, 56.0, 24.5, 19.1, 12.4; IR (film) 1582, 1560, 1528, 1447, 1339, 1315, 1238, 1184, 1153, 1125, 1015, 827 cm^{-1}; HRMS (ESI) Calcd for C$_{17}$H$_{18}$N$_2$NaO$_6$S$^+$ ([M+Na]$^+$) 401.0778. Found 401.0779; $[\alpha]_D^{21}$ +60.2 (*c* = 1.00, CHCl$_3$).
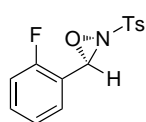
9: Prepared from *N*-Bs-4-nitrobenzaldimine **8** (29.3 mg, 0.101 mmol, 1 equiv) by General Procedure 1 as a white solid (27.5 mg, 0.0898 mmol, 89%) with 97% ee as determined by HPLC analysis; HPLC OJ3, H/IPA = 60:40, flow rate = 1.0 mL/min, λ = 258 nm, 37.4 min (major isomer), 46.6 min (minor isomer); mp 105–107 °C; ^{1}H NMR (500 MHz, CDCl$_3$) δ 8.27 (2H, d, *J* = 8.7 Hz), 8.06 (2H, dd, *J* = 7.7, 1.2 Hz), 7.80 (1H, tt, *J* = 7.7, 1.2 Hz), 7.66 (2H, t, *J* = 7.7 Hz), 7.65 (2H, d, *J* = 8.7 Hz), 5.60 (1H, s); ^{13}C NMR (126 MHz, CDCl$_3$): δ 150.2, 137.5, 135.7, 134.7, 129.9, 129.8, 129.7, 124.3, 74.9; IR (film) 1609, 1520, 1449, 1346, 1294, 1240, 1184, 1165, 1084, 827 cm^{-1}; HRMS (ESI) Calcd for C$_{13}$H$_{10}$N$_2$NaO$_5$S$^+$ ([M+Na]$^+$) 329.0203. Found 329.0202; $[\alpha]_D^{21}$ +84.1 (*c* = 1.01, CHCl$_3$).
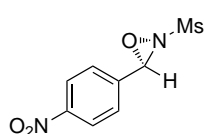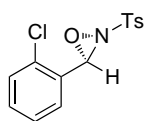
11: Prepared from *N*-Ms-4-nitrobenzaldimine **10** (22.6 mg, 0.0990 mmol, 1 equiv) by general procedure 1 as a white solid (20.8 mg, 0.0852 mmol, 86%) with 93% ee as determined by HPLC analysis; HPLC OJ3, H/IPA = 60:40, flow rate = 1.0 mL/min, λ = 257 nm, 52.7 min (major isomer), 59.0 min (minor isomer); mp 122–124 °C; ^{1}H NMR (500 MHz, CDCl$_3$) δ 8.30 (2H, d, *J* = 8.9 Hz), 7.69 (2H, d, *J* = 8.9 Hz), 5.55 (1H, s), 3.26 (3H, s); ^{13}C NMR (126 MHz, CDCl$_3$): δ 150.2, 137.2, 129.7, 124.3, 74.0, 38.7; IR (film) 2922, 1709, 1609, 1524, 1339, 1296, 1240, 1157, 1107, 968, 822 cm^{-1}; HRMS (ESI) Calcd for $C_8H_8N_2NaO_5S^+$ ([M+Na]$^+$) 267.0046. Found 267.0044; $[\alpha]_D^{21}$ +156.9 (*c* = 1.00, CHCl$_3$).
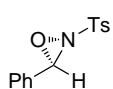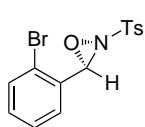
3b [12]: Prepared from *N*-Ts-benzaldimine **2b** (25.7 mg, 0.0991 mmol, 1 equiv) by general procedure 1 as a white solid (24.6 mg, 0.0894 mmol, 90%) with 95% ee as determined by HPLC analysis; HPLC OD3, H/IPA = 10:1, flow rate = 1.0 mL/min, λ = 210 nm, 7.6 min (major isomer), 10.4 min (minor isomer); mp 85–87 °C; ^{1}H NMR (400 MHz, CDCl$_3$) δ 7.93 (2H, d, *J* = 8.4 Hz), 7.48–7.37 (7H, m), 5.55 (1H, s), 2.49 (3H, s); ^{13}C NMR (101 MHz, CDCl$_3$): δ 146.7, 131.8, 131.7, 130.9, 130.4, 129.8, 129.1, 128.6, 76.7, 22.2; IR (film) 2922, 2851, 1593, 1460, 1341, 1296, 1244, 1159, 1086, 814, 802 cm^{-1}; HRMS (ESI) Calcd for $C_{14}H_{13}NNaO_3S^+$ ([M+Na]$^+$) 298.0508. Found 298.0507; $[\alpha]_D^{23}$ +110.2 (*c* = 1.00, CHCl$_3$).
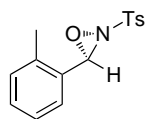
3c [12]: Prepared from *N*-Ts-2-fluorobenzaldimine **2c** (27.0 mg, 0.0974 mmol, 1 equiv) by general procedure 1 as a white solid (23.6 mg, 0.0805 mmol, 83%) with 95% ee as determined by HPLC analysis; HPLC OD3, H/IPA = 10:1, flow rate = 1.0 mL/min, λ = 227 nm, 6.2 min (major isomer), 7.0 min (minor isomer); mp 81–83 °C; ^{1}H NMR (400 MHz, CDCl$_3$) δ 7.93 (2H, d, *J* = 8.4 Hz), 7.43 (2H, d, *J* = 8.7 Hz), 7.45–7.40 (1H, m), 7.26 (1H, ddd, J_{H-H} = 8.0, 1.3 Hz, J_{F-H} = 6.0 Hz), 7.15 (1H, t, *J* = 7.4 Hz), 7.11 (1H, dd, J_{H-H} = J_{F-H} = 9.4 Hz), 5.79 (1H, s), 2.50 (3H, s); ^{13}C NMR (101 MHz, CDCl$_3$) δ 162.9 (d, J_{F-C} = 256.4 Hz), 146.9, 133.2 (d, J_{F-C} = 7.7 Hz), 131.5, 130.4, 129.9, 128.8, 124.9, 118.6 (d, J_{F-C} = 11.6 Hz), 116.0 (d, J_{F-C} = 20.3 Hz), 71.3 (d, J_{F-C} = 6.8 Hz), 22.2; ^{19}F NMR (376 MHz, CDCl$_3$): δ −120.3; IR (film) 1592, 1491, 1395, 1346, 1254, 1188, 1177, 1161, 1094, 1086, 837, 814 cm^{-1}; HRMS (ESI) Calcd for $C_{14}H_{12}FNNaO_3S^+$ ([M+Na]$^+$) 316.0414. Found 316.0413; $[\alpha]_D^{22}$ +85.0 (*c* = 1.01, CHCl$_3$).
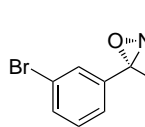
3d: Prepared from *N*-Ts-2-chlorobenzaldimine **2d** (29.3 mg, 0.100 mmol, 1 equiv) by general procedure 1 as a white solid (22.3 mg, 0.0720 mmol, 72%) with 95% ee as determined by HPLC analysis; HPLC OJ3, H/IPA = 80:20, flow rate = 1.0 mL/min, λ = 210 nm, 18.0 min (major isomer), 24.2 min (minor isomer); mp 78–80 °C; ^{1}H NMR (400 MHz, CDCl$_3$) δ 7.93 (2H, d, *J* = 8.2 Hz), 7.46–7.33 (4H, m), 7.32–7.22 (2H, m), 5.85 (1H, s), 2.49 (3H, s); ^{13}C NMR (101 MHz, CDCl$_3$) δ 146.9, 135.3, 132.3, 131.3, 130.4, 130.0, 129.0, 128.8, 127.6, 74.1, 22.2, one carbon was missing probably due to overlapping; IR (film) 2916, 1595, 1352, 1240, 1186, 1175, 1163, 1090, 1053 cm^{-1}; HRMS (ESI) Calcd for $C_{14}H_{12}{}^{35}ClNNaO_3S^+$ ([M+Na]$^+$) 332.0119. Found 332.0118; $[\alpha]_D^{22}$ +23.0 (*c* = 1.01, CHCl$_3$).

3e [12]: Prepared from *N*-Ts-2-bromobenzaldimine **2e** (33.9 mg, 0.100 mmol, 1 equiv) by general procedure 1 as a white solid (27.5 mg, 0.0776 mmol, 78%) with 95% ee as determined by HPLC analysis; HPLC OJ3, H/IPA = 4:1, flow rate = 1.0 mL/min, λ = 210 nm, 20.5 min (major isomer), 25.7 min (minor isomer); mp 82–84 °C; ^{1}H NMR (400 MHz, CDCl$_3$) δ 7.94 (2H, d, *J* = 8.5 Hz), 7.59 (1H, dd, *J* = 6.6, 2.5 Hz), 7.43 (2H, d, *J* = 8.5 Hz), 7.34–7.22 (3H, m), 5.80 (1H, s), 2.49 (3H, s); ^{13}C NMR (101 MHz, CDCl$_3$) δ 146.9, 133.2, 132.5, 131.2, 130.6, 130.4, 130.0, 129.1, 128.2, 124.4, 76.4, 22.2; IR (film) 2924, 2857, 1695, 1587, 1435, 1342, 1236, 1186, 1161, 1084, 1026, 812 cm^{-1}; HRMS (ESI) Calcd for C$_{14}$H$_{12}$^{79}BrNNaO$_3$S$^+$ ([M+Na]$^+$) 375.9613. Found 375.9613; $[\alpha]_D^{23}$ +44.3 (*c* = 1.01, CHCl$_3$).
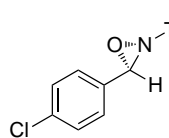
3f [12]: Prepared from *N*-Ts-2-tolualdimine **2f** (27.8 mg, 0.102 mmol, 1 equiv) by general procedure 1 as a white solid (25.5 mg, 0.0881 mmol, 86%) with 96% ee as determined by HPLC analysis; HPLC OD3, H/IPA = 10:1, flow rate = 1.0 mL/min, λ = 229 nm, 6.7 min (major isomer), 11.0 min (minor isomer); mp 52–54 °C; ^{1}H NMR (400 MHz, CDCl$_3$) λ 7.93 (2H, d, *J* = 8.4 Hz), 7.42 (2H, d, *J* = 8.4 Hz), 7.32 (1H, ddd, *J* = 8.8, 7.4, 1.4 Hz), 7.24 (1H, d, *J* = 7.8 Hz), 7.21–7.17 (2H, m), 5.67 (1H, s), 2.51 (3H, s), 2.49 (3H, s); ^{13}C NMR (101 MHz, CDCl$_3$) δ 146.5, 137.9, 131.6, 130.7, 130.6, 130.1, 129.5, 128.9, 126.8, 126.4, 74.7, 21.9, 18.6; IR (film) 2924, 1595, 1491, 1464, 1342, 1250, 1186, 1165, 1088, 812 cm^{-1}; HRMS (ESI) Calcd for C$_{15}$H$_{15}$NNaO$_3$S$^+$ ([M+Na]$^+$) 312.0665. Found 312.0662; $[\alpha]_D^{22}$ +58.0 (*c* = 1.19, CHCl$_3$).

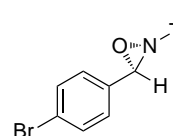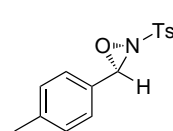**3g** [12]: Prepared from *N*-Ts-3-bromobenzaldimine **2g** (33.9 mg, 0.100 mmol, 1 equiv) by general procedure 1 as a white solid (29.9 mg, 0.0844 mmol, 84%) with 97% ee as determined by HPLC analysis; HPLC OJ3, H/IPA = 80:20, flow rate = 1.0 mL/min, λ = 210 nm, 18.2 min (major isomer), 28.0 min (minor isomer); mp 104–106 °C; ^{1}H NMR (400 MHz, CDCl$_3$) δ 7.92 (2H, d, *J* = 8.4 Hz), 7.59 (1H, ddd, *J* = 8.0, 2.0, 1.0 Hz), 7.55 (1H, t, *J* = 1.7 Hz), 7.44 (2H, d, *J* = 8.1 Hz), 7.40 (1H, dt, *J*s = 8.0, 1.4 Hz), 7.29 (1H, d, *J* = 7.7 Hz), 5.41 (1H, s), 2.50 (3H, s); ^{13}C NMR (101 MHz, CDCl$_3$): δ 147.0, 134.8, 133.2, 131.6, 131.4, 130.6, 130.5, 129.8, 127.4, 123.2, 75.6, 22.2; IR (film) 1595, 1437, 1350, 1238, 1188, 1173, 1092, 1086, 1070, 814 cm^{-1}; HRMS (ESI) Calcd for C$_{14}$H$_{12}$^{79}BrNNaO$_3$S$^+$ ([M+Na]$^+$) 375.9613. Found 375.9614; $[\alpha]_D^{22}$ +86.8 (*c* = 1.04, CHCl$_3$).
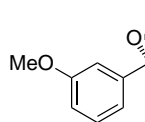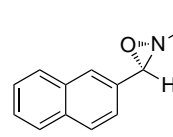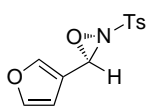
3h: Prepared from *N*-Ts-3-anisaldimine **2h** (28.6 mg, 0.0988 mmol, 1 equiv) by general procedure 1 as a colorless oil (29.8 mg, 0.0976 mmol, 99%) with 95% ee as determined by HPLC analysis; HPLC OD3, H/IPA = 10:1, flow rate = 1.0 mL/min, λ = 210 nm, 8.9 min (major isomer), 11.5 min (minor isomer); ^{1}H NMR (400 MHz, CDCl$_3$) δ 7.93 (2H, d, *J* = 8.2 Hz), 7.42 (2H, d, *J* = 8.2 Hz), 7.30 (1H, t, *J* = 8.0 Hz), 7.06 (1H, dt, *J* = 8.0, 1.3 Hz), 6.99 (1H, ddd, *J* = 8.0, 2.7, 1.3 Hz), 6.90 (1H, dd, *J* = 2.7, 1.3 Hz), 5.42 (1H, s), 3.78 (3H, s), 2.49 (3H, s); ^{13}C NMR (101 MHz, CDCl$_3$) δ 160.2, 146.8, 132.3, 131.7, 130.4, 130.1, 129.8, 121.2, 118.2, 112.6, 76.6, 55.7, 22.2; IR (film) 2963, 2926, 2841, 1595, 1493, 1348, 1267, 1167, 1090, 1040, 906 cm^{-1}; HRMS (ESI) Calcd for C$_{15}$H$_{15}$NNaO$_4$S$^+$ ([M+Na]$^+$) 328.0614. Found 328.0611; $[\alpha]_D^{20}$ +103.9 (*c* = 2.27, CHCl$_3$).

3i [12]: Prepared from *N*-Ts-4-chlorobenzaldimine **2i** (29.5 mg, 0.100 mmol, 1 equiv) by general procedure 1 as a white solid (27.5 mg, 0.0888 mmol, 89%) with 96% ee as determined by HPLC analysis; HPLC OJ3, H/IPA = 80:20, flow rate = 1.0 mL/min, λ = 234 nm, 19.6 min (major isomer), 23.7 min (minor isomer); mp 85–87 °C; ^{1}H NMR (400 MHz, CDCl$_3$) δ 7.92 (2H, d, *J* = 8.0 Hz), 7.43 (2H, d, *J* = 8.4 Hz), 7.38–7.37 (4H, m), 5.43 (1H, s), 2.49 (3H, s); ^{13}C NMR (101 MHz, CDCl$_3$) δ 146.9, 137.9, 131.7, 130.4, 129.9, 129.8, 129.4, 75.9, 22.2, one carbon was missing probably due to overlapping; IR (film) 1597, 1495, 1356, 1344, 1186, 1180, 1157, 1016, 816 cm^{-1}; HRMS (ESI) Calcd for C$_{14}$H$_{12}$^{35}ClNNaO$_3$S$^+$ ([M+Na]$^+$) 332.0119. Found 332.0118; [α]$_D^{22}$ +88.5 (*c* = 1.05, CHCl$_3$).

3j [12]: Prepared from *N*-Ts-4-bromobenzaldimine **2j** (33.6 mg, 0.0993 mmol, 1 equiv) by general procedure 1 as a white solid (30.2 mg, 0.0853 mmol, 86%) with 96% ee as determined by HPLC analysis; HPLC OJ3, H/IPA = 80:20, flow rate = 1.0 mL/min, λ = 210 nm, 19.6 min (major isomer), 23.6 min (minor isomer); mp 92–93 °C; ^{1}H NMR (400 MHz, CDCl$_3$) δ 7.92 (2H, d, *J* = 8.5 Hz), 7.54 (2H, d, *J* = 8.5 Hz), 7.43 (2H, d, *J* = 8.5 Hz), 7.30 (2H, d, *J* = 8.5 Hz), 5.42 (1H, s), 2.49 (3H, s); ^{13}C NMR (101 MHz, CDCl$_3$) δ 146.9, 132.4, 131.6, 130.4, 130.1, 130.0, 129.7, 126.3, 76.0, 22.2; IR (film) 1505, 1350, 1188, 1176, 1161, 1094, 1086, 1070, 1013, 816 cm^{-1}; HRMS (ESI) Calcd for C$_{14}$H$_{12}$^{79}BrNNaO$_3$S$^+$ ([M+Na]$^+$) 375.9613. Found 375.9613; [α]$_D^{23}$ +70.9 (*c* = 1.06, CHCl$_3$).

3k [12]: Prepared from *N*-Ts-4-tolualdimine **2k** (27.3 mg, 0.0999 mmol, 1 equiv) by general procedure 1 as a white solid (26.2 mg, 0.0905 mmol, 91%) with 95% ee as determined by HPLC analysis; HPLC OJ3, H/IPA = 80:20, flow rate = 1.0 mL/min, λ = 230 nm, 24.0 min (major isomer), 28.0 min (minor isomer); mp 77–79 °C; ^{1}H NMR (400 MHz, CDCl$_3$) δ 7.92 (2H, d, *J* = 8.4 Hz), 7.41 (2H, d, *J* = 8.4 Hz), 7.32 (2H, d, *J* = 8.4 Hz), 7.19 (2H, d, *J* = 8.1 Hz), 5.41 (1H, s), 2.48 (3H, s), 2.36 (3H, s); ^{13}C NMR (101 MHz, CDCl$_3$) δ 146.7, 142.1, 131.9, 130.4, 129.8, 128.5, 127.9, 76.8, 22.2, 21.8, one carbon was missing probably due to overlapping; IR (film) 1593, 1385, 1348, 1236, 1186, 1171, 1159, 1119, 1094, 1088, 816 cm^{-1}; HRMS (ESI) Calcd for C$_{15}$H$_{15}$NNaO$_3$S$^+$ ([M+Na]$^+$) 312.0665. Found 312.0663; [α]$_D^{23}$ +95.3 (*c* = 1.00, CHCl$_3$).
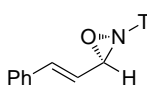
3l [12]: Prepared from *N*-Ts-2-naphthaldimine **2l** (31.1 mg, 0.100 mmol, 1 equiv) by general procedure 1 as a white solid (32.4 mg, 0.096 mmol, 99%) with 90% ee as determined by HPLC analysis; HPLC OD3, H/IPA = 10:1, flow rate = 1.0 mL/min, λ = 230 nm, 10.0 min (major isomer), 10.8 min (minor isomer); mp 92–93 °C; ^{1}H NMR (400 MHz, CDCl$_3$) δ 8.02 (1H, s), 7.96 (2H, d, *J* = 8.5 Hz), 7.90–7.82 (3H, m), 7.58–7.50 (2H, m), 7.44 (2H, d, *J* = 8.5 Hz), 7.39 (1H, dd, *J* = 8.5, 1.4 Hz), 5.62 (1H, s), 2.50 (3H, s); ^{13}C NMR (101 MHz, CDCl$_3$) δ 146.7, 135.0, 132.8, 131.7, 130.3, 130.0, 129.7, 129.1, 128.6, 128.2, 128.1, 127.9, 127.1, 123.7, 76.9, 22.1; IR (film) 1593, 1344, 1202, 1171, 1088, 822 cm^{-1}; HRMS (ESI) Calcd for C$_{18}$H$_{15}$NNaO$_3$S$^+$ ([M+Na]$^+$) 348.0665. Found 348.0664. [α]$_D^{23}$ +59.4 (*c* = 0.504, CHCl$_3$).

3m: Prepared from *N*-Ts-3-furaldimine **2m** (24.8 mg, 0.0995 mmol, 1 equiv) by general procedure 1 as a colorless oil (25.3 mg, 0.0954 mmol, 96%) with 93% ee as determined by HPLC analysis; HPLC OD3, H/IPA = 10:1, flow rate = 1.0 mL/min, λ = 227 nm, 8.3 min (major isomer), 9.8 min (minor isomer); ^{1}H NMR (400 MHz, CDCl$_3$) δ 7.91 (2H, d, *J* = 8.4 Hz), 7.78 (1H, d, *J* = 0.8 Hz), 7.42 (2H, d, *J* = 8.4 Hz), 7.41 (1H, s), 6.36 (1H, d, *J* = 0.8 Hz), 5.48 (1H, s), 2.49 (3H, s); ^{13}C NMR (101 MHz, CDCl$_3$) δ 146.8, 145.4, 144.6, 131.6, 130.4, 129.7, 118.4, 108.6, 71.5, 22.2; IR (film) 3140, 2918, 1595, 1508, 1344, 1163, 1088, 1016, 874, 808 cm^{-1}; HRMS (ESI) Calcd for C$_{12}$H$_{11}$NNaO$_4$S$^+$ ([M+Na]$^+$) 288.0301. Found 288.0301; $[\alpha]_D^{20}$ +80.5 (*c* = 0.670, CHCl$_3$).
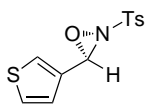
3n: Prepared from *N*-Ts-3-thienylaldimine **2n** (26.6 mg, 0.100 mmol, 1 equiv) by general procedure 1 as a white solid (25.5 mg, 0.0906 mmol, 91%) with 94% ee as determined by HPLC analysis; HPLC OD3, H/IPA = 10:1, flow rate = 1.0 mL/min, λ = 210 nm, 10.3 min (major isomer), 17.2 min (minor isomer); mp 55–57 °C; ^{1}H NMR (400 MHz, CDCl$_3$) δ 7.91 (2H, d, *J* = 8.5 Hz), 7.66 (1H, dd, *J* = 3.0, 1.1 Hz), 7.42 (2H, d, *J* = 8.5 Hz), 7.32 (1H, dd, *J* = 5.3, 3.0 Hz), 7.05 (1H, dd, *J* = 5.3, 1.1 Hz), 5.53 (1H, s), 2.48 (3H, s); ^{13}C NMR (101 MHz, CDCl$_3$) δ 146.8, 133.2, 131.8, 130.4, 129.8, 129.4, 127.5, 126.2, 73.1, 22.2; IR (film) 3103, 2920, 1597, 1495, 1400, 1373, 1155, 1121, 1030, 1003, 812 cm^{-1}; HRMS (ESI) Calcd for C$_{12}$H$_{11}$NNaO$_3$S$_2^+$ ([M+Na]$^+$) 304.0073. Found 304.0071; $[\alpha]_D^{23}$ +51.8 (*c* = 1.65, CHCl$_3$).

3o: Prepared from *N*-Ts-(*E*)-cinnamaldimine **2o** (28.4 mg, 0.0995 mmol, 1 equiv) by general procedure 1 as a white solid (25.5 mg, 0.0846 mmol, 85%) with 96% ee as determined by HPLC analysis; HPLC OD3, H/IPA = 19:1, flow rate = 1.0 mL/min, λ = 258 nm, 22.9 min (major isomer), 25.2 min (minor isomer); mp 67–68 °C; ^{1}H NMR (400 MHz, CDCl$_3$) δ 7.90 (2H, d, *J* = 8.2 Hz), 7.48–7.38 (4H, m), 7.38–7.30 (3H, m), 7.12 (1H, d, *J* = 16.4 Hz), 5.88 (1H, dd, *J* = 16.4, 7.9 Hz), 5.15 (1H, d, *J* = 7.9 Hz), 2.48 (3H, s); ^{13}C NMR (101 MHz, C$_6$D$_6$) δ 145.8, 142.0, 134.9, 133.0, 130.0, 129.54, 129.48, 128.8, 127.6, 120.2, 77.6, 21.2; IR (film) 2922, 2851, 1595, 1344, 1186, 1163, 1123, 1090, 974, 812 cm^{-1}; HRMS (ESI) Calcd for C$_{16}$H$_{15}$NNaO$_3$S$^+$ ([M+Na]$^+$) 324.0665. Found 324.0664; $[\alpha]_D^{22}$ +152.3 (*c* = 2.03, CHCl$_3$).
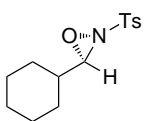
3r [12]: Prepared from *N*-Ts-cyclohexanecarbaldimine **2r** (26.7 mg, 0.101 mmol, 1 equiv) by general procedure 2 as a white solid (26.0 mg, 0.0924 mmol, 91%) with 98% ee as determined by HPLC analysis; HPLC OD3, H/IPA = 95:5, flow rate = 0.5 mL/min, λ = 226 nm, 12.3 min (major isomer), 13.2 min (minor isomer); mp 32–33 °C; ^{1}H NMR (400 MHz, CDCl$_3$) δ 7.85 (2H, d, *J* = 8.2 Hz), 7.39 (2H, d, *J* = 8.2 Hz), 4.47 (1H, s), 2.47 (3H, s), 1.80–1.71 (4H, m), 1.70–1.63 (1H, m), 1.62–1.55 (1H, m), 1.29–1.09 (5H, m); ^{13}C NMR (101 MHz, CDCl$_3$) δ 146.4, 132.1, 130.3, 129.5, 81.5, 38.9, 27.4, 27.2, 26.2, 25.3, 22.1; IR (film) 2928, 2855, 1595, 1450, 1344, 1165, 1090, 858, 814 cm^{-1}; HRMS (ESI) Calcd for C$_{14}$H$_{19}$NNaO$_3$S$^+$ ([M+Na]$^+$) 304.0978. Found 304.0976; $[\alpha]_D^{23}$ +104.9 (*c* = 1.70, CHCl$_3$).
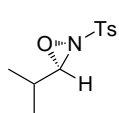
3s [12]: Prepared from *N*-Ts-isobutyraldimine **2s** (22.3 mg, 0.0990 mmol, 1 equiv) by general procedure 2 as a white solid (18.8 mg, 0.0777 mmol, 78%) with 95% ee as determined by HPLC analysis; HPLC OD3, H/IPA = 19:1, flow rate = 0.5 mL/min, λ = 226 nm, 11.0 min (minor isomer), 12.1 min (major isomer); ^{1}H NMR (400 MHz, CDCl$_3$) δ 7.86 (2H, d, *J* = 8.2 Hz), 7.39 (2H, d, *J* = 8.2 Hz), 4.48 (1H, d, *J* = 6.5 Hz), 2.47 (3H, s), 1.89 (1H, octet, *J* = 6.5 Hz), 1.03 (3H, d, *J* = 6.5 Hz), 1.01 (3H, d, *J* = 6.5 Hz); ^{13}C NMR (101 MHz, CDCl$_3$) δ 146.5, 132.0, 130.3, 129.5, 82.3, 29.9, 22.1, 16.9, 16.8; IR (film) 2970, 2934, 1597, 1470, 1346, 1188, 1163, 1090, 854, 814 cm^{-1}; HRMS (ESI) Calcd for C$_{11}$H$_{15}$NNaO$_3$S$^+$ ([M+Na]$^+$) 264.0665. Found 264.0664; $[\alpha]_D^{23}$ +112.1 (*c* = 2.07, CHCl$_3$).
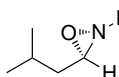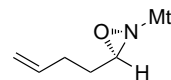
5b: Prepared from *N*-Mts-isovaleraldimine **4b** (26.4 mg, 0.0987 mmol, 1 equiv) by general procedure 2 as a colorless oil (25.8 mg, 0.0910 mmol, 92%) with 95% ee as determined by HPLC analysis; HPLC IC3, H/IPA = 98:2, flow rate = 1.0 mL/min, λ = 210 nm, 9.4 min (major isomer), 10.6 min (minor isomer); ^{1H} NMR (400 MHz, CDCl$_3$) δ 7.00 (2H, s), 4.73 (1H, t, *J* = 5.4 Hz), 2.70 (6H, s), 2.32 (3H, s), 1.93 (1H, nonet, *J* = 6.7 Hz), 1.70 (1H, ddd, *J* = 14.3, 6.7, 5.4 Hz), 1.66 (1H, ddd, *J* = 14.3, 6.7, 5.4 Hz), 1.01 (6H, t, *J* = 6.7 Hz); ^{13}C NMR (101 MHz, CDCl$_3$) δ 144.9, 142.0, 132.4, 76.9, 39.9, 25.3, 23.4, 23.1, 22.8, 21.5, one carbon atom was missing probably due to overlapping; IR (film) 2959, 1603, 1468, 1406, 1342, 1165, 1055, 1034, 853 cm^{-1}; HRMS (ESI) Calcd for C$_{14}$H$_{21}$NNaO$_3$S$^+$ ([M+Na]$^+$) 306.1134. Found 306.1131; $[\alpha]_D^{22}$ +120.6 (*c* = 2.25, CHCl$_3$).
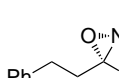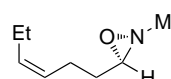
5c: Prepared from *N*-Mts-hydrocinnamaldimine **4c** (31.0 mg, 0.0982 mmol, 1 equiv) by general procedure 2 as a white solid (28.4 mg, 0.0856 mmol, 87%) with 96% ee as determined by HPLC analysis; HPLC IC3, H/IPA = 98:2, flow rate = 1.0 mL/min, λ = 210 nm, 17.3 min (major isomer), 19.0 min (minor isomer); ^{1}H NMR (400 MHz, CDCl$_3$) δ 7.29 (2H, t, *J* = 7.2 Hz), 7.21 (1H, t, *J* = 7.2 Hz), 7.18 (2H, d, *J* = 7.2 Hz), 7.00 (2H, s), 4.77 (1H, t, *J* = 4.7 Hz), 2.78 (2H, t, *J* = 8.1 Hz), 2.68 (6H, s), 2.33 (3H, s), 2.23–2.08 (2H, m); ^{13}C NMR (101 MHz, CDCl$_3$) δ 145.0, 142.0, 140.1, 132.4, 129.8, 129.0, 128.6, 126.7, 76.9, 32.7, 29.9, 23.5, 21.5; IR (film) 2918, 2849, 1603, 1456, 1340, 1231, 1165, 1055, 1034, 856, 837 cm^{-1}; HRMS (ESI) Calcd for C$_{18}$H$_{21}$NNaO$_3$S$^+$ ([M+Na]$^+$) 354.1134. Found 354.1135; $[\alpha]_D^{23}$ +87.6 (*c* = 1.69, CHCl$_3$).
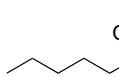
5d: Prepared from *N*-Mts-caproaldimine **4d** (24.9 mg, 0.0885 mmol, 1 equiv) by general procedure 2 as a colorless oil (23.0 mg, 0.0773 mmol, 87%) with 94% ee as determined by HPLC analysis; HPLC IC3, H/IPA = 99:1, flow rate = 1.0 mL/min, λ = 210 nm, 14.7 min (major isomer), 17.1 min (minor isomer); ^{1}H NMR (400 MHz, CDCl$_3$) δ 7.00 (2H, s), 4.71 (1H, t, *J* = 5.0 Hz), 2.70 (6H, s), 2.32 (3H, s), 1.85–1.77 (2H, m), 1.49 (2H, quintet, *J* = 7.4 Hz), 1.39–1.25 (4H, m), 0.89 (3H, t, *J* = 6.9 Hz); ^{13}C NMR (101 MHz, CDCl$_3$) δ 144.9, 142.1, 132.4, 130.0, 77.6, 31.5, 31.0, 23.6, 23.4, 22.7, 21.5, 14.2; IR (film) 2928, 2860, 1603, 1560, 1456, 1404, 1342, 1227, 1186, 1165, 1034, 853 cm^{-1}; HRMS (ESI) Calcd for C$_{15}$H$_{23}$NNaO$_3$S$^+$ ([M+Na]$^+$) 320.1291. Found 320.1290; $[\alpha]_D^{24}$ +90.4 (c=1.09, CHCl$_3$).

5e: Prepared from *N*-Mts-4-pentenylaldimine **4e** (26.7 mg, 0.101 mmol, 1 equiv) by general procedure 2 as a colorless oil (24.0 mg, 0.0835 mmol, 83%) with 96% ee as determined by HPLC analysis; HPLC IC3, H/IPA = 99:1, flow rate = 1.0 mL/min, λ = 210 nm, 17.2 min (major isomer), 19.2 min (minor isomer); ^{1}H NMR (400 MHz, CDCl$_3$) δ 7.00 (2H, s), 5.80 (1H, ddt, J = 17.3, 10.3, 6.9 Hz), 5.08 (1H, dq, J = 17.3, 1.4 Hz), 5.03 (1H, dq, J = 10.3, 1.4 Hz), 4.75 (1H, t, J = 4.9 Hz) 2.69 (6H, s), 2.32 (3H, s), 2.23 (2H, q, J = 4.9 Hz), 2.00–1.85 (2H, m); ^{13}C NMR (101 MHz, CDCl$_3$) δ 176.6, 144.4, 140.6, 136.2, 132.2, 131.7, 116.7, 35.2, 29.0, 23.3, 21.4; IR (film) 2980, 2941, 1603, 1449, 1344, 1165, 1055, 1034, 918, 854 cm^{-1}; HRMS (ESI) Calcd for C$_{14}$H$_{19}$NNaO$_3$S$^+$ ([M+Na]$^+$) 304.0978. Found 304.0975; $[\alpha]_D^{22}$ +108.4 (c = 4.41, CHCl$_3$).

5f: Prepared from *N*-Mts-(*Z*)-4-heptenylaldimine **4f** (29.1 mg, 0.0992 mmol, 1 equiv) by general procedure 2 as a colorless oil (23.3 mg, 0.0753 mmol, 76%) with 95% ee as determined by HPLC analysis; HPLC IC3, H/IPA = 99:1, flow rate = 1.0 mL/min, λ = 210 nm, 14.2 min (major isomer), 15.3 min (minor isomer); ^{1}H NMR (400 MHz, CDCl$_3$) δ 7.00 (2H, s), 5.45 (1H, tt, J = 7.3, 1.4 Hz), 5.31 (1H, tt, J = 7.3, 1.4 Hz), 4.74 (1H, t, J = 4.8 Hz), 2.69 (6H, s), 2.33 (3H, s), 2.22 (2H, q, J = 7.3 Hz), 2.04 (2H, quintet, J = 7.3 Hz), 1.89 (1H, dtd, J = 14.7, 7.3, 4.8 Hz), 1.86 (1H, dtd, J = 14.7, 7.3, 4.8 Hz), 0.96 (3H, t, J = 7.6 Hz); ^{13}C NMR (101 MHz, CDCl$_3$) δ 144.9, 142.1, 134.0, 132.4, 130.0, 126.5, 77.3, 31.3, 23.5, 21.7, 21.5, 20.8, 14.5; IR (film) 2970, 2934, 1628, 1603, 1560, 1456, 1339, 1319, 1155, 1055, 1034, 853 cm^{-1}; HRMS (ESI) Calcd for C$_{16}$H$_{23}$NNaO$_3$S$^+$ ([M+Na]$^+$) 332.1291. Found 332.1294; $[\alpha]_D^{24}$ +7.3 (c = 1.00, CHCl$_3$).

2.4.2.6   General Procedure for Kinetic Resolution of α-Chiral Imines
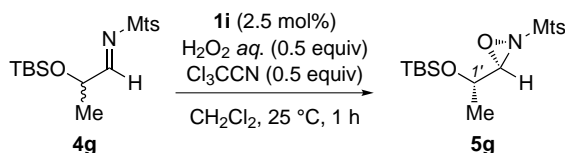

To a solution of chiral iminophosphorane **1i** (4.33 mg, 0.0050 mmol, 0.025 equiv), *N*-sulfonyl imine **4g** (72.0 mg, 0.20 mmol, 1 equiv), and Cl$_3$CCN (12.0 μL, 0.120 mmol, 0.6 equiv) in CH$_2$Cl$_2$ (4.0 mL) was added an aqueous 35% solution of H$_2$O$_2$ (8.8 μL, 0.5 equiv, titrated by using KMnO$_4$) at 25 °C under Ar atmosphere. After being stirred for 1 h, the reaction was quenched by the addition of a saturated aqueous solution of Na$_2$SO$_3$ (5 mL). The aqueous phase was extracted with EA (2 × 10 mL). The combined organic extracts were dried over Na$_2$SO$_4$ and filtered. The organic phase was concentrated under reduced pressure. The residue thus obtained was purified by column chromatography on silica gel (H/EA = 50/1 as eluent) to afford a diastereomeric mixture of oxaziridine **5g** as colorless oil (34.4 mg, 0.0897 mmol, 46%). The diastereomeric ratio of **5g** was determined by HPLC analysis (dr = 87.9:0.2:7.2:4.7).

5g: HPLC IC3, H/IPA = 99:1, flow rate = 0.5 mL/min, λ = 210 nm, 10.9 min (major diastereomer

of (1'*S*)-isomer), 12.3 min (minor diastereomer of (1'*R*)-isomer), 15.5 min (major diastereomer of (1'*R*)-isomer), 16.5 min (minor diastereomer of (1'*S*)-isomer); ^{1}H NMR (400 MHz, CDCl$_3$) *major isomer* δ 7.01 (2H, s), 4.59 (1H, d, *J* = 6.3 Hz), 3.66 (1H, quintet, *J* = 6.3 Hz), 2.69 (6H, s), 2.33 (3H, s), 1.28 (3H, d, *J* = 6.3 Hz), 0.88 (9H, s), 0.05 (6H, s); ^{13}C NMR (101 MHz, CDCl$_3$) *major isomer* δ 145.1, 142.2, 132.4, 129.6, 79.3, 69.0, 26.0, 23.5, 21.5, 19.4, 18.4, −4.4, −4.6; IR (film) 2954, 2930, 2859, 1602, 1464, 1350, 1254, 1188, 1173, 1115, 988, 835 cm^{-1}; HRMS (ESI) Calcd for $C_{18}H_{31}NNaO_4SSi^+$ ([M+Na]$^+$) 403.1635. Found 408.1634.

2.4.3 Derivatizations

2.4.3.1 Intramolecular Oxygen Atom-Transfer Reaction of 5e
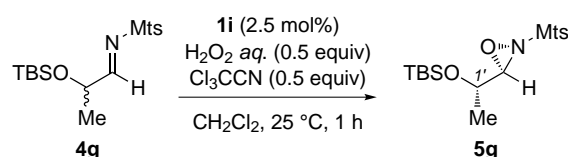

A solution of oxaziridine **5e** (21.0 mg, 0.0731 mmol) in CHCl$_3$ (3.0 mL) was stirred for 77 h at 60 °C under Ar atmosphere. After cooling to room temperature, all volatiles were evaporated off to give crude epoxy imine **13a**. The imine **13a** was used for the following reaction without further purification.

### 2.4.3.2 Reductive Cyclization to *N*-Mts Pyrrolidine Methanol 14a
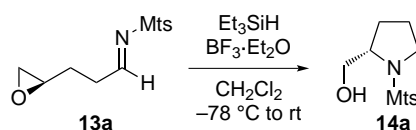
To a solution of the crude imine **13e** in CH$_2$Cl$_2$ (0.70 mL) was added BF$_3$ · Et$_2$O (12.0 μL, 0.095 mmol) at −78 °C under Ar. Then, Et$_3$SiH (26.0 μL, 0.21 mmol) was slowly added over 5 min, and the reaction mixture was stirred for 0.5 h at −78 °C and for 2.5 h at room temperature. The reaction was quenched by the addition of a saturated aqueous solution of NaHCO$_3$. The aqueous phase was extracted with EA twice and organic extracts were washed with brine. The combined organic extracts were dried over Na$_2$SO$_4$ and filtered. After concentration, the resulting residue was purified by column chromatography on silica gel (H/EA = 60/40 as an eluent) to afford **14a** in 74% yield (15.3 mg, 0.0540 mmol).
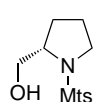
14a: HPLC AD3, H/EtOH = 95:5, flow rate = 1.0 mL/min, λ = 210 nm, 44.9 min (minor isomer), 48.1 min (major isomer); ^{1}H NMR (400 MHz, CDCl$_3$) δ 6.97 (2H, s), 4.00 (1H, dq, *J* = 9.6, 4.6 Hz), 3.59 (1H, dd, *J* = 11.4, 5.0 Hz), 3.53 (1H, dd, *J* = 11.4, 5.0 Hz), 3.32 (1H, dt, *J* = 10.1, 6.9 Hz), 3.08 (1H, dt, *J* = 10.1, 6.4 Hz), 2.66 (6H, s), 2.40 (1H, brs), 2.31 (3H, s), 2.12–2.00 (1H, m), 1.94–1.81 (3H, m); ^{13}C NMR (101 MHz, CDCl$_3$) δ 143.3, 140.5,

132.6, 132.4, 65.5, 60.9, 49.0, 29.5, 24.9, 23.3, 21.3; IR (film) 3503 (br), 2974, 2940, 1603, 1456, 1308, 1194, 1148, 1059, 1043, 854 cm^{-1}; HRMS (ESI) Calcd for $C_{14}H_{21}NNaO_3S^+$ ([M+Na]$^+$) 306.1134. Found 306.1129; $[\alpha]_D^{20}$ −5.3 (c = 1.80, CHCl$_3$).
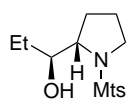
14b: HPLC AD3, H/EtOH = 95:5, flow rate = 1.0 mL/min, λ = 210 nm, 20.1 min (minor isomer), 24.5 min (major isomer); ^{1}H NMR (400 MHz, CDCl$_3$) δ 6.97 (2H, s), 3.93 (1H, dq, J = 8.2, 4.4 Hz), 3.45 (1H, dt, J = 11.0, 6.5 Hz), 3.37 (1H, td, J = 7.1, 4.4 Hz), 2.98 (1H, dt, J = 11.0, 6.9 Hz), 2.77 (1H, brs), 2.67 (6H, s), 2.30 (3H, s), 2.04 (1H, dq, J = 12.4, 7.4 Hz), 1.93–1.78 (2H, m), 1.78–1.64 (1H, m), 1.54 (1H, dqd, J = 15.1, 7.8, 2.7 Hz), 1.37–1.24 (1H, m), 0.96 (3H, t, J = 7.4 Hz); ^{13}C NMR (101 MHz, CDCl$_3$) δ 143.3, 140.6, 132.5, 132.2, 75.1, 64.2, 49.1, 29.1, 26.5, 25.5, 23.4, 21.3, 10.1; IR (film) 3505, 2920, 1603, 1558, 1454, 1400, 1333, 1290, 1142, 1055, 962, 860 cm^{-1}; HRMS (ESI) Calcd for $C_{16}H_{25}NNaO_3S^+$ ([M+Na]$^+$) 334.1447. Found 334.1445; $[\alpha]_D^{21}$ +0.66 (c = 1.00, CHCl$_3$).

2.4.3.3 Preparation of Authentic Sample of 14a from Commercially Available (*S*)-Pyrrolidine Methanol
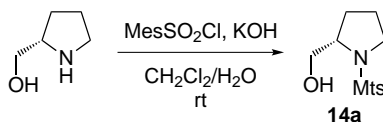
To a solution of L-prolinol (18.4 mg, 0.182 mmol) in CH$_2$Cl$_2$ (1.0 mL) were added a 50% aqueous solution of KOH (0.2 mL) and MesSO$_2$Cl (133.2 mg, 0.609 mmol) at room temperature. An ordinary work-up and subsequent purification by column chromatography on silica gel yielded **14a** (37.9 mg, 0.127 mmol) as a colorless oil.

2.4.3.4 Oxyamination of *N*-Acyl Indole with 3b [25j]
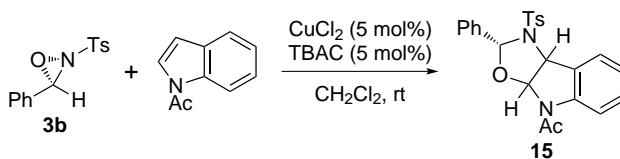
A 0.02 M solution of copper(II) chloride and tetra-*n*-butylammonium chloride in CH$_2$Cl$_2$ (0.50 mL, 0.010 mmol), prepared by following the literature procedure, [25j] was added to a solution of *N*-acetyl indole (32.3 mg, 0.203 mmol) in CH$_2$Cl$_2$ (0.50 mL) at room temperature. Oxaziridine **3b** (103.3 mg, 0.404 mmol) was added and the reaction mixture was stirred for 21.5 h under Ar. The mixture was concentrated and the diastereomeric ratio of the products was determined by ^{1}H NMR analysis of the crude residue in CDCl$_3$. Subsequent purification by ash column chromatography on silica gel (CHCl$_3$/EA = 99:1 as an eluent) gave **15** as a mixture of diastereomers in 76% yield (67.0 mg, 0.154 mmol). Diastereomers were partially separated by using PTLC for spectroscopic assignments. **15**: HPLC IB, H/EtOH = 95:5, flow rate = 0.5 mL/min, λ = 210 nm, 60.5 min

(major isomer of major diastereomer), 65.9 min (minor isomer of minor diastereomer), 84.8 min (minor isomer of major diastereomer), 88.8 min (major isomer of minor diastereomer); ^{1}H NMR (400 MHz, CDCl$_3$) *major isomer* δ 8.24 (1H, d, J = 7.8 Hz), 7.92 (1H, J = 7.3 Hz), 7.40 (2H, t, J = 8.2 Hz), 7.26–7.19 (2H, m), 7.17–7.10 (3H, m), 7.10–7.04 (2H, m), 6.99 (2H, d, J = 8.2 Hz), 6.25 (1H, d, J = 6.0 Hz), 6.12 (1H, d, J = 6.0 Hz), 5.58 (1H, s), 2.38 (3H, s), 2.35 (3H, s); *minor isomer* δ 7.88 (2H, d, J = 8.2 Hz), 7.68 (1H, d, J = 8.2 Hz), 7.43 (2H, d, J = 8.2 Hz), 7.35 (1H, d, J = 7.3 Hz), 7.16–7.06 (3H, m), 7.06–6.97 (3H, m), 6.93 (1H, t, J = 7.3 Hz), 6.63 (1H, s), 5.69 (1H, d, J = 6.4 Hz), 5.63 (1H, d, J = 6.4 Hz), 2.51 (3H, s), 2.34 (3H, s); ^{13}C NMR (101 MHz, CDCl$_3$) *major isomer* δ 170.1, 143.7, 143.6, 137.6, 131.4, 130.9, 130.0, 129.3, 128.0, 127.8$_1$, 127.7$_8$, 126.1, 125.2, 116.4, 89.6, 89.5, 64.2, 24.3, 21.8, one carbon was missing probably due to overlapping; *minor isomer* δ 169.4, 145.3, 141.9, 137.4, 134.7, 130.6, 130.3, 128.5, 128.2, 127.9, 126.4, 125.8, 125.7, 124.6, 116.5, 92.6, 91.5, 63.7, 24.2, 22.1; IR (film) *major isomer* 3034, 2926, 2893, 1684, 1479, 1395, 1354, 1339, 1157, 1092, 1057 cm^{-1}; *minor isomer* 3034, 2926, 1680, 1479, 1395, 1356, 1281, 1165, 1090, 1038 cm^{-1}; HRMS (ESI) *major isomer* Calcd for $C_{24}H_{22}N_2NaO_4S^+$ ([M+Na]$^+$) 457.1192. Found 457.1192; *minor isomer* Calcd for $C_{24}H_{22}N_2NaO_4S^+$ ([M+Na]$^+$) 457.1192. Found 457.1193.

2.4.4   Solvent and Protective Group Effect on the Oxidation of imines with 1a

Aromatic hydrocarbon seems to be a uniquely effective solvent for the oxidation of **2a** and toluene is the solvent of choice. MeCN does not have sufficient electrophilicity to activate hydroperoxide. *N*-Sulfonyl group was found to be the best protective group for the imine nitrogen.

Table 2.3 Solvent and Protective Group Effect

entry[a]	G	solvent	yield (%)b	ee (%)[c]	comments
1	Ts (**2a**)	toluene	99	68	Entry 1 of Table 2.1
2	Ts (**2a**)	CH$_2$Cl$_2$	18	42	
3	Ts (**2a**)	Et$_2$O	trace	-	**2a** was remained.
4	Ts (**2a**)	THF	20	46	
5	Ts (**2a**)	MeCN	20	1	
6	Ts (**2a**)	MeCN	not observed	-	without Cl$_3$CCN
7	Boc	toluene	< 10	not determined	crude ^{1}H NMR
8	P(O)Ph$_2$	toluene	< 10	not determined	crude ^{1}H NMR

[a]Reactions were performed on 0.1 mmol scale with 1.2 equiv of 35% aqueous solution of H_2O_2, 1.2 equiv of Cl$_3$CCN, and 5 mol% of **1a** in solvent (2.0 mL) at 0 °C for 4.5 h. [b]Isolated yield. [c]Enantiomeric excess was analyzed by chiral stationary phase HPLC.

2.4.5 Results of the Reactions with Achiral Organic Base Catalysts

Relatively strong organic bases are able to promote the Payne-type oxidation of *N*-tosyl imine **2a** under similar conditions.

Table 2.4 Achiral organic base catalyzed oxidation of **2a**

entry[a]	base	yield (%)[b]	comments
1	Et$_3$N	trace	
2	TMG	88	7% of **2a** was remained.[c]
3	DBU	72	3% of **2a** was remained.[c]
4	BEMP	88	5% of **2a** was remained.[c]

[a]Reactions were performed on 0.1 mmol scale with 1.2 equiv of 35% aqueous solution of H$_2$O$_2$, 1.2 equiv of Cl$_3$CCN, and 5 mol% of base in toluene (2.0 mL) at 0 °C for 4.5 h. [b]Isolated yield. [c]Determined by ^{1}H NMR analysis of crude aliquots.

2.4.6 Experimental Support for Intramolecular Oxygen-Transfer Process

Intramolecular oxygen-transfer involved in the derivatization of **4** from **5e** was strongly supported by the following cross-over experiment.
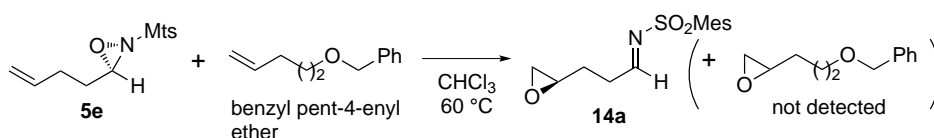
Procedure for the cross-over experiment: A solution of oxaziridine **5e** (26.1 mg, 0.0928 mmol) and benzyl pent-4-enyl ether (15.7 mg, 0.0891 mmol) in CHCl$_3$ (3.7 mL) was stirred for 72 h at 60 °C under Ar atmosphere. After cooling to room temperature, all volatiles were evaporated off. The ^{1}H NMR analysis of the crude residue revealed that almost all **5e** was converted into **14a** without concomitant epoxidation of benzyl pent-4-enyl ether. This observation strongly suggests that intramolecular oxygen transfer mechanism is operative in the formation of **14a** from **5e**.

References and notes

(1) Lawesson, S.-O.; Schroll, G. In *The Chemistry of Carboxylic Acids and Esters*; Patai, S., Ed.; John Wiley: New York, NY, 1969; Chapter 14, pp 669–703.

(2) (a) Shu, L.; Shi, Y. *Tetrahedron Lett.* **1999**, *40*, 8721. (b) Shu, L.; Shi, Y. *Tetrahedron* **2001**, *57*, 5213. (c) Wang, Z.-X.; Shu, L.; Frohn, M.; Tu, Y.; Shi, Y. *Org. Synth.* **2003**, *80*, 9.

(3) (a) Peris, G.; Jakobsche, C. E.; Miller, S. J. *J. Am. Chem. Soc.* **2007**, *129*, 8710. (b) Jakobsche, C. E.; Peris, G.; Miller, S. J. *Angew. Chem., Int. Ed.* **2008**, *47*, 6707. (c) Peris, G.; Miller, S. J. *Org. Lett.* **2008**, *10*, 3049. (d) Kolundzic, F.; Noshi, M. N.; Tjandra, M.; Movassaghi, M.; Miller, S. J. *J. Am. Chem. Soc.* **2011**, *133*, 9104.

(4) For leading references on epoxidation using RCN–H$_2$O$_2$, see: (a) Payne, G. B.; Deming, P. H.; Williams, P. H. *J. Org. Chem.* **1961**, *26*, 659. (b) Payne, G. B. *Tetrahedron* **1962**, *18*, 763. (c) Bach, R. D.; Knight, J. W. *Org. Synth.* **1981**, *60*, 63. (d) Arias, L. A.; Adkins, S.; Nagel, C. J.; Bach, R. D. *J. Org. Chem.* **1983**, *48*, 888

(5) For reviews on phosphonium salt catalyses, see: (a) Werner, T. *Adv. Synth. Catal.* **2009**, *351*, 1469. (b) Enders, D.; Nguyen, T. V. *Org. Biomol. Chem.* **2012**, *10*, 5327.

(6) For a review on organic base catalysis, see: Palomo, C.; Oiarbide, M.; López, R. *Chem. Soc. Rev.* **2009**, *38*, 632.

(7) Triaminoiminophosphoranes are also known as a P1-phosphazenes, which was developed by Schwesinger, see: (a) Schwesinger, R.; Schlemper, H. *Angew. Chem., Int. Ed. Engl.* **1987**, *26*, 1167. For review, see: (b) *Superbases for Organic Synthesis: Guanidines, Amidines, Phosphazenes and Related Organocatalysts*; Ishikawa, T., Ed.; John Wiley: West Sussex, U.K., 2009.

(8) (a) Uraguchi, D.; Ooi, T. *J. Synth. Org. Chem. Jpn.* **2010**, *68*, 1185. (b) Uraguchi, D.; Nakamura, S.; Ooi, T. *Angew. Chem., Int. Ed.* **2010**, *49*, 7562. (c) Uraguchi, D.; Ueki, Y.; Ooi, T. *Angew. Chem., Int. Ed.* **2011**, *50*, 3681. (d) Uraguchi, D.; Ueki, Y.; Ooi, T. *Chem. Sci.* **2012**, *3*, 842. (e) Corbett, M. T.; Uraguchi, D.; Ooi, T.; Johnson, J. S. *Angew. Chem., Int. Ed.* **2012**, *51*, 4685. (f) Uraguchi, D.; Yoshioka, K.; Ueki, Y.; Ooi, T. *J. Am. Chem. Soc.* **2012**, *134*, 19370. (g) Uraguchi, D.; Ueki, Y.; Sugiyama, A.; Ooi, T. *Chem. Sci.* **2013**, *4*, 1308.

(9) Uraguchi, D.; Tsutsumi, R.; Ooi, T. *J. Am. Chem. Soc.* **2013**, *135*, 8161.

(10) For examples of the oxaziridine synthesis, see: (a) Emmons, W. D. *J. Am. Chem. Soc.* **1956**, *78*, 6208. (b) Boyd, D. R.; Malone, J. F.; McGuckin, M. R.; Jennings, W. B.; Rutherford, M.; Saket, B. M. *J. Chem. Soc., Perkin Trans. 2* **1988**, 1145. (c) Martiny, L.; Jørgensen, K. A. *J. Chem. Soc., Perkin Trans. 1* **1995**, 699. (d) Damavandi, J. A.; Karami, B.; Zolfigol, M. A. *Synlett* **2002**, 933.

(11) For the imine oxidations by means of RCN–H$_2$O$_2$ system, see: (a) Schirmann, J.-P.; Weiss, F. *Tetrahedron Lett.* **1972**, *13*, 633. (b) Kraïem, J.; Kacem, Y.; Khiari, J.; Ben Hassine, B. *Synth.*

Commun. **2001**, *31*, 263. (c) Kraïem, J.; Ben Othman, R.; Ben Hassine, B. *C.R. Chim.* **2004**, *7*, 1119. (d) Tka, N.; Kraïem, J.; Ben Hassine, B. *Synth. Commun.* **2012**, *42*, 2994.

(12) Lykke, L.; Rodríguez-Escrich, C.; Jørgensen, K. A. *J. Am. Chem. Soc.* **2011**, *133*, 14932.

(13) Olivares-Romero, J. L.; Li, Z.; Yamamoto, H. *J. Am. Chem. Soc.* **2012**, *134*, 5440.

(14) Dong, S.; Liu, X.; Zhu, Y.; He, P.; Lin, L.; Feng, X. *J. Am. Chem. Soc.* **2013**, *135*, 10026.

(15) For a review on asymmetric hydroxylation of enolates with *N*-sulfonyloxaziridines, see: Davis, F. A.; Chen, B.-C. *Chem. Rev.* **1992**, *92*, 919.

(16) (a) Davis, F. A.; Nadir, U. K.; Kluger, E. W. *J. Chem. Soc., Chem. Commun.* **1977**, 25. (b) Davis, F. A.; Jenkins, R., Jr.; Yocklovich, S. G. *Tetrahedron Lett.* **1978**, *19*, 5171. (c) Davis, F. A.; Harakal, M. E.; Awad, S. B. *J. Am. Chem. Soc.* **1983**, *105*, 3123. (d) Davis, F. A.; Billmers, J. M.; Gosciniak, D. J.; Towson, J. C.; Bach, R. D. *J. Org. Chem.* **1986**, *51*, 4240. (e) Davis, F. A.; Sheppard, A. C. *Tetrahedron* **1989**, *45*, 5703. (f) Petrov, V. A.; Resnati, G. *Chem. Rev.* **1996**, *96*, 1809. (g) Andreae, S.; Schmitz, E. *Synthesis* **1991**, 327.

(17) Anderson, D. R.; Woods, K. W.; Beak, P. *Org. Lett.* **1999**, *1*, 1415.

(18) Brodsky, B. H.; Du Bois, J. *J. Am. Chem. Soc.* **2005**, *127*, 15391.

(19) Instead of the desired oxaziridine **3a**, the corresponding peroxyhemiaminal of type **a** (Figure 2.2) was obtained. The stereoselectivity of this simple addition of hydroperoxide ion was not determined because of the instability of the peroxyhemiaminal.

(20) Iminophosphorane **1i** can be recovered as corresponding hydrogen chloride salt **1i**·HCl during purification procedure.

(21) For this type of abbreviation for multi-substituted benzenesulfonyl groups, see, for example: (a) Ramage, R.; Green, J.; Blake, A. J. *Tetrahedron* **1991**, *47*, 6353. (b) Ooi, T.; Uematsu, Y.; Fujimoto, J.; Fukumoto, K.; Maruoka, K. *Tetrahedron Lett.* **2007**, *48*, 1337.

(22) When α-unsubstituted aliphatic *N*-Ts aldimine **2** (R^1 = Ph(CH$_2$)$_2$) was subjected to the standard conditions (general procedure 2), the corresponding oxaziridine was obtained with high enantioselectivity (94% ee) albeit in moderate chemical yield (57%).

(23) (a) Saito, I.; Nagata, R.; Yuba, K.; Matsuura, T. *Tetrahedron Lett.* **1983**, *24*, 1737. (b) Sasakura, N.; Nakano, K.; Ichikawa, Y.; Kotsuki, H. *RSC Adv.* **2012**, *2*, 6135.

(24) For review on aminohydroxylation of olens using oxaziridines, see: Knappke, C. E. I.; von Wangelin, A. J. *ChemCatChem* **2010**, *2*, 1381.

(25) For recent examples of transformations of *N*-sulfonyl oxaziridines, see: (a) Michaelis, D. J.; Shaffer, C. J.; Yoon, T. P. *J. Am. Chem. Soc.* **2007**, *129*, 1866. (b) Partridge, K. M.; Anzovino, M. E.; Yoon, T. P. *J. Am. Chem. Soc.* **2008**, *130*, 2920. (c) Michaelis, D. J.; Ischay, M. A.; Yoon, T. P. *J. Am. Chem. Soc.* **2008**, *130*, 6610. (d) Michaelis, D. J.; Williamson, K. S.; Yoon, T. P. *Tetrahedron* **2009**, *65*, 5118. (e) Benkovics, T.; Du, J.; Guzei, I. A.; Yoon, T. P. *J. Org. Chem.* **2009**, *74*, 5545. (f) Allen, C. P.; Benkovics, T.; Turek, A. K.; Yoon, T. P. *J. Am. Chem. Soc.* **2009**, *131*, 12560. (g) Partridge, K. M.; Guzei, I. A.; Yoon, T. P. *Angew. Chem., Int. Ed.* **2010**, *49*, 930. (h) Williamson, K. S.;

Yoon, T. P. *J. Am. Chem. Soc.* **2010**, *132*, 4570. (i) DePorter, S. M.; Jacobsen, A. C.; Partridge, K. M.; Williamson, K. S.; Yoon, T. P. *Tetrahedron Lett.* **2010**, *51*, 5223. (j) Benkovics, T.; Guzei, I. A.; Yoon, T. P. *Angew. Chem., Int. Ed.* **2010**, *49*, 9153. (k) Williamson, K. S.; Yoon, T. P. *J. Am. Chem. Soc.* **2012**, *134*, 12370.

(26) (a) Kraïem, J.; Grosvalet, L.; Perrin, M.; Ben Hassine, B. *Tetrahedron Lett.* **2001**, *42*, 9131. (b) Fabio, M.; Ronzini, L.; Troisi, L. *Tetrahedron* **2007**, *63*, 12896. (c) Motiwala, H. F.; Gülgeze, B.; Aubé, J. *J. Org. Chem.* **2012**, *77*, 7005. (d) Richy, N.; Ghoraf, M.; Vidal, J. *J. Org. Chem.* **2012**, *77*, 10972.

(27) (a) Lu, K.; Kwon, O. *Org. Synth.* **2009**, *86*, 212. (b) Chemla, F.; Hebbe, V.; Normant, J.-F. *Synthesis* **2000**, 75.

Chapter 3

Mechanistic Study on the Oxidation of *N*-Sulfonyl Imines with Hydrogen Peroxide– Trichloroacetonitrile System

3.1   Introduction

During the course of condition optimization of triaminoiminophosphorane **1**-catalyzed enantios-elective Payne-type oxidation of *N*-sulfonyl imines described in Chapter 2, the author generally observed the formation of a diastereomeric mixture of dimeric peroxides as major byproducts by the ^{1}H NMR analysis of a crude mixture when aliphatic *N*-Ts aldimine **2** was employed as the substrate. For example, when *N*-Ts cyclohexane carbaldimine **2a** was subjected to the standard condition for aromatic imines, dimeric peroxide **4a** was formed along with the desired oxazirdine **3a** in low isolated yield (Scheme 3.1).

Scheme 3.1 Formation of dimeric peroxide byproduct **4a**
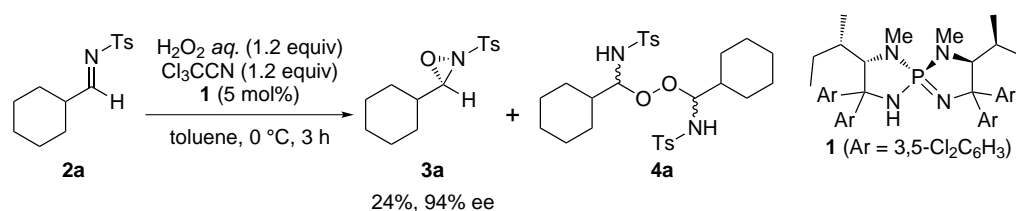
The formation of **4** could be accounted for by the fact that the aminophosphonium hydroperox-ide first reacts with imine **2** to give a tautomeric mixture of peroxyhemiaminal intermediates **a** and **a'** and the peroxyanion form **a'** instantly attacks another imine **2** (Figure 3.1). This interpretation prompted us to consider another mechanism (path B), where key intermediate **b** is generated by the addition of **a'** to trichloroacetonitrile (Cl$_3$CCN), in parallel with the Payne-type mechanism (path A).
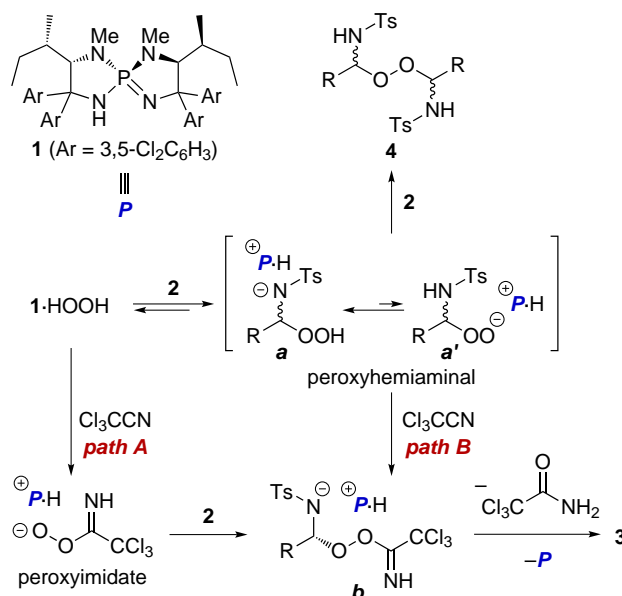
Figure 3.1 Two possible reaction pathways of oxaziridination

Preliminary NMR experiments to monitor the reaction showed the following facts: (1) the stating imine **2** is smoothly converted to the corresponding peroxyhemiaminal a when it is treated with **1** and ethereal hydrogen peroxide (H_2O_2) in the absence of Cl_3CCN under homogenous condition, (2) the above addition of hydroperoxide to imine **2** is reversible; the elimination of hydroperoxide ion from a actually occurred to give the starting imines **2**. [1]

Despite the complicated situation revealed by the above observation, the author concluded that the present reaction proceeds via Payne-type oxidation pathway (path A) by conducting another cross-over experiment by NMR. The detail is described in the following section.

3.2   Results and Discussion

To elucidate the actual reaction pathway, the cross-over experiments were conducted, in which the predominant pathway could be determined by comparing the reactivities of imine **2** and peroxyhemiaminal **a**·H under the influence of **1** and Cl_3CCN. Thus, a $CDCl_3$ solution of peroxyhemiaminal **2b'** was prepared by the treatment of *N*-Mts-isovaleraldimine **2b** with an ethereal solution of H_2O_2 [2] in the presence of a catalytic quantity of iminophosphorane **1** at ambient temperature; the ¹H NMR analysis showed that **2b** was instantly converted to **2b'** (Figure 3.2a). After the simultaneous addition of *N*-Mts-hydrocinnamaldimine **2c** and excess amount of Cl_3CCN to the reaction mixture, the ¹H NMR spectral analysis revealed almost exclusive formation of **3c** in 63% yield with 97% ee (Scheme 3.2, top and Figure 3.2b), suggesting the dominant contribution of path A. Importantly, **3b** predominantly formed by switching the roles of **2b** and **2c** (Scheme 3.2, bottom and Figure 3.2d).

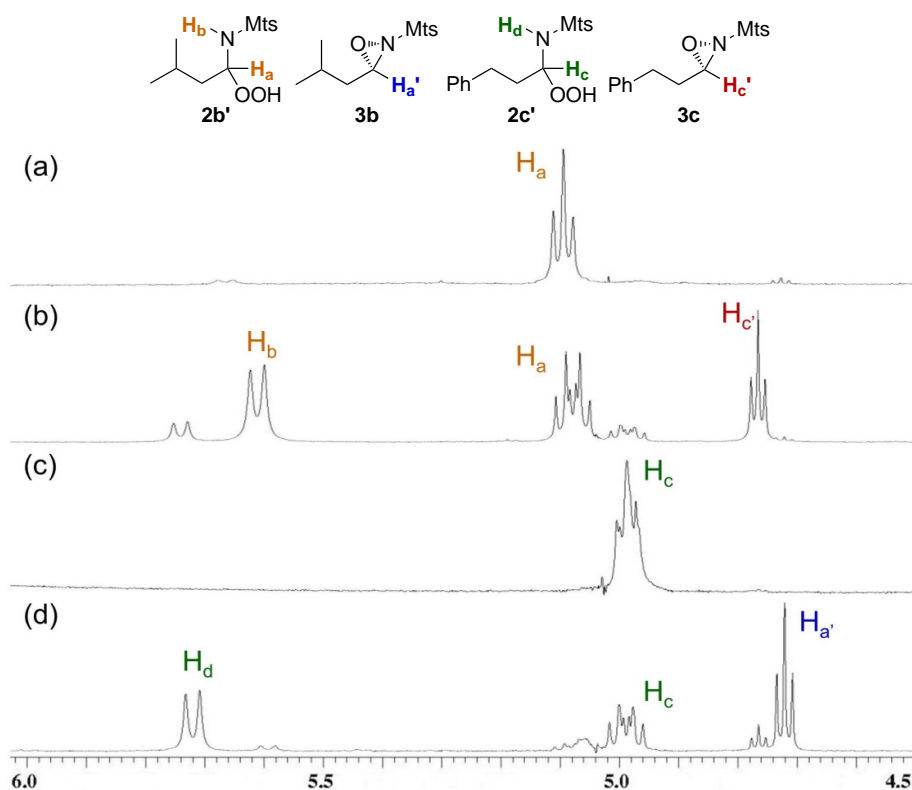**Scheme 3.2** Cross-over experiments using aliphatic imines
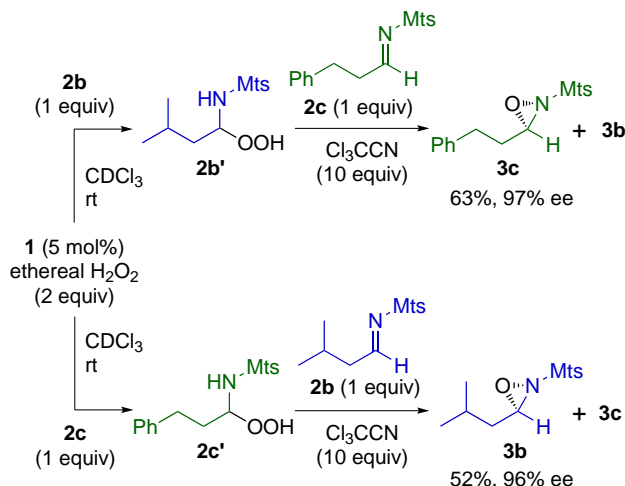
Figure 3.2 ^{1}H NMR Analysis of cross-over experiment

These observations clearly demonstrated that hydroperoxide ion rather than the peroxyhemi-aminal ion preferentially attacked Cl_3CCN with the aid of **1**·H to afford the oxaziridines **3**. Moreover, the enantiomeric excesses of **3b** and **3c** thus obtained were the same as those of the products obtained from the independent reactions with **2b** and **2c** under similar conditions (Scheme 3.3). Although the intervention of path B could not be completely excluded, the experimental results strongly supported that iminophosphorane selectively catalyzes this asymmetric oxazirination via the initially proposed path A.

Scheme 3.3 Oxaziridination of aliphatic *N*-Mts imines in the $CDCl_3 \cdot Et_2O$ solvent system
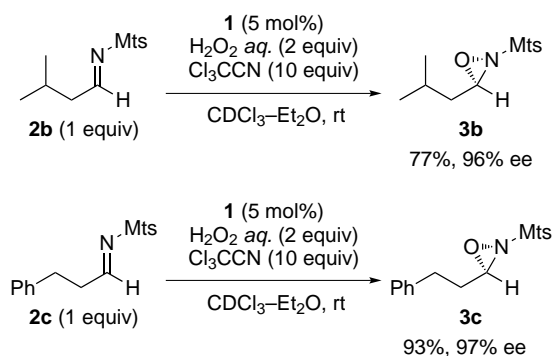
3.3   **Conclusion**

The reaction mechanism of **1**-catalyzed enantioselective oxidation of *N*-sulfonyl imines with H_2O_2–Cl_3CCN systems was investigated.   The cross-over experiments by means of NMR confirmed the operation of the initially proposed Payne-type oxidation mechanism wherein H_2O_2 first reacts with Cl_3CCN to form peroxyimidate as active species, which subsequently adds to imines **2** to afford the final product **3**.

3.4 Experimental Section

3.4.1 General Information

^{1}H NMR spectra were recorded on a JEOL JNM-ECS400 (400 MHz) spectrometer. Analytical thin layer chromatography (TLC) was performed on Merck precoated TLC plates (silica gel 60 GF254, 0.25 mm). Flash column chromatography was performed on PSQ60AB (spherical, av. 55 μm; Fuji Silysia Chemical ltd.). Enantiomeric excesses were determined by HPLC analysis using chiral columns [ϕ 4.6 mm × 250 mm, DAICEL CHIRALCEL OD-3 (OD3) and CHIRAL-PAK IC-3 (IC3)] with n-hexane (H), 2-propanol (IPA), and ethanol (EtOH) as eluent. Toluene and dichloromethane (CH_2Cl_2) were supplied from Kanto Chemical Co., Inc. as "Dehydrated"" and further purified by passing through neutral alumina under nitrogen atmosphere. Aminophos-phonium chloride **1**·HCl, [3] iminophosphorane **1**, [3] and N-sulfonyl imines **2** [4] were prepared by following the literature procedures. Trifluoroacetic acid (TFA) and trifluoromethanesulfonic acid (TfOH) were kindly supplied from Asahi Glass Co., Ltd. and Central Glass Co., Ltd., respectively. Other simple chemicals were purchased and used as such.

3.4.2 Preparation of an Ethereal Solution of H_2O_2 [2]

A 35% aqueous solution of H_2O_2 (titrated by using $KMnO_4$) was extracted with Et_2O. The ethereal phase was separated and dried over $MgSO_4$. The concentration of the ethereal solution of H_2O_2 thus obtained was determined to be 1.5–1.7 M by titration with $KMnO_4$.

3.4.3 Cross-Over Experiment (Figure 1.25)
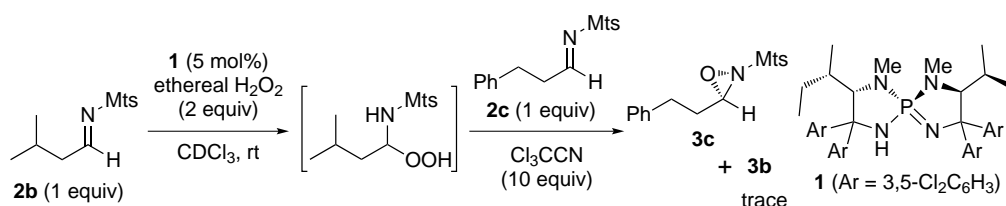
Chiral iminophosphorane **1** (0.87 mg, 0.0010 mmol) and N-Mts-isovaleraldimine **2b** (5.35 mg, 0.0200 mmol) were placed into a test tube and $CDCl_3$ (0.45 mL) was introduced to the tube at room temperature. An ethereal solution of H_2O_2 (27.0 μL) [2] was then added with stirring. After 5 min (The ^{1}H NMR analysis at this stage gave a spectrum (a).), a solution of N-Mts-hydrocinnamaldimine **2c** (6.31 mg, 0.0200 mmol) and Cl_3CCN (20.0 μL, 0.200 mmol) in $CDCl_3$ (0.10 mL) was rapidly added. Subsequent ^{1}H NMR analysis (400 MHz) gave a spectrum (b). After dilution of the mixture with EtOAc (EA), the reaction was quenched by the addition of saturated aqueous solution of Na_2SO_3. The aqueous phase was extracted twice by EA and the combined organic phase was dried over Na_2SO_4. After filtration, the filtrate was concentrated *in vacuo*. The

crude residue thus obtained was purified by column chromatography on silica gel (H/EA as eluent) to afford oxaziridine **3c**. The enantiomeric excess of 3c was determined to be 96% by HPLC analysis (IC3, H/IPA = 98:2, flow rate = 1.0 mL/min, λ = 210 nm, 17.3 min (major isomer), 19.0 min(minor isomer)). In a similar way, to the solution of **2b** and **1** in $CDCl_3$ were sequentially added ethereal H_2O_2 (The ^{1}H NMR analysis at this stage gave a spectrum (c).) and a solution of **2c** and Cl_3CCN. Subsequent ^{1}H NMR analysis gave a spectrum (d). The enantiomeric excess of **3b** thus obtained was 97% (IC3, H/IPA = 98:2, flow rate = 1.0 mL/min, λ = 210 nm, 9.4 min (major isomer), 10.6 min (minor isomer)).

3.4.4 Oxaziridination of Aliphatic *N*-Mts Imines in the $CDCl_3$–Et_2O Solvent System
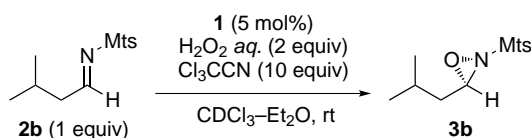
To a solution of **1** (0.87 mg, 0.0050 mmol), **2b** (5.35 mg, 0.0200 mmol), and Cl_3CCN (20.0 μL, 0.200 mmol) in $CDCl_3/Et_2O$ (0.55 mL, 27.0 μL) was added an aqueous 35% solution of H_2O_2 (3.5 μL, titrated by using $KMnO_4$) at room temperature. The work-up and purification according to the above procedure gave oxaziridine **3b**. The enantiomeric excess of **3b** thus obtained was determined to be 96% by HPLC analysis. Oxaziridine **3c** was obtained by the same procedure and its enantiomeric excess was 97%.

References and notes

(1) The existence of the retro reaction of the addition of hydroperoxide to imine **2** was confirmed by the following NMR experiment. To the solution of *N*-Ts pivalaldimine **2d** and **1** in CDCl$_3$ was added ethereal H$_2$O$_2$ (0.5 equiv) at room temperature. The ^{1}H NMR analysis at this stage showed the formation of the corresponding peroxyhemiaminal **2d'** and the existence of unreacted **2d**. This observation might suggest the complete consumption of H$_2$O$_2$ in the mixture judging from the rapidness of the reaction between imines **2** and H$_2$O$_2$. When imine **2a** was added to this mixture, the corresponding peroxyhemiaminal **2a**' formed. Moreover, the regeneration of imine **2d** was confirmed by comparison of the integration of ^{1}H NMR signals with that of 1,3,5-trimethoxybenzene as internal standard. These results clearly showed the scrambling of hydroperoxide between **2a'** and **2d'**, indicating the intervention of elimination of hydroperoxide ion from **2a'** and **2d'**.

(2) (a) Saito, I.; Nagata, R.; Yuba, K.; Matsuura, T. *Tetrahedron Lett.* **1983**, *24*, 1737. (b) Sasakura, N.; Nakano, K.; Ichikawa, Y.; Kotsuki, H. *RSC Adv.* **2012**, *2*, 6135.

(3) Uraguchi, D.; Yoshioka, K.; Ueki, Y.; Ooi, T. *J. Am. Chem. Soc.* **2012**, *134*, 19370.

(4) (a) Lu, K.; Kwon, O. *Org. Synth.* **2009**, *86*, 212. (b) Chemla, F.; Hebbe, V.; Normant, J.-F. *Synthesis* **2000**, 75.

List of Publications

Publications Related to the Thesis

1. "Catalytic Asymmetric Oxidation of *N*-Sulfonyl Imines with Hydrogen Peroxide–Trichloroacetonitrile System" Uraguchi, D.; Tsutsumi, R.; Ooi, T. *J. Am. Chem. Soc.* **2013**, *135*, 8161–8164.
2. "Catalytic Asymmetric Payne Oxidation under the catalysis of *P*-Spiro Chiral Tri-aminoiminophosphorane: Application to the Synthesis of *N*-Sulfonyl Oxaziridines" Uraguchi, D.; Tsutsumi, R.; Ooi, T. *Tetrahedron*, **2014**, *70*, 1691–1701.
3. "The Practical Preparation of Chiral *N*-Sulfonyl Oxaziridines via Catalytic Asymmetric Payne Oxidation" Tsutsumi, R.; Kim, S.; Uraguchi, D.; Ooi, T. *Synthesis* **2014**, in press. DOI: 10.1055/s-0033-1340818

Other Publications

1. "Total Synthesis of (−)-Brevisin: A Concise Synthesis of a New Marine Polycyclic Ether" Ohtani, N.; Tsutsumi, R.; Kuranaga, T.; Shirai, T.; Wright, J. L. C.; Baden, D. G.; Satake, M.; Tachibana, K. *Heterocycles* **2009**, *80*, 825–830.
2. "An Improved Synthesis of (−)-Brevisamide, a Marine Monocyclic Ether Amide of Dinoflagellate Origin" Tsutsumi, R.; Kuranaga, T.; Wright, J. L. C.; Baden, D. G.; Ito, E.; Satake, M.; Tachibana, K. *Tetrahedron* **2010**, *66*, 6775–6782.
3. "Synthesis of the ABC Ring Fragment of Brevisin, a New Dinoflagellate Polycyclic Ether" Kuranaga, T.; Ohtani, N.; Tsutsumi, R.; Baden, D. G.; Wright, J. L. C.; Satake, M.; Tachibana, K. *Org. Lett.* **2011**, *13*, 696–699.

Acknowledgement